

INVESTIGATIONS ON PART GEOMETRY AND SURFACE FINISH BY ELECTRICAL DISCHARGE MACHINING (EDM)

**A Thesis Submitted
In Partial Fulfilment of the Requirements for the
Degree of**

DOCTOR OF PHILOSOPHY

**in
Mechanical Engineering**

by

**Shrikant Vidya
(2K17/Ph.D./ME/29)**

Under the Supervision of

Dr. Reeta Wattal

Professor
Department of Mechanical Engineering
Delhi Technological University

Dr. P. V. Rao

Professor
Department of Mechanical Engineering
Indian Institute of Technology, Delhi



Department of Mechanical Engineering

DELHI TECHNOLOGICAL UNIVERSITY

Delhi-110042, India

December, 2024



DELHI TECHNOLOGICAL UNIVERSITY

BAWANA ROAD DELHI-110042 (INDIA)

CANDIDATE'S DECLARATION

I, Shrikant Vidya (2K17/Ph.D./ME/29) hereby declare that the work done in this thesis titled **“INVESTIGATIONS ON PART GEOMETRY AND SURFACE FINISH BY ELECTRICAL DISCHARGE MACHINING (EDM)”** is an original and own work carried out by me under the supervision of Dr. Reeta Wattal, Professor, Department of Mechanical Engineering, Delhi Technological University, Delhi and Dr. P. V. Rao, Professor, Department of Mechanical Engineering, Indian Institute of Technology, Delhi. The thesis has been prepared under the guidelines and regulations of Delhi Technological University, Delhi. The research work reported and the findings concluded and presented in the thesis have not been submitted and reported for any award of the degree or diploma either part or full time in any university or institute. As per my knowledge and understanding, this research work is free from all plagiarized content.

SHRIKANT VIDYA

(2K17/Ph.D./ME/29)

Department of Mechanical Engineering

Delhi Technological University

Place: Delhi

Date:



DELHI TECHNOLOGICAL UNIVERSITY

BAWANA ROAD DELHI-110042 (INDIA)

CERTIFICATE BY THE SUPERVISORS

Certified that **Shrikant Vidya** (2K17/Ph.D./ME/29) has carried out his research work presented in this thesis entitled **“INVESTIGATIONS ON PART GEOMETRY AND SURFACE FINISH BY ELECTRICAL DISCHARGE MACHINING (EDM)”** for the award of **Doctor of Philosophy** from Department of Mechanical Engineering, Delhi Technological University, Delhi, under our supervision. The thesis embodies results of original work and studies are carried out by the student himself and the contents of the thesis do not form the basis for the award of any other degree to the candidate or to anybody else from this or any other University/Institution.

Signature

(Dr. Reeta Wattal)

Professor

Department of Mechanical Engineering

Delhi Technological University

Signature

(Dr. P. V. Rao)

Professor

Department of Mechanical Engineering

Indian Institute of Technology, Delhi

Date:

ABSTRACT

The integration of advanced Electrical Discharge Machining (EDM) technology, incorporating short and electronically pulsed discharges with precise tool electrode movements, has enabled the production of intricate 3D micro geometries. The process is renowned for its ability to precisely machine superalloys that are traditionally challenging to machine. Nevertheless, it is crucial to regulate the process stability in order to ensure failure free operation and the production of defect free components. The current work aims to investigate the machining performance of die sinking EDM in machining of micro cavities of different shapes – holes, channels, triangular cavities, square cavities, pentagonal cavities and hexagonal cavities on steel samples using copper electrode.

In this investigation, small area EDM machining of microholes, channels and polygonal cavities is performed over EN-24 alloy steel with shaped tool electrodes. Further, these machined features are critically analysed through optical microscope, profile projector and SEM (scanning electron microscope) to assess the performance and capabilities of EDM machining in terms of dimensional accuracy, shape error, geometric tolerance, tool wear rate, recast layer formation and occurrence of micro cracks. Energy-dispersive X-ray (EDX) analysis is carried out for the machined surfaces to examine the presence of elements at their surface. The parametric analysis in die-sinking EDM of pentagonal cavities has also been conducted to examine how input parameters relate with performance metrics using Taguchi's L25 orthogonal array (OA). The assessment of rate of tool wear and rate of material removal is predicated on volumetric removal while the measurement of surface roughness has been carried out at three positions to give average value.

The experimental results reveal that the occurrence of random secondary discharges, alterations in discharge location and the joint impact of ion bombardment and thermo mechanical waves result in overcutting, corner rounding as well as tool wear. Among micro holes and micro channels, it is found that round micro holes have the best dimensional control whereas micro channels have rather inadequate dimensional

control. The tool wear rate is lower in channel machining because there is a greater discharge area, which also results in a smaller incidence of side discharge. According to the calculated geometric tolerance, the produced cavities are found to be of acceptable quality with fine tolerance. In reference to investigation of tool wear in polygonal cavities, it has been found that the polygonal cavity's complexity directly affects the rate of wear of tool. Hence, in case of machining of hexagonal cavities, there is maximum wear of tool while minimum tool wear occurs during the machining of triangular cavities. The formation of a recast layer becomes more prominent when working with complex and higher-order polygons. Sudden changes in the tool path's direction can cause uneven energy distribution, leading to inconsistent material removal and a thicker, irregular recast layer in higher-order polygons.

According to parametric analysis, the most important factor in the machining of pentagonal cavities is current followed by pulse-on-time and pulse-off-time. In case of tool wear rate also, the most significant factor is the current followed by pulse-on-time and pulse-off-time. Current is the most contributing factor for surface roughness while the influence of pulse-on-time is insignificant.

In nutshell, on the basis of experimental results, it can be revealed that die-sinking EDM integrated with advanced technologies is capable for producing micro geometries under optimum operating conditions.

ACKNOWLEDGEMENTS

I begin this acknowledgment by expressing my gratitude to the Supreme Creator, who has guided me through the challenges I encountered during this research work. Without the benevolent support of the Divine, this task would not have been possible.

I would like to extend my heartfelt gratitude to my supervisors, Prof. Reeta Wattal and Prof. P. V. Rao for their invaluable guidance and insightful recommendations throughout my research. Their unwavering support and encouragement during my doctoral studies have been truly invaluable. They have significantly contributed not only to my research skills and knowledge but also to my development in professionalism, communication and leadership. Their mentorship has been a source of inspiration to me and I aspire to one day provide the same level of guidance and support to future students. One of the most unique and memorable aspects of my journey with them as a supervisor is the supportive and inclusive research environment they created. In this environment, I have always felt valued and respected both as a researcher and as an individual. Their kindness, patience and sense of humour have made even the most challenging moments of my Ph.D. journey more manageable.

I would like to convey my thanks to Prof. Atul Agrawal, DRC chairman, Department of Mechanical Engineering, Delhi Technological University for his unwavering support and guidance. My special thanks to student research committee (SRC) members- Prof. S. K. Garg, Professor, Delhi Technological University, Prof. R. S. Mishra, Professor, Delhi Technological University, Prof. Sudharshan Ghosh, Department of Mechanical Engineering, IIT Delhi, Prof. Arshad Noor Siddiquee, Department of Mechanical Engineering, JMI, Delhi, Prof. R. C. Singh, Department of Mechanical Engineering, Delhi Technological University and Prof. Uma Nagia, Department of Electrical Engineering, Delhi Technological University for providing me their expert opinions and adding valuable suggestions. My sincere thanks goes to

Prof. B. B. Arora, Head-Department of Mechanical Engineering, Delhi Technological University for his continuous support during my research work.

I wish to acknowledge and thank the assistance and valuable suggestions provided by my colleagues and my seniors in the research group - Dr. Bharat Sanga, Dr. Anmol Bhatia, Dr. Himmat Singh, Mr. Harishankar, Mrs. Alka Sharma, Mr. Dhruv Kumar and Mr. Bijendra. I am especially thankful to Mr. M. K. Biswal and Mr. Viji K. for their help and cooperation during the experimentation in the Advanced Manufacturing Centre of CSIR-CMERI, Durgapur.

I wish to express my sincere gratitude to the Governing Body, Galgotias University, Greater Noida for constant encouragement and necessary approvals to continue and complete my research work at DTU, Delhi. I would like to thank all the faculty members of Department of Mechanical Engineering, Galgotias University for their whole hearted support throughout my research work. Special mention to Prof. P. K. S. Nain, Prof. S. K. Singh, Dr. Nav Rattan and Dr. Abhilash Purohit for their inputs and supports at various stages of this research. I would also like to thank all my friends, especially Mr. Subodh Kumar, Mr. K. S. Srikanth and Ms. Supriya Mishra for their help and continuous support during my research work.

Last but not the least, I would like to express my gratitude to my parents Mr. R. K. Nigam and Mrs. Asha Kumari for all their sacrifices, love and unconditional support throughout my life. I thank my sister Mrs. Nutan Kumari and my brother Mr. K. K. Vidya for their moral support. Finally, I thank with love, my wife Mrs. Shikha Kumari and son Shashwat for standing by me through all my toils, absence and impatience. The journey would not be this amazing without each of your inspiration and support.

TABLE OF CONTENTS

Title	Page No.
Candidate's Declaration	ii
Certificate	iii
Abstract	iv-v
Acknowledgements	vi-vii
Table of Contents	viii-x
List of Figures	xi-xiii
List of Tables	xiv-xv
List of Symbols and Abbreviations	xvi-xvii
CHAPTER 1 INTRODUCTION	1-19
1.1 INTRODUCTION	1
1.2 OVERVIEW OF EDM	2
1.2.1 Variants of EDM	3
1.2.2 EDM Process Parameters	6
1.2.3 EDM Dielectric	13
1.2.4 Electrode Material	14
1.3 CHARACTERISTICS OF EDM	15
1.3.1 Benefits of EDM	15
1.3.2 Limitations of EDM	16
1.3.3 Applications of EDM	17
1.4 FORMAT OF THE THESIS	18
CHAPTER 2 LITERATURE REVIEW	20-52
2.1 INTRODUCTION	20

2.2	MATERIAL REMOVAL MECHANISM	21
2.3	PLASMA CHARACTERISTICS	25
2.4	PROCESS PERFORMANCE AND OPTIMIZATION	28
2.5	PERFORMANCE ANALYSIS AND IMPROVEMENT	35
2.6	TOLERANCE ANALYSIS	49
2.7	GAPS IN LITERATURE	51
2.8	PROBLEM STATEMENT AND OBJECTIVE OF THE RESEARCH WORK	52
CHAPTER 3 METHODOLOGY AND EXPERIMENTATION		53-64
3.1	INTRODUCTION	53
3.2	METHODOLOGY	54
3.3	DIE-SINKING EDM TOOL AND ITS PERIPHERALS	54
3.4	MATERIAL SELECTION	56
3.5	MACHINING PARAMETERS	60
3.6	MEASUREMENTS AND ANALYSIS	60
3.6.1	Dimensional Measurement and Shape error	61
3.6.2	Tool wear rate (TWR)	62
3.6.3	Surface roughness	63
3.6.4	Surface characterization	63
3.6.5	Geometric tolerance analysis	64
CHAPTER 4 RESULTS AND DISCUSSIONS		65-91
4.1	PERFORMANCE ANALYSIS IN DIE-SINKING EDM OF MICRO HOLES AND CHANNELS	65
4.1.1	Dimensional Accuracy and Shape Error	67
4.1.2	Geometric Tolerance Estimation	69
4.1.2.1	Out of Roundness (for circular geometries)	71

4.1.2.2	Straightness (for micro channels)	73
4.1.3	Tool Wear Rate	77
4.1.4	Surface Characteristics and Elemental Characterization	78
4.2	PERFORMANCE ANALYSIS IN DIE-SINKING EDM OF POLYGONAL MICRO CAVITIES	81
4.2.1	Tool Wear Rate	83
4.2.2	Surface Characterization of Polygonal Cavities	86
4.2.3	EDS Analysis of Polygonal Cavities	87
4.2.4	Software Based Analysis of Angularity Error	90
CHAPTER 5	PARAMETRIC ANALYSIS IN DIE-SINKING EDM OF PENTAGONAL CAVITIES	92-124
5.1	INTRODUCTION	92
5.2	EXPERIMENTAL EQUIPMENT AND DESIGN	93
5.3	PARAMETRIC ANALYSIS OF MATERIAL REMOVAL RATE (MRR)	98
5.4	PARAMETRIC ANALYSIS OF TWR	107
5.5	PARAMETRIC ANALYSIS OF SURFACE ROUGHNESS (SR)	115
CHAPTER 6	CONCLUSIONS AND FUTURE SCOPE	125-129
6.1	CONCLUSIONS	125
6.2	SCOPE OF FUTURE WORK	128
	REFERENCES	130-149
	LIST OF PUBLICATIONS AND RECOGNITIONS	150-151
	CURRICULUM VITAE	152-153

LIST OF FIGURES

FIGURE NO.	DESCRIPTION	PAGE NO.
Figure 1.1	Illustration of the EDM Process	5
Figure 1.2	EDM Spark Description	5
Figure 1.3	Pulse Wave Form	7
Figure 2.1	Arc Plasma Expansion for Two Models	26
Figure 2.2	Area graph of (a) MRR for different Tool Shapes (b) TWR for different Tool Shapes	30
Figure 3.1	Flowchart of the Methodology	54
Figure 3.2	EDM Xpert-1 Tool	57
Figure 3.3	Dimensional Representation of Workpiece (in mm)	57
Figure 3.4	Olympus Optical Microscope	61
Figure 3.5	NIKON Profile Projector	62
Figure 3.6	Mitutoyo Surface Roughness Tester – SJ-400	63
Figure 3.7	ZEISS EVO Series SEM EVO 50 and EVO 18	64
Figure 4.1	Die-sinking EDM Machining Setup	66
Figure 4.2	Microscopic Images (5X) of (a) Micro hole (b) Micro channel	68
Figure 4.3	Minimum zone circle approach to find roundness error	72
Figure 4.4	Analysis Process of Straightness of Micro channels using Olympus Analysis Five Software	74
Figure 4.5	Average Tool Wear Rate of Micro holes and Channels	77
Figure 4.6	SEM Micrographs of Cavity Representing Recast Layer Formation: (a) Micro hole (b) Micro channel	79

Figure 4.7	Machined surface EDX analysis of (a) Micro hole (b) Micro channel	80
Figure 4.8	Schematic Representation of Polygonal Tools: (a) Triangular (b) Square (c) Pentagonal (d) Hexagonal	82
Figure 4.9	Microscopic Images of Cavities: (a) Triangular (b) Square (c) Pentagonal (d) Hexagonal	83
Figure 4.10	Graphical Representation of Tool Wear Rate for Different Geometries	85
Figure 4.11	SEM Analysis of Cavities Representing Recast Layer with Micro Cracks: (a) Triangular (b) Square (c) Pentagonal and (d) Hexagonal	87
Figure 4.12	EDS Analysis of Machined Surface of Different Cavities: (a) Triangular (b) Square (c) Pentagonal (d) Hexagonal	89
Figure 4.13	Microscopic Images along with Analysis Procedure of Cavities	90
Figure 5.1	(a) Tool Preparation (b) EDM Machining Setup	96
Figure 5.2	(a) Machined Sample (b) Microscopic Image of Cavity	98
Figure 5.3	Primary Effects of Mean Values for MRR	102
Figure 5.4	Primary Effects of Signal to Noise Ratios on material for MRR	103
Figure 5.5	Residual plot of MRR	104
Figure 5.6	Contour Plots for MRR: (a) Current (I) vs Pulse-on Time (T_{ON}) (b) Current (I) vs Pulse-off Time (T_{OFF}) (c) Pulse-on Time (T_{ON}) vs Pulse-off Time (T_{OFF})	105
Figure 5.7	Interaction plot of MRR	107
Figure 5.8	Primary Effects of Mean Values for TWR	109
Figure 5.9	Primary Effects of Signal to Noise Ratios for TWR	109

Figure 5.10	Normal Probability Plot of TWR	111
Figure 5.11	Contour Plots for TWR: (a) Current (I) vs Pulse-on Time (T_{ON}) (b) Pulse-on Time (T_{ON}) vs Pulse-off Time (T_{OFF}) (c) Current (I) vs Pulse-off Time (T_{OFF})	114
Figure 5.12	Interaction plot of TWR	115
Figure 5.13	Primary Effects of Mean Values for SR	116
Figure 5.14	Primary Effects of Signal to Noise Ratios for SR	117
Figure 5.15	Residual Plot of SR	120
Figure 5.16	Contour Plots for SR: (a) Current (I) vs Pulse-on Time (T_{ON}) (b) Current (I) vs Pulse-off Time (T_{OFF}) (c) Pulse-on Time (T_{ON}) vs Pulse-off Time (T_{OFF})	123
Figure 5.17	Interaction Plot of SR	124

LIST OF TABLES

TABLE NO.	DESCRIPTION	PAGE NO.
Table 3.1	Composition of EN-24 Alloy Steel	58
Table 3.2	Properties of Tool Electrode	58
Table 3.3	Common Parameters used for Machining	60
Table 4.1	Dimensions of Geometries	66
Table 4.2	Dimensional error for micro holes and channels	68
Table 4.3	Geometric Characteristics Symbols	70
Table 4.4	Roundness Error of Micro holes	72
Table 4.5	Dimensions of Micro-channel at different points	74
Table 4.6	Straightness Tolerance of Micro channels	76
Table 4.7	Tool Wear Rate for Different Geometries	77
Table 4.8	Angularity Error for Cavities	91
Table 5.1	Control Parameters with their Levels	95
Table 5.2	Experimental Layout	97
Table 5.3	Design Matrix of Process Parameters with Performance Measures	99
Table 5.4	Calculated S/N Ratios for MRR	100
Table 5.5	Response values for S/N Ratios - MRR	101
Table 5.6	Mean Response Values - MRR	102
Table 5.7	ANOVA Table for MRR	103
Table 5.8	Calculated SN ratios for TWR	108
Table 5.9	Response Values for TWR - S/N Ratios	110

Table 5.10	Response Values for TWR - Means	110
Table 5.11	ANOVA Table for the TWR	112
Table 5.12	Calculated S/N Ratios for Surface Roughness	118
Table 5.13	Response Values for S/N Ratios - SR	119
Table 5.14	Response Values for Means - SR	120
Table 5.15	ANOVA Table for the SR	121

LIST OF SYMBOLS AND ABBREVIATIONS

EDM	:	Electrical Discharge Machining
T _{ON}	:	Pulse on Time
T _{OFF}	:	Pulse off Time
MRR	:	Material Removal Rate
TWR	:	Tool Wear Rate
SR	:	Surface Roughness
HAZ	:	Heat Affected Zone
WLT	:	White Layer Thickness
OA	:	Orthogonal Array
DOE	:	Design of Experiment
ANOVA	:	Analysis of Variance
SEM	:	Scanning Electron Microscopy
MZC	:	Minimum Zone Circle
MCC	:	Minimum Circumscribed Circle
MIC	:	Maximum Inscribed Circle
LSC	:	Least Square Circle
I	:	Current
V	:	Voltage
R _a	:	Average Surface Roughness
EDS	:	Energy Dispersive X-Ray Spectroscopy
SD	:	Standard Deviation
R ²	:	Coefficient of Determination
R ² (adj)	:	Adjusted Coefficient of Determination

SS	:	Sum of Squares
LS	:	Least Square
R^2	:	Degree of Variance
DF	:	Degree of Freedom
LTB	:	Lower-The-Better
HTB	:	Higher-The-Better
y_{ijk}	:	Experimental Value of the j^{th} Response Variable in the i^{th} trial at the k^{th} Replication
n	:	Number of Repeated Experiments
p	:	Number of Replies
m	:	Number of Experimental Runs
e_i	:	Deviations in the Calculation of Straightness Tolerance
l_0, y_0	:	Least Square Solutions in Calculation of Straightness Tolerance
$h_{\text{straightness}}$:	Straightness Tolerance

CHAPTER 1

INTRODUCTION

1.1 INTRODUCTION

The machining of challenging materials like super alloys, ceramics, and composites is becoming more complex due to technological advancements and increased global competition. The high precision and surface quality required for these materials raises the cost of machining. Irrespective of the material's hardness, the notable characteristics of contact-free machining and 3D machining of Electrical Discharge Machining (EDM) have made it popular among other non-conventional machining techniques such as Electro-Chemical Machining (ECM), Ultrasonic Machining (USM) and Laser Machining. High-strength, high temperature alloys, complicated geometries and electro-conductive challenging-to-machine materials can be machined using EDM in small quantities as well as on a job-shop basis. The EDM process has been extensively studied by scientists over the years, yielding a wealth of theoretical and experimental notions.

The following special characteristics of the EDM process make modern machining possible:

(i) Contactless machining, which allows for machining to be done without exerting pressure on the material is a characteristic of the technique. As a result, "difficult-to-machine" materials such as curved and inclined surfaces as well as thin sheet materials can be machined at high pressure without creating vibration, chatter or mechanical stress

- (ii) The procedure makes it possible to create three-dimensional characteristics by means of a solid tool and the motions that go along with it, which makes it possible to machine intricate shapes. Furthermore, even more complicated shapes can be produced by combining the process with additional micro-machining methods such as chemical etching, laser radiation, Lithographie, Galvanoformung and Abformung (LIGA) technology and ultrasonic machining
- (iii) Any material that conducts electricity regardless of its hardness can be processed using the EDM process.

1.2 OVERVIEW OF EDM

Electrical Discharge Machining (EDM) is a non-conventional machining technique that utilizes electrical energy to produce sparks and remove material through thermal energy [1]. This process can be used to create complex shapes in limited quantities or on a per-order basis. EDM proves particularly advantageous for machining challenging materials like high-strength, temperature-resistant metals. However, for EDM to be effective, the work material must be electrically conductive. The key components of EDM include:

The dielectric circulation unit: The dielectric fluid is strained and directed into the space between the electrodes by this unit, facilitating the removal of machined material.

The servo-controlled tool feed unit: It is in charge of preserving a steady machining gap so that active discharges can occur between the electrodes.

The DC pulse generator: It supplies voltage and current for a predetermined duration, crucial for sparking and material removal during the EDM process.

The method of electrical discharge machining involves the occurrence of electric sparks between the tool electrode and the work material to remove metal through erosion. The tool electrode and work material both are immersed in a dielectric fluid and the servo system ensures that a minimal space is maintained between them. The workpiece is often assigned a positive charge, while the tool is assigned a negative charge. Once the voltage across the gap reaches a certain threshold, a spark is released within a time frame ranging from 10 μ s to a few hundred μ s. When the discharge channel becomes conductive, ions and electrons collide, resulting in the formation of a plasma channel. As a result, there is a rapid decrease in electric resistance, which enables the current density to increase significantly and generate a powerful magnetic field. The spark creates high pressure and the temperature ranges from 8000 to 12,000 °C [2], resulting in the melting and erosion of materials. Material removal occurs through vaporization and partial melting, forming a crater at the site of erosion. The plasma channel collapses upon withdrawal of the potential difference, generating shock waves that evacuate the molten material. Figure 1.1 illustrates the EDM process, highlighting the key components and their interactions while Figure 1.2 illustrates the process of plasma channel development, along with a detailed explanation of the spark.

1.2.1 Variants of EDM

EDM has two main variants:

(a) Die-sinking EDM

An electrically charged, geometrically-configured, shaped electrode is used in the die-sinking EDM machining process. The electrode's capacity to imprint intricate

geometries onto even the smallest and most resilient steel components through the utilization of negative energy allows for the treatment of such parts. This technique alternatively referred to as cavity-type EDM or volume EDM is extensively utilized in the die and mould-making sector. In an insulating liquid, two metal parts are submerged and linked to a current source that is automatically turned on and off in accordance with the controller's specifications during the die-sinking EDM process. When the current is activated, an electrical tension builds up between the two metal components. A spark will jump between them if they are brought within even a fraction of an inch of each other, discharging the electrical tension. The spark causes the metal to melt to the required shape for the metal sheet, which is determined by the geometry of the electrode. Before erosion occurs, some hundred thousand sparks must occur each second.

(b) Wire-cut EDM

In wire-cut EDM machining, heat from electrical sparks is used to cut through metal using de-ionized water and a thin, single-strand metallic wire. This method is favoured when there is a need for low residual stresses as it doesn't require substantial cutting forces for material removal. However, there's a risk of material deformation due to unrelieved stresses during machining. For precise and intricate cutting of hard conductive materials, wire EDM proves to be a valuable technique.

In wire EDM machining, there is occurrence of an electrical discharge when there is a flow of electricity between a wire or electrode and a workpiece. As sparks jump across the gap, removal of material takes place from both the workpiece and the electrode. To prevent shorting out during sparking, a nonconductive material is used.

The waste product is flushed away using a dielectric fluid and the process is repeated as necessary.

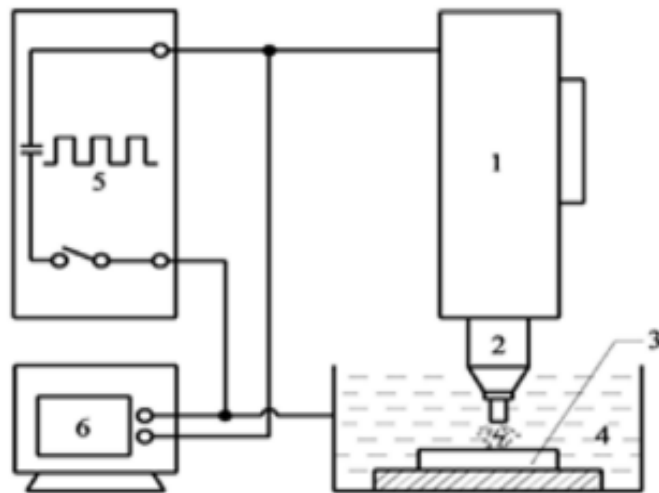


Figure 1.1: Illustration of the EDM Process

1. Servo-control, 2. Tool electrode, 3. Workpiece, 4. Dielectric fluid,
5. Pulse generator, 6. Oscilloscope [3]

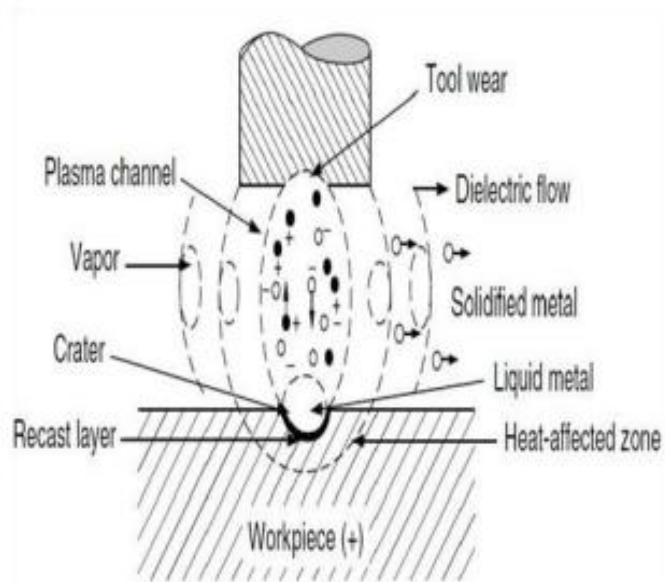


Figure 1.2: EDM Spark Description [1]

1.2.2 EDM Process Parameters

The parameters for EDM machines vary depending on their designs. In order to carry out effective machining, it is vital to identify the key process factors that impact the responses. These parameters can be classified as input or process factors and response or performance parameters. The set of parameters used is specific to each machine.

Input / Process Parameters

Electrical parameters

- **Spark On-time (pulse on time or T_{on}):** The on-time refers to the duration, measured in microseconds, during which the current is allowed to flow in each cycle. The quantity of energy transferred during the on-time period, which is determined by the highest current and the duration of the on-time, is directly related to the amount of material that is taken away. Studies have demonstrated that as the duration of the pulse increases, the roughness of the surface reduces. Simultaneously, the hardness of the work material, length and breadth of cracks and width of the recast layer rise with the rise in pulse duration.
- **Spark Off-time (pulse off time or T_{off}):** The pulse-off time (T_{off}), measured in microseconds between sparks, plays a crucial role as it permits the molten substance to congeal and flow across the arc gap. This setting controls the cutting steadiness and speed. If the off-time is too small, it can lead to the generation of unstable sparks. Studies have shown that a longer pulse interval results in a lower material removal rate (MRR) [4]. Studies have also

shown that low MRR is caused by small pulse interval times; nevertheless, as pulse interval times are increased, MRR first rises and thereafter falls gradually [5]. Indeed, the dielectric in the gap needs sufficient time to regain its dielectric strength, which is why very short pulse interval times can increase the likelihood of arcing. Research conducted by Zied [6] on the relationship between voltage, pulse off-time, and electro-discharge machining of AISI T1 high-speed steel indicates that the rate of material removal is less influenced by changes in pulse interval time during finish machining when pulse on-time is low. Figure 1.3 shows a representation of the pulse waveform.

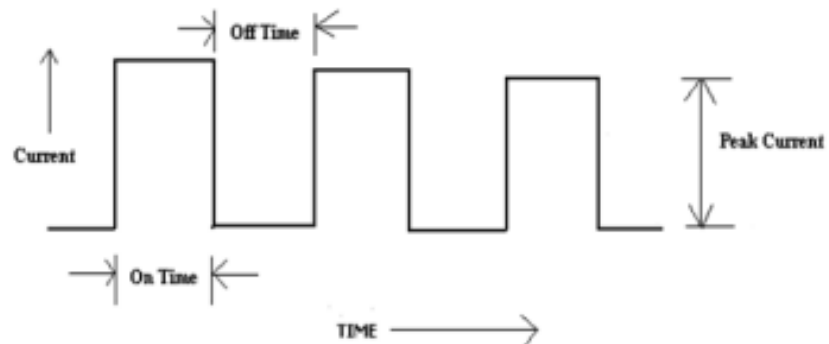


Figure 1.3: Pulse Wave Form [7]

- **Electrode gap (Spark gap):** EDM involves maintaining a certain distance between the tool electrode and the work material, known as the gap distance. This gap distance is controlled by electromechanical and hydraulic systems that respond to the average gap voltage. During the machining process, it's critical to maintain an appropriate gap distance for best performance and stability. In addition, the system must react fast to variations in the gap distance, such as open or short circuits. Although the average gap voltage

cannot be directly measured, it can serve as an indirect indicator of the gap width, allowing for estimation [7].

- **Duty cycle (τ):** The percentage of a full cycle that the current is permitted to flow is represented by the duty cycle parameter in EDM. It stands for a portion of the whole cycle duration during which the current is flowing. The calculation of duty cycle is performed by dividing the specific pulse duration by the whole duration of the cycle

$$\text{Duty cycle} = \frac{T_{on}}{T_{on} + T_{off}} \quad (1.1)$$

Amorim et al. [8] found that increasing the duty factor leads to an elevated rate of material removal. This occurs when the duty cycle is raised to a level where a layer of black coating forms over the surface of the work material. However, when the duty cycles exceed this threshold, the process of machining becomes unstable. Nevertheless, the pace at which material is removed increases as the duty factor increases. However, a greater duty factor can lead to instability in the machining process due to the deposit of a black layer on the surface of the work material [9]. As the duty cycle increases, the amount of energy delivered to the workpiece also increases leading to a higher intensity of the spark which results in an elevated MRR.

- **Polarity:** The polarity of the tool electrode or work material can lead to both positive and negative impacts on the EDM process. The polarity can have an effect on the speed, wear, finish and stability of the process. Studies suggest that linking the tool electrode to the positive terminal (+) instead of the negative terminal (-) leads to an increased rate of material removal. This

phenomenon occurs due to the transmission of a greater amount of energy during the process of charging. The ionization process occurs when neutral molecules between the workpiece and electrode are struck by electrons from the cathode. Ionization, however, takes place at the surface's positive terminal. Since the rate of removal of material is influenced by the drop in anode potential, the negative polarity is typically chosen over the positive polarity because it produces a larger MRR and better surface finish [10]. In a micro-slitting experiment on the alloy of titanium using an electrode as a rotating disk made up of copper, Chow et al. [11] reported that the MRR decreases with the workpiece's positive polarity because of the recast layer formation caused by the dissociation of carbon elements in the dielectric fluid.

- **Discharge Voltage:** The breakdown strength of the dielectric and the spark gap in EDM is directly linked with the discharge voltage. Before any electrical current can be started, the voltage across the open gap needs to rise until it forms a pathway of ionized particles through the dielectric. Once the electric current is established, the voltage steadily decreases until it stabilizes at the desired operating gap. The current voltage is now used to determine the size of the spark gap between the electrode and the leading edge of the workpiece. By increasing the voltage setting, the gap is widened resulting in improved flushing conditions and enhanced stability of the cut. When the open circuit voltage is increased, the rate of tool wear as well as surface roughness increase more rapidly than the rate of removal of material removal. This is due to rise in electric field strength.

Non-Electrical Parameters

- **Rotation of Tool Electrode:** In EDM, rotational speed is the number of revolutions per minute (RPM) that an electrode tool with a cylindrical or disc-shaped shape may make. Centrifugal force is produced when the electrode speed rises, hastening the clearing of debris from the area of machining. The electrode rotates perpendicular to the work surface. According to Mohan et al. [12], centrifugal force generates a layer of dielectric in the discharge gap, which fosters a better surface quality, inhibits arching, and raises the material removal rate. When spinning electrodes were compared to stationary electrodes, it was reported by Soni and Chakraverti [13] that both the surface finish and the MRR were improved because of the greater action of flushing and efficiency of sparking with less wear of the tool.
- **Flushing:** A critical step in electrical discharge machining (EDM) is flushing, which is filling the spark gap with filtered and clean dielectric fluid. Several flushing techniques are employed to effectively eliminate metal particles. By going through a filter system, the pressurized dielectric fluid carries away the eroded particles and clears debris from the fluid medium [14]. Chen et al. [15] observed that utilizing distilled water as the dielectric solution increased the rate of removal of material and decreased the relative wear ratio of electrode in their investigation on the EDM of Ti 6Al 4V.
- **Tool Geometry:** Tool electrode shapes, such as square, rectangle, cylindrical, circular, and so forth, are referred to as tool geometry. A study by Murali et al. [16] achieved an aspect ratio of 2.3 by using graphite foil for straight

grooving operations rather than pin-shaped electrodes. Singh et al. [17] machined 6061Al/Al₂O₃P composite using square and rectangular and square electrodes with aspect ratios of 0.6 and 1.0, respectively. The electrode wear ratio (EWR) was found to be influenced by the electrode's form, with electrodes with a smaller aspect ratio having a greater EWR. Larger electrodes can therefore result in improved EDM performance.

- **Tool Material (Electrode):** The selection of tool material for the EDM process is crucial for achieving desired machining results. Good thermal conductivity is a property that tool material should have to help with the dissipation of heat generated during machining. High temperatures are involved in the EDM zone thus it has to withstand the process by having a high melting point. Given its high melting point as well as low wear rate coupled with good electrical and thermal conductivity, copper is used many times as tool material. Of the various materials used in EDM, copper-tungsten, copper-graphite, silver-tungsten and brass are some other materials while graphite (because of its excellent lubrication properties, low wear rate and high heat conductivity) happens to be the most common among them. They have high melting points; hence they have good electrical conductivity as well as resistance to wear and tear. Since graphite is endowed with remarkable properties of low rate of attrition but high thermal conductivity making it an excellent lubricant, it is thus not surprising that it has emerged as a very attractive material when it comes to EDM tools alongside copper-tungsten; However, there are others like copper-graphite or silver-tungsten except brass. These are substances with very high melting points so they do conduct electricity easily while being difficult for them to be worn out.

Response / Performance Measures

- **Material removal rate (MRR):** Material removal rate, which represents the rate at which material is eliminated throughout the machining process per unit time is a major EDM measurement for values. In a high number of industrial applications that need high productivity, a higher MRR shows quicker machining therefore is recommended. It is vital to balance the MRR with other performance metrics such as the quality of the surface and the rate of electrode wear because an increase in MRR can also cause a decrease in these measures.
- **Tool wear rate (TWR):** Tool wear rate happens to be a crucial performance characteristic within EDM because it shows how much an electrode has worn away while being processed. With a lower TWR, we get more optimal performance because it implies that the electrode wears down less thereby enabling the electrode to stay for long without any repairs or sharpening.
- **Surface roughness (SR):** It represents the mean level of surface irregularities. In the industrial sector, R_a is the most commonly utilized surface roughness parameter. The machining performance improves with a smaller R_a value during the EDM process as R_a is a lower-the-better characteristic.
- **Surface Integrity:** The white layer, the heat-affected zone (HAZ) and the unaffected parent metal make up the three separate layers that make up the surface layer created during EDM. The white layer often termed as the "surface layer" or "surface film," represents the topmost layer of the material exposed to the atmosphere and is distinguished by its unique look as well as

by its metallurgical and chemical properties. The term "White Layer Thickness" (WLT) refers to the width of the white recast deposit. The area beneath the recast layer where the EDM processes have caused some degree of thermal change is known as the HAZ. The area below the hazard area zone that has not been impacted by the EDM process is known as the untouched parent metal. Surface roughness (SR) is influenced by various factors in the EDM process, such as the discharge energy, pulse duration, flushing and electrode material. As the discharge energy increases, the SR also tends to increase due to the creation of the layer that has resolidified on top of the HAZ. By decreasing the loss of alloying elements from the workpiece, the application of dielectric fluid containing powders can raise the micro-hardness and decrease the incidence of micro-cracks on the surface machined by EDM.

1.2.3 EDM Dielectric

As previously discussed, in the EDM process, material is primarily removed using melting and evaporation. Thermal processing must be done in an oxygen-free atmosphere to guarantee process control and avoid oxidation. Oxidation may cause the workpiece's surface conductivity to decrease, making machining more difficult. In order to prevent electrical breakdown, the dielectric fluid that is utilized needs to produce an environment of machining that is devoid of oxygen, has great resistance to dielectric, good ionization capability and is thermally resistant when sparking occurs. Since tap water ionizes too soon and breaks down because of contaminants like salts, kerosene and deionized water are frequently

employed as dielectric fluids in electrodynamic diodes (EDDs). To remove molten material effectively, the dielectric medium is often delivered through the tool and flushed around the spark zone.

1.2.4 Electrode Material

To minimize tool wear caused by positive ion impingement, the electrode material used in EDM should have properties that limit localized temperature rise and prevent excessive melting. This can be achieved by selecting or tailoring the material's properties. Indeed, electrode materials used in EDM must possess specific characteristics to accommodate the intricate geometric features commonly machined.

The basic characteristics of electrode materials include:

- Electrode materials used in EDM should possess high electrical conductivity. This characteristic lowers the local temperature rise for the same heat load by facilitating quicker heat conduction to the tool's bulk. As a result, there is less tool wear and greater machining process efficiency.
- Greater density is a crucial feature of the electrode materials used in EDM. Greater density would result in less volume removal or tool wear for the equivalent heat load and tool wear measured by weight. As a result, there is minimal dimensional loss or inaccurate machining. Higher density electrode materials are therefore recommended since they enable more exact and accurate cutting.
- An additional important feature of the electrode materials utilized in EDM is their high melting point. Less tool wear results from a higher melting point since the tool material melts more slowly.

- Easy manufacturability
- The material should be economically viable, balancing performance and expense

The diverse tool electrode materials that are normally utilized in industries are as follows:

- Graphite
- Brass
- Oxygen-free copper produced through electrolysis
- Tellurium copper – an alloy composed of 99% copper and 0.5% tellurium.

1.3 CHARACTERISTICS OF EDM

1.3.1 Benefits of EDM

1. EDM is an unconventional machining technique that produces no cutting forces. This produces burr-free edges and enables precise production of small, delicate parts.
2. Because EDM machines are so precise, they require less operator involvement to produce complex parts with excellent finishes. The process can be easily configured to run automatically, eliminating the need for constant manual operation and increasing overall efficiency. EDM is often applied in multiple industries such as aerospace, medical care and automobiles that require accuracy and flawless surface finishes because it can effortlessly come up with complicated structures and subtle elements.
3. EDM has an advantage over conventional machining methods in terms of being able to avoid hindrance from the hardness of the machined material, unlike the latter;

it can handle even hard materials without forming any distortion or altering their forms after heating since removal takes place because of melting or vaporization. Industries that find it challenging to make carbide, titanium, and hardened steel using traditional techniques prefer EDM.

4. Materials that are extremely difficult to machine with high precision can be produced through electrical discharge machining. The technique is based on the idea that the work material and the tool electrode are connected to an electric circuit with an electric current that causes sparks to jump between them, therefore it only applies to electrically conductive elements. Still, it could well appear as one of the best methods ever if you want something delicate repeating exactly after another every time made from something possessing electrical conductivity properties such as copper or carbon fibre instead of other products like plastics (non-conductors).

1.3.2 Limitations of EDM

- a) EDM can only machine electrically conductive materials, limiting its use to materials that are non-conductive like certain ceramics and plastics.
- b) Compared to traditional machining processes, EDM has a relatively slow material removal rate
- c) The method has the ability to modify the surface characteristics of the workpiece, such as generating a recast layer and causing residual stresses, which might require additional treatment
- d) The localized heating can cause changes in the metallurgical structure of the workpiece, leading to heat-affected zones (HAZ) that might affect the mechanical properties of the material

e) EDM requires precise control and setup, including the maintenance of dielectric fluid quality, electrode alignment, and proper gap control, making it a complex and potentially costly process to maintain

f) EDM is less effective for machining deep, narrow cavities compared to some other methods, as flushing the dielectric fluid becomes more challenging and tool wear is more pronounced.

1.3.3 Applications of EDM

1. The most common uses of EDM are for processing hard metals and alloys, as well as meeting the growing demand for smaller, intricate, multipurpose components in the microelectronics sector. This technology excels in producing detailed parts essential for advanced electronic applications.

2. It is employed in thread cutting, wire drawing, extrusion, forging and drilling curved holes.

3. It is utilized for tasks such as cutting internal threads, helical gears and fabrication of précised edges and corners.

4. EDM machining enables the attainment of greater tolerance limits.

1.4 FORMAT OF THE THESIS

Chapter-1: Introduction

In this chapter, the notion of micro-manufacturing is presented along with the role that electrical discharge machining plays in it. The fundamentals of the EDM process including the mechanism, control variables, dielectrics, electrode materials, characteristics and process difficulties are covered.

Chapter-2: Literature Review

A review of research conducted on EDM process optimization, plasma characteristics, material removal mechanism, performance analysis and improvement as well as tolerance analysis is discussed in this chapter. The objectives of the study and gaps in the literature are also mentioned in this chapter.

Chapter-3: Methodology and Experimentation

In this chapter, the specifics of the experimental work are covered. This chapter deals with the fundamental experimental design, material choice, machining specifications and the selection of the machine tool. The planning for experimentation as well as tools and devices used to assess and gauge EDM performance is also described in the chapter.

Chapter-4: Results and Discussions

This chapter presents the outcomes of the assessment of EDM performance in the fabrication of micro holes, channels and polygonal microcavities. The detailed analysis of the results obtained in shape inaccuracy, tool wear rate, production of recast layers, and elemental characterization is also covered in the chapter.

Chapter-5: Parametric Analysis in Die-sinking EDM of Pentagonal Cavities

The creation of pentagonal microcavities and the impact of variables on die-sinking EDM machining results are covered in this chapter. Single objective optimization using Taguchi is described in this chapter. This indicates the optimum machine settings for optimizations of the single response parameters.

Chapter-6: Conclusions and Future Scope

This chapter presents the key findings derived from the research conducted with potential future research directions in the same field.

CHAPTER 2

LITERATURE REVIEW

2.1 INTRODUCTION

When Electrical Discharge Machining (EDM) was introduced in the 1940s, it was initially referred to as ram or sinker EDM. Initially EDM was utilized primarily within the tool and die industry for removing broken taps and drills from dies under production. But, now EDM has gained widespread acceptance among manufacturers, particularly in the aircraft, aerospace, electronics and medical sectors.

The majority of published literature on EDM focuses on its industrial applications, addressing various aspects such as technology, key machining parameters like current and voltage, their influence on machining quality and EDM's effectiveness on different materials, material removal rates, and wear ratios of tool and workpiece electrodes. Additionally, numerous papers discuss the advantages and disadvantages of EDM as a micromachining technique. On the other hand only limited studies have been carried out on understanding the physical aspects of the process. The shape and Size effect in EDM is the primary focus of this research. Literature reviewed mostly covers the aspects related to mechanism of material removal, characteristics of plasma channel and optimization of parameters. A brief discussion about recent investigations of different engineers and researchers in context to the research are discussed in the following section:

2.2 MATERIAL REMOVAL MECHANISM

Wang et al. [18] conducted an analysis of the process involved in material removal of the electrode in EDM by means of short pulses, incorporating principles of heat conduction, plasma theory, and elasticity mechanics. They developed a thermodynamic model to understand the removal of electrode material during individual sparks, which they verified through finite element numerical simulations and experimental tests. Additionally, they explored and formulated another electrostatic force-based material removal model designed specifically for EDM that makes use of short pulses. This model facilitated the prediction of electrode wear and contributed to improving machining accuracy.

Lauwers et al. [19] explored material removal mechanism in EDM for various ceramic materials, such as zirconium dioxide-based, silicon nitride-based, and aluminium oxide-based ceramics having conductive phase additives like titanium nitride and titanium carbonitride. They identified additional removal mechanisms like oxidation and base material decomposition alongside typical EDM processes like melting/evaporation and spalling. Their study highlighted the influence of factors such as melting point, fracture toughness and thermal conductivity on spalling effects.

A thermo-electric model was established by Singh et al. [20] with the goal of assessing electrostatic force and stress distribution in Electrical Discharge Machining (EDM) during the discharge phase. They found electrostatic forces to be prominent in short pulses, while melting dominated in long pulses, explaining consistent crater depth variation. Dimensional analysis was used by Yahya and Manning [21] to

examine how electrical and physical parameters affected a die sinking electro-discharge machine's rate of material removal. A concise description of the metal removal procedure was given and a numerical model for the metal removal rate was created via dimensional analysis using the components that affected the rate of metal removal. The material characteristics factor, gap voltage, gap current, discharge pulse on time and sparking frequency were found to be proportionate to the material removal rate. Regression analysis had been used to generate a dimensionless constant C to forecast the rate of erosion at a particular gap current. Since the approach predicts outcomes that are in good accord with experimental data, its validity has been confirmed.

Erden and Kaftanoglu [22] developed a thermo-mathematical model for EDM, optimizing energy pulse shapes for maximum material removal, while Bergs et al. [23] improved heat transfer simulations during EDM, considering material removal during discharge and addressing simulation ambiguities. Yue et al. [24] investigated EDM of carbon-fiber-reinforced silicon carbide composites, emphasizing thermal stress effects on material removal. They employed innovative observation methods and simulations to understand fracture and stress distribution during EDM, aiding in achieving efficient material removal. Gostimirovic et al. [25] integrated mathematical and experimental approaches to study material removal in EDM, focusing on electro-thermal effects and optimizing EDM parameters based on temperature distributions.

In a study of material removal in EDM by Yue et al. [26] studied, it was found that metal vapour jets emerging from the workpiece and tool electrode create radial flow, aiding material removal. They observed that more material was removed per

discharge on a steel workpiece using a tool electrode with a lower boiling point.. High-speed video showed more effective debris removal using electrodes with lower boiling point. Molecular dynamics simulations confirmed that these electrodes produced more intense vapour jets, enhancing radial atom velocities. Measuring the reaction force of discharge revealed that brass wire with a zinc coating produced a larger force, indicating that jet-induced shear force aids material removal. They concluded that the higher rate of material removal with zinc-coated wire in wire cut EDM is due to the zinc coating's lower boiling point. The impact of magnetic field assistance on the material removal rate in both dry and wet electrical discharge machining (EDM) was examined by Govindan et al. [27]. With various factors such as current, bi-pulse current, voltage, pulse on-time and magnetic field, more than 100 single-discharge trials were carried out. According to the findings, magnetic field aid lowered the crater diameter by 80% and raised the MRR in dry EDM by about 130%. Magnetic field help in liquid EDM greatly increased material erosion uniformity while just slightly reducing crater diameter. The researchers attributed the increased MRR to several variables, including the restriction of plasma by Lorentz forces. Analytical modeling indicated that the involvement of Lorentz forces in constraining plasma and lowering the electron mean free path owing to the magnetic field accurately mirrored the experimental findings. Overall, the study showed how magnetic field aid may help increase the effectiveness and accuracy of EDM. Similarly, in order to simulate the EDM discharge process, a two-temperature model (TTM) was utilized by Yue et al. [28] in a 2-D sub-micrometer simulation. This simulation model made it possible to examine the effects of free electrons and lattice vibration on heat conduction at the same time. A sub-micrometer-sized discharge

crater that resembled the tiniest discharge crater ever documented was successfully recreated using the TTM-based sub-micrometer scale simulation. Additionally, the modelling findings showed that molten material was removed during the EDM discharge process in part due to pressure generated within the molten pool. Furthermore, it was shown that during the discharge, polycrystalline copper showed a greater inclination to produce fault structures and larger denatured layers than monocrystalline copper. Significantly, it was shown that the degree of fault structures and denatured layer in polycrystalline copper was correlated with its grain size, with smaller grains having stronger impacts. In order to investigate the mechanism of material removal and the influence of process factors on the dimensional accuracy, profile accuracy and machining speed of features machined on zirconia toughened alumina (ZTA) ceramics employing assistive electrode EDM, Bilal et al. [29] carried out an investigation. The results of the experiment reported that the rate of removal of material was improved by raising the peak current as well as spark on time. Over the machined surface, a thicker layer was seen to form as a consequence of these circumstances, though. Moreover, a greater value of the pulse interval duration was found to be crucial for the complete elimination of the intrinsic carbon layer during the machining of nonconductive ceramics, which may result in non-sparking circumstances. While shorter pulse on and pulse off periods led to enhanced circularity due to rough machining, increasing the peak current also improved circularity. Peak current and spark on time had an impact over the machined features' taperness. In conclusion, it was found that the main mechanisms for removing material from ZTA ceramics during the EDM process were thermal cracking and spalling, in addition to melting and evaporation. Lu et al. [30] developed a dry single

impulse EDM technique for machining RB-SiC and studied the material removal mechanism through surface topography and phase components. Using SEM, EDS, and Raman spectroscopy, they examined the Si matrix and SiC particles. By varying discharge energy with different pulse-on times, they found that short pulse-on times mainly removed the silicon matrix because of its lower melting temperature and electrical resistivity. SiC particle removal occurred through spalling from thermal shock and high-temperature decomposition. They also observed material migration and oxidation on the sample surfaces machined through EDM.

2.3 PLASMA CHARACTERISTICS

Natsu et al. [31] employed spectroscopic analysis to determine the true temperature determined by Abel's inversion and compared it with the apparent temperature distribution in the EDM arc plasma. They reported that, depending on the operating parameters, the centre of the arc plasma had the maximum plasma temperature during discharge, which ranged from 4000K to 8000K. Factors like electrode thickness discharge current and gap distance influenced the temperature of the plasma, with thinner electrodes, greater gap distances, and higher discharge currents resulting in higher plasma temperatures and larger plasma diameters. Additionally, they noted that plasma deionization occurred faster with narrower gap distances.

Panda Deepak Kumar [32] presented a solution for the computation of components related to thermal stress in closed form generated during EDM machining utilising single spark. The analytical model provided simpler mathematical expressions compared to finite element models and showed significant resemblance to previous results. Thermal stresses were found to extend around the crater, exceeding ultimate

stress levels, with factors like power, pulse duration and radius of the plasma channel affecting their magnitude. Higher heat flux and longer pulse durations led to increased thermal damage, with a network of cracks initiating from the crater's top edge. Controlling surface roughness helped minimize the damaged layer surrounding the crater. In a study by Natsu et al. [33] the plasma arc expansion in electrical discharge machining was noted using a video camera and a new model called the initial phase expansion model was suggested. This model, verified experimentally through plasma temperature measurements revealed that the arc plasma expansion during the machining process occurs rapidly, typically completing within microseconds following dielectric breakdown. They demonstrated that the initial phase expansion model bears a close resemblance to the real-world EDM (Electrical Discharge Machining) process, as indicated by the computed discharge crater characteristics, surpassing the accuracy of conventional models (Figure 2.1).

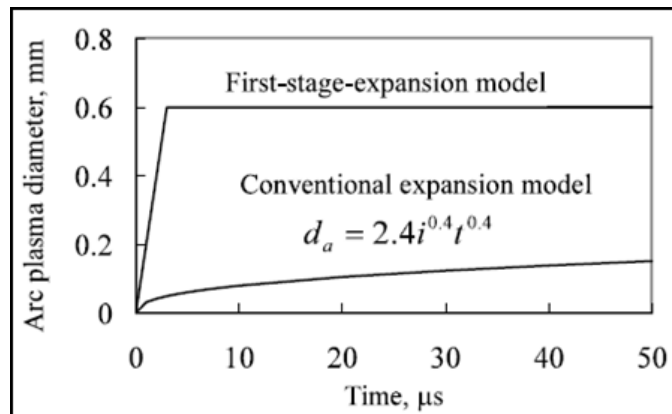


Figure 2.1: Arc Plasma Expansion for Two Models [33]

Pandey et al. [34] performed computation based analysis to investigate the variation in size of plasma channel with pulse-on duration in Electrical Discharge Machining (EDM), introducing a 2-D disc heat source model. They observed that adapting this

model to account for the time-dependent nature of diameter of plasma channel led to better alignment between theoretical predictions and experimental results. This enhancement improved the accuracy of forecasting the thickness of the HAZ and the amount of thermal damage to tool electrode during EDM. The temperature distribution on workpiece and tool surfaces during a single discharge in EDM was simulated by Shabgard et al. [35] using ABAQUS finite element software, incorporating temperature-dependent material properties and plasma channel radius expansion over time. Their numerical analysis assessed parameters influencing plasma flushing efficiency, indicating positive effects of increased pulse current and negative effects of increased pulse on-time on plasma flushing. Regression models based on these findings predicted recast layer thickness on electrodes, offering insights without expensive empirical testing.

Li et al. [36] employed high-speed camera observation and image processing to examine the mobility of arc plasma and how it relates to the development of craters during single-pulse discharge in EDM. They observed varying arc plasma movement speeds and ranges, influencing crater morphology, particularly affected by discharge current, gap distance, and electrode shape. Additionally, they noted constrained arc plasma movement in oil compared to air. Tanveer et al. [37] developed a plasma discharge model for analyzing plasma characteristics in EDM, incorporating chemical kinetics, fluid flow and mechanisms of heat transfer. Their 1D domain model considered surface reactions on electrode walls and investigated plasma characteristics under different EDM parameters, offering insights into plasma generation mechanisms and potential applications in melt-pool modeling. A high-speed photography and FEM was utilized by Yue et al. [38] to study discharge

process dynamics in EDM. They observed random plasma motion causing molten pool movement, influencing material removal and crater topography. Application of an external magnetic field directed plasma motion and molten pool flow, affecting material removal mechanisms and resulting crater shapes.

The simulation studies on arc plasma in EDM were conducted by Li et al. [39], integrating flow field, heat transfer, and electromagnetic field considerations. They observed significant influence of vapour generated from tool electrode and workpiece heating on arc plasma diameter, with different compositions altering dielectric medium properties and affecting plasma characteristics. Additionally, they investigated the impact of different gas dielectrics on arc plasma behaviour, highlighting the importance of dielectric choice in EDM.

2.4 PROCESS PERFORMANCE AND OPTIMIZATION

Utilizing a full factorial design with an emphasis on the factors of pulse-on-time and discharge current, Lee and Tai [40] investigated the relationship between Electrical Discharge Machining factors and the formation of surface crack. Their examination of D2 and H13 tool steels elucidated the effects on surface finish, white layer width, induced stress and the occurrence of cracks during EDM. They concluded that surface roughness increased proportionally with pulse current and spark-on-time for both steels. The width of the white recast layer increased with higher pulse current and pulse-on-time, with the latter having a more significant effect, and was greater for H13 steel due to its higher thermal conductivity. Cracks originated from the surface of the workpiece and penetrated perpendicularly into the white recast layer, with fewer tendencies for crack formation in H13 steel due to its higher thermal

conductivity. Increased pulse-on-time led to thicker white layers and induced stress, promoting crack formation, while increased pulse current resulted in higher material removal rates and thicker white layers, but similar crack densities.

The influence of different tool shapes considering size factor in EDM processes on the rate of removal of material and tool wear by means of Response Surface Methodology (RSM) was investigated by Sohani et al. [41]. They developed mathematical models of second order to set up relations between process parameters and responses using Central Composite Design. Analysis of Variance with Fisher's test verified model adequacy. Their findings indicated highly significant influence of spark-on-time and discharge current on the rate of removal of material and rate of wear of tool electrode, with tool area as well as pulse-off-time also significantly affecting rate of removal of material and rate of tool electrode wear. MRR increased linearly with discharge current, while TWR increased nonlinearly. Initially, MRR increased with pulse-on-time and then decreased, while TWR initially decreased rapidly before stabilizing. While TWR dropped linearly with tool area, MRR grew linearly with an increase in pulse-off-time. Graphical analysis (Figure 2.2) suggested circular tools with size considerations yielded the highest rate of removal of material and lowest rate of wear of tool electrode, subsequently triangular, rectangular, and square tools. A research based study on the impact of intensity, spark-on-time and spark-off time on a variety of output aspects of the machining like dimensional accuracy and surface quality was carried out by Puertas et al. [42]. Their findings highlighted that intensity significantly affects surface roughness, and they observed a significant interaction between pulse-on time and intensity. The authors recommended using high intensity values and low pulse-on times for optimal results.

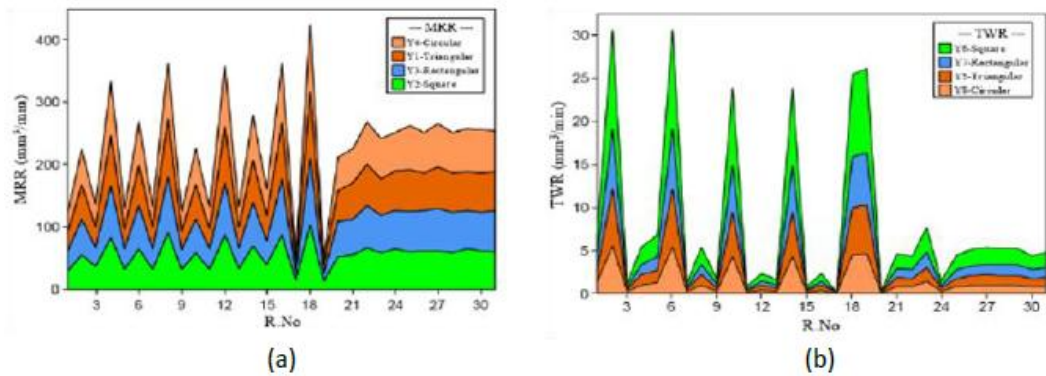


Figure 2.2: Area graph of (a) MRR for different Tool Shapes (b) TWR for different Tool Shapes [41]

Guu Y.H. [3] explored the influence of discharge energy on surface features during machining of AISI D2 tool steel via EDM. They found that higher discharge energy led to poorer surface structure and increased micro-crack depth. Their study suggested using low discharge energy to minimize damage, and emphasized the importance of polishing components to reduce micro-cracks before use. A rotary EDM process was introduced by Guu et al. [43] for machining hard-to-cut cylindrical workpieces. They compared this approach with conventional EDM and found that rotary EDM improved machining efficiency and surface quality. The study revealed that debris particles increased discharge instability in traditional EDM, while centrifugal force in rotary EDM enhanced gap flushing, resulting in higher material removal rates (MRR) and smoother surfaces. Anish et al. [44] developed quadratic models to analyze key EDM parameters for pure titanium machining. Their study highlighted the significance of factors such as spark gap voltage, peak current, spark-off-time and spark-on-time on machining rate, surface finish, and dimensional deviations. They concluded that these parameters strongly influence EDM performance with a 95% level of confidence.

Nikalje et al. [45] deliberated the influence of spark-on-time, discharge current and spark-off-time on performance measures like rate of removal of material, relative wear ratio, tool electrode wear ratio as well as surface finish. They utilized the Taguchi method for optimization and found optimal levels of factors varied for different performance characteristics. A quadratic model was developed by Patel et al. [46] to represent EDM behaviour and conducted experiments with Al₂/SiC_W/TiC ceramic composite as the workpiece. Their study revealed that pulse-on time significantly influences surface roughness, while an increase in discharge current also increases surface roughness.

Tzeng and Chen [47] used fuzzy logic and taguchi techniques to create a high-speed electrical discharge machining process. They identified duty cycle, pulse time and peak discharge current as crucial factors, accounting for a significant deviation in the process. The response surface methodology was utilized by Kansal et al. [48] to recognize the correlation between process factors and performance parameters like rate of material removal and surface finish. They identified peak current and silicon powder concentration as key factors affecting MRR and surface roughness. In a study by Arooj et al. [49], the investigation of the effect of electric current variation on surface morphology was done during die sinking EDM of aluminum alloy. They observed a correlation between current values and surface characteristics, reporting an increase in globule formation with higher currents. ZhanBo et al. [50] explored the viability of three dimensional surface machining by dry electrical discharge machining and identified optimal combinations of parameters for maximum MRR and minimum tool wear. They found that depth of cut and gas pressure significantly affects MRR and tool wear. An approximate theoretical model for determining the

final surface roughness was introduced by Zhang et al. [51]. The electrode used in the experiments was copper, and the work piece material was AISI 1045 steel. The study found that when discharge voltage, discharge current, and pulse duration rise, so does the completed surface's roughness. Guu et al. [52] stated that EDM creates a wavy surface, increases surface roughness which results in damage from machining. Using atomic force microscopy (AFM), they analyzed surface characteristics and proposed an empirical model for Fe-Mn-Al alloy. Energy dispersive spectroscopy measured chemical composition, and a micro hardness tester assessed surface hardness. It was found that AFM effectively provides nanometre-scale 3D images and more melting expulsions from higher discharge energies result in deeper, bigger craters and worse surface quality. They also reported that pulse-on duration significantly affects surface texture more than pulsed current. Micro cracks, voids, and damage increase having longer pulse-on times and higher pulsed current. Also, the machined surface chemistry differs due to electrode material diffusion but surface hardness remains similar to the non-EDM workpiece. In a research by Senthil et al. [53], the optimization of process parameters was carried out in the machining of Al-CuTiB₂ metal matrix composites (MMCs) by electrical discharge machining. In-situ casting was employed to synthesize MMCs and L18 orthogonal arrays (OA) were used to optimize the EDM process parameters. The spark on time, discharge current and spark off time were taken into consideration as input factors while surface finish, tool wear rate and metal removal rate are reaction parameters. To resolve the EDM process's multi-criteria optimization, a multi-attribute decision making (MADM) technique called the technique for order preference by similarity to ideal solution (TOPSIS) was employed. The outcomes of TOPSIS and the proper

parameters for the electrical discharge machining process were verified by researchers. Tang and Du [54] combined Taguchi methods and grey relational analysis for EDM parametric optimization. The outcomes of their study showed that the relationship between pulse width and pulse interval had the most notable influence on rate of wear of electrode, rate of removal of material and surface roughness. Hascalik and Caydas [55] studied the EDM of titanium alloy (Ti-6Al-4V) utilising graphite, electrolytic copper and aluminum electrodes, focusing on the effects of pulse current and pulse duration on surface integrity. They used SEM, XRD, EDS, and hardness analysis to evaluate their results. It was reported that as current density and pulse duration raised, the rate of material removal, surface roughness, rate of electrode wear and average width of white layer also increased. On the other hand, very long pulse lengths (200 ms) decreased surface roughness and MRR. When copper electrode was utilized, surface hardness increased as a result of Ti₂₄C₁₅ carbide production, resulting in apparent fissures in the re-solidified layer while in case of Graphite electrode; there was improvement in MRR, reduction in electrode wear, surface crack density and surface finish. Rebelo et al. [56] characterized the surface integrity of steels through a variety of experimental evaluations employed in mould manufacture after EDM. They examined metallurgical structure, surface crack networks, residual stress and surface roughness, focusing on their dependence on processing parameters. It was reported that cracks emanating from and encircling the overlapping surface craters grew in size as the machining pulse energy rose. They also came to the conclusion that greater cracks and deeper penetration in the recast layer were caused by increased machining pulse energy. Cementite, a novel phase, was detected in the white layer

through the application of microprobe analysis and x-ray diffraction. Various zones influenced by heat were noted according to the amount of machining energy and initial steel states modelled via x-ray diffraction peak broadening and x-ray diffraction accurately determined high tensile residual stresses. ZrB₂-based composite ceramics by Nakamura et al. [57] using EDM and strength and surface roughness were evaluated. They found that strength increased and roughness decreased with decreased pulse current, duration, and duty factor. A hybrid optimization technique was employed by Dewangan et al. [58] to optimize multiple performance description of surface integrity in EDM simultaneously. They found that spark on time had the most considerable impact on surface integrity. Marichamy et al. [59] utilized the Taguchi method to optimize electrical discharge machining parameters for duplex brass plates, identifying peak current as a significant factor affecting material removal rates and surface roughness. Kumar et al. [60] investigated the impact of EDM parameters on Al-B₄C composite machining, finding that current and electrode material significantly affected MRR, EWR, and SR. A kriging model and particle swarm optimization was utilized by Dang et al. [61] to determine optimal EDM conditions for maximizing MRR and minimizing EWR while controlling SR. Their results highlighted the complex relationship between parameters and responses. Baghel et al. [62] developed a model for predicting MRR during diamond grinding assisted EDM of ceramic composites, highlighting the influence of process factors on surface features and contours and removal rate of material. Mahdeih et al. [63] examined ultra-fine-grained aluminium machined using EDM and observed the effects of machining factors on surface characteristics and quality. In a study by Phan et al. [64], the optimization in vibration assisted electrical

discharge machining of high carbon silicon tool steel was performed using Taguchi–TOPSIS computational approach, showing improvements in quality factors. Researchers have published similar studies on the use of multi-criteria decision making techniques such as Taguchi based Data Envelopment Analysis based Ranking (DEAR) and Taguchi-grey analysis, as well as vibration aided machining of silicon-based steel [65, 66]. Maradia et al. [67] optimized EDM drilling parameters using the E-smeshing technique, finding significant impacts on drilling time and electrode wear. Dikshit et al. [68] optimized die-sinking EDM machining of Inconel 625 utilising central composite design, observing the significance of factors on rate of material removal and surface finish. Chakraborty et al. [69] studied wire EDM of Ti6Al4V with a powder mixed dielectric, identifying significant impacts of dielectric type and powder addition on machining performance. The surface characterization of DSS-2205 alloy machined via EDM with different electrode materials was carried out by Ablyaz et al. [70], highlighting the influence of process factors on the rate of material removal and surface finish. Viswanth et al. [71] investigated the impact of pongamia green dielectric in EDM, optimizing process variables to enhance MRR while minimizing EWR and SR. Their study provided insights into the significance of various factors on machining performance.

2.5 PERFORMANCE ANALYSIS AND IMPROVEMENT

To boost the operational competence of Electrical Discharge Machining, Kliuev et al. [72] merged the drilling and shaping processes of holes used for cooling with diffusers in the blades of turbine, utilizing a unified tool electrode. They noticed a 20% drop in the electrode wear rate and an enhancement in the rate of material

removal. Additionally, a reduction in the white layer and surface roughness was noted when this integrated drilling and shaping method was employed.

The use of copper, brass, and copper tungsten electrodes for drilling Inconel 718 was compared in a study on the machining performance of hybrid EDM by Ahmed et al. [73]. They reported that the highest rate of removal of material was achieved while using a brass electrode, followed by copper (Cu) and copper tungsten (CuW) electrodes at all chosen current settings. But when employing a copper tungsten electrode, followed by brass and copper electrodes, the rate of electrode wear was lowest. Additionally, they noticed that when using copper (Cu) and brass electrodes instead of copper tungsten (CuW) electrodes, the machined surface quality was higher. Chuvaree and Kanlayasiri [74] introduced an innovative flushing technique for EDM in deep hole processes. They created a tool electrode that is especially intended to facilitate the removal of debris from the machining gap, resulting in stable and effective cutting. The study demonstrated that the tool electrode having feature of interior flushing and multi holes integrated interior flushing were more effective compared to side flushing. Results showed that using a multi-hole interior flushing electrode reduced machining time by 26.10% (for a depth of 50 mm). Additionally, even though the surface roughness (Ra) increased by 58.04%, the Material Removal Rate (MRR) increased by 35.28% when electrode rotation and multi-hole interior flushing were applied. The influence of electrode shape on the performance of die sinking EDM was reported by Khan et al. [75]. Using mild steel work material and copper electrodes, they examined the effects of electrode shape on electrode wear rate, rate of material removal, ratio of electrode wear and average surface finish. According to the study, electrodes with a round form had the highest

MRR, followed by electrodes with square, triangular, and diamond shapes. However, diamond-shaped electrodes showed the highest EWR and WR. Regarding surface roughness, round electrodes demonstrated the lowest roughness, subsequently by square, triangular, and diamond-shaped electrodes, although the significance of electrode shape over surface roughness was deemed inconsequential. The electrical discharge machining of metal matrix composites supplemented with particles and employing a hexagonal electrode with a through hole was studied by Lin et al. [76]. They observed better performance, which they attributed to a wider debris gap during discharge. The study found that current had the biggest impact on machining performance followed by flushing pressure and duty cycle. In a related work, Nair et al. [77] machined Ti6Al4V using brass as the electrode and negative polarity, analyzing the impact of input parameters on machining efficiency. They found that longer discharge times and higher currents resulted in thicker recast layers, faster rates of material loss, and rougher surfaces. An experimental study was conducted by Bozdana and Ulutas [78] on the EDM process for creating blind and through holes over Inconel 718. They used tubular brass electrodes with different channel configurations. The study revealed that the utilization of multi-channel electrodes for drilling holes resulted in superior outcomes including reduced drilling time, enhanced dimensional accuracy and increased surface quality. Chern and Chuang [79] implemented vibration-EDM using a vibrating worktable for micro-punching machining. They reported that micro-EDM with vibration machining achieved increased feed rates and improved surface finishes. Circular and noncircular micro-electrodes were produced using vibration-EDM, and experiments to punch micro-

holes on stainless steel and brass strips yielded successful results. Furthermore, the study investigated the influence of factors on the quality of punched micro holes.

In a study by Khan [80], the analysis of electrode wear across both the cross-section and the length of the electrode during EDM of aluminium and mild steel using copper and brass electrodes were done. The study revealed that electrode wear increased with an increase in both voltage as well as current, wearing throughout the cross-section being more pronounced. The brass electrode exhibited the highest wear ratio during steel machining, whereas the maximum rate of material removal was reported when machining of aluminium was carried out using brass electrodes. Li et al. [81] investigated the influence of flushing techniques on machining performance indices using experiments and simulations. They observed that a clustered electrode with multiple inner holes for flushing led to increased material removal rates and a higher relative tool wear ratio, attributed to a more efficient flushing process.

Syed and Palaniyandi [82] conducted experimental investigations on adding aluminium metal powder to dielectric fluid in EDM. They used Taguchi design of experiments to vary parameters and measured performance in terms of rate of material removal, wear ratio of electrode, average surface finish, and thickness of white layer. This study highlighted the significant impact of polarity on machining performance. Yilmaz and Okka [83] undertook a relative experimental study on EDM drilling of aerospace alloys. They conducted a comparison between tubular electrodes constructed of brass and copper examining both single-channel and multi-channel designs to investigate the effects of electrode type and material. The investigation unveiled that single-channel electrodes exhibited superior rates of material removal and lower ratios of electrode wear whereas electrodes with many

channels yielded improved surface finishes for both aerospace alloys. The micro machining of copper plates was performed by Weng and Her [84] using EDM with electrodes of tungsten carbide. They experimented with micro-scale hole and slot cutting on a conventional CNC-EDM machine, successfully completing the processes. To enhance productivity in micro part manufacturing via EDM, they investigated a batch production method utilizing multi-electrodes, developing a new technique for preparing such electrodes. Results indicated the feasibility of batch production using EDM and highlighted the effectiveness of batch production with multi-electrodes. The investigation of the impact of machined holes on flushing efficiency in EDM was carried out by Flano et al. [85]. They proposed different configurations and their performance were evaluated in terms of time of machining and electrode wear. Notably, continuous pockets or open holes outperformed separated or closed holes. Furthermore, they observed a notable alteration in the material removal rate when empty spaces of holes were drilled within the slot, offering deeper insights into EDM phenomena. Employing their suggested electrode reduced processing time by as much as 65% when machining slots with a depth of 10 mm, with machining stability guaranteed if flushing pockets extended throughout the entire depth. Puri and Gohil [86] provided an experimental analysis of how EDM parameters affect material removal rate in EDM turning of titanium alloy Ti-6Al-4V. They employed Taguchi's DoE technique, developing a numerical model for rate of removal of material through regression analysis and analyzing factor effects using ANOVA. SN ratio analysis helped to identify optimal conditions.

An experimental study on EDM milling in a gaseous environment was conducted by Li et al. [87], incorporating electrode wear compensation and finish machining

techniques. They compared dry EDM milling (EDMM) with compressed air and kerosene, demonstrating higher processing precision in dry EDMM due to low electrode wear. They suggested a method for segmental machining decomposition that tackles electrode wear compensation and finishing aspects, achieving finish machining with reduced accumulative error and easy operation. Moarrefzadeh [88] established mathematical interactions between input and output process factors of EDM using regression methods, employing Genetic algorithm for optimal parameter determination. They conducted numerical simulations in ANSYS software to study the thermal profile and optimize process parameters, revealing non-Gaussian distributions of arc pressure, current density, and heat transfer at the workpiece surface. Electrical discharge machining of carbon nanofibre (CNF) for field emission display (FED) applications was introduced by Kim et al. [89]. They used EDM to planarize CNFs, conducting the process in air to prevent contamination. Machining characteristics were studied with varying capacitance and voltage to improve the uniformity of CNF field emission. Liu et al. [90] investigated the impact of pulse shapes of EDM discharge over material removal mechanisms and process performance of Silicon nitride. They noted significant variations in material removal and identified diverse material removal mechanisms depending on the pulse shape used. A strategy was devised for manufacturing ceramic components in Silicon nitride, and its efficacy was confirmed through the fabrication of a high-temperature mesoscopic gas turbine. Egashira et al. [91] explored the potential of electrical discharge machining with extremely small amount of discharge energy, achieving machining at voltages lower than 15V with maximum energy of discharge per pulse as small as approximately to 3 nJ. They utilized an RC discharge circuit and

ultrasonically vibrated workpieces to prevent short-circuiting and debris accumulation, resulting in smooth surfaces free of observable discharge craters.

A fundamental investigation into electrical discharge machining was conducted by Shankar et al. [92] with a focus on understanding the behaviour of an arc and theory of heat transfer. They employed the finite element method to simultaneously solve the field equations involved in determination of electric potential and temperature in the spark region. They iteratively changed the arc radii at various cross-sections until convergence was attained using the condition of steady current at any cross-section of a spark. It was reported that the generated spark form was non-cylindrical and had variable radii at various cross-sections. Moreover, they conducted calculations to determine the proportion of heat put in absorbed by the anode, cathode and dielectric. They then compared the calculated relative electrode wear with experimental findings. Khanra et al. [93] explored how the energy input in EDM affects the structure and composition of debris produced during machining. They employed a Zirconium diboride-copper composite as the tool and mild steel plate as the workpiece material, all within a kerosene medium. Analysis using SEM/EDS of various debris particles unveiled that low EDM energy input produced smaller particles with limited satellites, whereas high energy input led to the formation of hollow spheres with dents, surface cracks and burnt core structures. To investigate the effects of pulsed current on electrode wear, surface finish, diametral overcut, and material removal rate in EN-31 tool steel EDM, an experimental study was performed by Singh et al. [94]. They adjusted the pulsed current with opposite polarity while performing machining operations with various electrodes. The results

showed that when pulsed current increased, EDM output characteristics increased as well, with copper and aluminium electrodes showing the best machining speeds.

Lee et al. [95] presented a study on electrical discharge machining of D2 and H13 tool steels using tool electrodes of varying diameters. In order to investigate surface cracking influenced by electrode size, EDM settings, and material thermal conductivity, the idea of a Crack Critical Line (CCL) was established. Results revealed that the distribution of surface crack was affected by machining factors and diameter of electrodes, with cracks less likely to appear at reduced current pulse and increased pulse on duration. The effects of steel type on surface integrity of EDM using hardenable and non-hardenable steels was studied by Ghanem et al. [96]. EDM resulted in three layers in hardenable steels while non-hardenable steels showed formation of a recast layer with dendritic structure. Metallurgical changes in hardenable steels near the surface resulted in hardening and the development of high tensile residual stress, which contributed to crack formation. In contrast, non-hardenable steels showed minimal structural alterations. A finite element model was created by Yadav et al. [97] to calculate the temperature field and thermal stresses brought on by Gaussian distributed heat flux during EDM. They analyzed the effects of process variables on temperature and thermal stress distributions, displaying areas with high temperature gradients and zones experiencing substantial stresses, occasionally surpassing the material's yield strength. Shen et al. [98] introduced a novel machining technique termed high-speed dry electrical discharge milling (EDM) and contrasted it with liquid dielectric EDM. They investigated microscopic features like surface roughness, white layer thickness, micro-hardness, cracks, and voids in machined Inconel 718. Results indicated that high-speed dry EDM milling

yielded better surface finish, thinner white layers, and fewer cracks as compared to liquid dielectric EDM. The influence of a range of dielectric fluids over the performance of electrical discharge machining was examined by Li et al. [99] during the drilling of Nickel alloy. Four dielectric fluids were selected, and their impact on surface integrity was analyzed. According to the results, kerosene was a far better dielectric fluid than water-based dielectrics, emulsions, and de-ionized water in terms of reducing the creation of recast layers. Furthermore, several other studies have investigated the effects of dielectric fluids in EDM across different EDM variants [100-103]. Amorim et al. [104] investigated electrical discharge machining utilizing dielectric fluid comprising of suspended powder particles, revealing considerable enhancements in stability of the process and surface finish of EDM-machined components. The study delved into the powder-mixed EDM (PMEDM) process to generate a resolidified layer, serving as a coating with better mechanical properties compared to the base material. Various sizes of fine molybdenum powder particles suspended in dielectric fluid were explored across various EDM finishing conditions and machining durations, focusing on surface modification of AISI H13 tool steel. Samples underwent assessment for chemical composition, hardness and microstructure employing optical microscopy, energy-dispersive spectrometry, scanning electron microscopy, nano indentation as well as X-ray diffraction. Results revealed an improvement of the modified surface layer with molybdenum, leading to the formation of Iron-Molybdenum and Molybdenum Carbide phases, alongside solid solution consisting of molybdenum, resulting in a fourfold increase in hardness compared to the metal matrix. Optimal outcomes were attained with discharge current of 1A and particle sizes less than 15 μm , yielding a Mo-enriched, uniformly

modified layer with a hardness of 14 GPa and a consistent 5 μm thickness, lacking of pores and cracks. Machining durations exhibited negligible effects on the character of the resolidified layer. The study provided pivotal factors for the PMEDM process utilizing Mo to enhance surface mechanical properties. Marashi et al. [105] enhanced the surface features of machined steel of AISI D2 grade with EDM by introducing titanium nano powder into the dielectric fluid under a range of machining factors such as peak current and discharge duration. Surface profilometry, AFM and FESEM analyses were employed to evaluate surface roughness, morphology, and micro-defects. EDX analysis assessed the Ti nano-powder deposition on the surface, while ESEM and EDX examined the Ti nano-powder concentration in the dielectric. Results indicated a significant enhancement in surface morphology and roughness when Ti nano-powder was added under all machining factors except T_{on} of 340 μs . The most notable improvement occurred at T_{on} of 210 μs , where there was improvement of approximately 69% in removal rate of material and 35% in average surface roughness approximately for peak currents of value 6 ampere and 12 ampere respectively. The elemental analysis suggested minimal deposition of Ti on the machined surface, while increased concentration of Ti was observed around the areas of crack. A novel electric discharge machining method was introduced by Upadhyay et al. [106] that utilizes magneto-rheological fluid as a substitute of traditional oil such as kerosene. This study aimed to identify process factors affecting removal rate of material in this new EDM process. This approach of hybrid machining approach offered enhanced surface quality and cutting efficiency owing to the viscoelastic nature of MR fluid, which provides polishing effects and high material removal rates. Experimentation revealed the effects of discharge current, duty cycle, pulse duration,

alumina particle concentration over surface roughness and MRR leading to significant enhancements in surface finish and material removal rate. It was found that combining EDM with magneto-rheological fluid results in increase in rate of removal of material and improvement in surface finish considerably within a definite limit of carbonyl iron percentage in the magneto-rheological fluid. A hybrid technique that combines abrasive jet machining and electrical discharge machining in gas was investigated by Lin et al. [107]. For tool steel of SKD 61 grade, they used a Taguchi-based L18 orthogonal array to optimize process parameters such peak current, machining polarity, pulse duration, grain size, gas pressure, and servo reference voltage. In order to determine the significant machining parameters influencing rate of electrode wear, rate of material removal and surface finish, response data were analysed using signal-to-noise ratios and ANOVA. Response plots of signal-to-noise ratios were used to evaluate the most advantageous combination of machining factors. The outcomes revealed considerable parameters influencing MRR, EWR, and SR, with enhancements in S/N ratios at optimal parameter levels, thereby improving machining efficiency for modern manufacturing applications. Using a variety of dielectrics as working fluids, Zhang et al. [108] closely examined the material removal behaviours in electrical discharge machining. They looked at kerosene, de-ionized water, oxygen, air and water-in-oil emulsion as five different kinds of dielectrics. Metallographic methods were utilized to ascertain the crater's geometrical parameters, taking into account of the recast material. The study conducted a comparative analysis of the volume of removed material, along with the efficiency of removal across various dielectrics. The researchers established correlations between material removal behaviours and the evolution of bubbles

generated through discharge in various dielectrics, utilizing computer simulation. The findings underscored the significant influence of pressure above the discharge point on material removal characteristics. This investigation is expected to improve comprehension of the intricate process of material removal of electrical discharge machining. The optimization of the rate at which material is removed and the rate at which the tool wears in powder mixed electrical discharge machining (EDM) of Inconel-800 was investigated by Kumar et al. [109]. The impact of three types of micro powder particles and three electrodes for testing were investigated, along with a number of other input elements such as peak current, spark off time, tool, spark on time as well as powder materials. The experimental design was conducted using the Response Surface Methodology (RSM) box-Behnken approach, while the multi response measure optimization was carried out using the Desirability Approach. Using ANOVA, the validity of predicted mathematical models was evaluated. Electron microscopy, energy dispersive spectroscopy and X-ray diffraction were employed to analyze the microstructure and the effects of different factors on the machined surface. The results showed that peak current, tool material, pulse on-time, and powder material all had a significant influence on the rate of removal of material while peak current, tool material, pulse on-time, and tool material also had an impact on the rate of wear of tool. The rate of removal of material was impacted by powder particles, however the rate of wear of tool and removal of material was unaffected by pulse off-time. Employing the approach of desirability, the optimal parameter arrangement was determined to be a current of value of 1 A, pulse on-time of value of 0.98 μ s, 0.03 μ s as pulse off time, tool material of 0.31, and suspended particles of 0.64. Additionally, the oil was mixed with micro powders to act as a dielectric,

which enhanced the machined profile's stability and surface finish [110]. Tamang et al. [111] conducted an experimental analysis and parametric optimization of the electrical discharge machining (EDM) process to produce micro holes with a diameter of 500 μm on stainless steel (grade 304). The study considered process parameters such as current (I), spark on time (T_{on}) and gap voltage (V) which were optimized to enhance hole quality, specifically focusing on taper angle and overcut. Statistical regression models were proposed to predict taper angle and overcut, and the influence of the parameters were analyzed through plots. Best possible parameters were determined for both single and multiple performance characteristics. Taguchi analysis was employed to optimize each objective individually, and the results were compared with desirability analysis. The optimal parameter combination identified through ANOVA with the maximum signal-to-noise ratio for 10 A for current, 50 V for gap voltage, and 150 μs for pulse on time, resulting in enhanced quality of hole with minimal taper angle and overcut. This outcome closely matched the findings of the desirability analysis. Rotating curvilinear electrodes and Reuleaux Triangle-guided tool paths were utilized by Ziada et al. [112] to fabricate polygons with sharp corners in sinking EDM. Their approach aimed to enhance flushing through the discharge gap and maximize the frontal area of the tool by rotating and translating the electrode during machining. Gu et al. [113] investigated the utilization of bundled electrodes with a multi-hole inner flushing technique for machining Ti6Al4V using die sinking EDM. They noted that this technique allowed for rough machining over wider areas, resulting in decreased wear of electrode and enhanced material removal rate. In a similar investigation, Singh et al. [114] documented that employing argon gas-perforated tool assistance in electrical discharge machining

resulted in decreased electrode wear rates and smoother machined surfaces compared to methods involving air assistance and solid rotary tools. Tanjilul et al. [115] introduced a debris removal system for deep hole EDM drilling, which combined simultaneous flushing and vacuum assistance to enhance the flushing and debris removal process. Their research unveiled enhancements in drilling time and surface roughness of the produced holes. Additionally, they created a computational fluid dynamics (CFD) model to analyze the system's performance. Furthermore, various researchers have utilized micro-EDM, a micro-level variant of EDM, to fabricate micro holes and channels using diverse tool and work electrode materials [116-119]. Multiple studies have employed micro-EDM and micro-Electrical discharge milling to fabricate different geometries and assess the process behaviour and machining performance involved. For example, a mist of deionized water jet was used by Li et al. [120] to achieve high-precision and rapid machining of deep micro holes while enhancing debris removal. The effectiveness of micro-EDM in creating straight micro holes with exact edges was demonstrated through the investigation of the effect of input factors on the rate of material removal, overcut and machining time, including capacitance, feed rate, and voltage by Singh et al. [121]. In their analysis of the form, shape as well as surface characteristics of channels created through micro-EDM milling, Karthikeyan et al. [122] found that redeposition is affected by the rotational motion of the tool. In order to produce micro holes, channels and different geometries, Vidya et al. [123] used micro-EDM milling. They assessed the machining performance in terms of surface integrity, shape error and surface characteristics. They came to the conclusion that while cavities of triangular shape show the best surface finish, circular holes exhibit higher dimensional accuracy.

They also found that the rotation of the tool had a substantial impact on surface quality, causing globule development, formation of recast layers and the movement of eroded particles. Furthermore, several researches have explored technologies aimed at improving the performance of micro-EDM in micro-hole drilling [124-127]. Meshram et al. [128] introduced the curved EDM process for producing curved channels, noting improved machining efficiency through optimization, using both solid and hollow electrodes. A ranking method based on data envelopment analysis was employed by Phan et al. [129] to apply Decision-making involving multiple criteria in the machining process of SKD61 die steel, focusing on optimizing process factors like pulse current, voltage and spark-on-time in EDM to enhance surface finish and rate of material removal. Paswan et al. [130] investigated the use of highly carbonated liquid as a dielectric medium in EDM, observing increased removal rate of material and significant material removal from the workpiece compared to traditional EDM oil. They noted the influence of process factors on EDM and their impact on surface morphology and micro-crack density. Additionally, Jiang et al. [131] considered the use of a Cu-Ni electrode for machining polycrystalline diamond (PCD) using a dielectric containing suspended graphene powder. Their findings highlighted significant enhancements in material removal rate and surface quality compared to conventional EDM techniques.

2.6 TOLERANCE ANALYSIS

Research on tolerance analysis has extensively examined parameters such as roundness, flatness, and straightness using various methodologies. Selvarajan et al. [132] conducted an experimental investigation on electrical discharge machining of a

Silicon nitride ceramic composite, employing copper as a electrode. They noted the challenging machinability of Si₃N₄-TiN composite with conventional methods but found that spark EDM facilitated precise geometric and dimensional tolerances. Analysis of machining factors like spark on time, spark off time, current, spark gap voltage and the pressure of dielectric revealed their significant influence on output characteristics. Optimization using Taguchi L25 orthogonal array and grey relational analysis showed pulse on time, current and spark gap voltage as key factors affecting output characteristics, which were confirmed through experiments.

A novel approach using twin support vector machines (TWSVMs) was proposed by Liu et al. [133] to evaluate roundness error. Their method demonstrated effectiveness and accuracy in roundness error assessment, with potential for online evaluation in industrial processing to enhance efficiency. Exponential penalty function and Primal-dual interior point method algorithms were employed by Arezki et al. [134] for aspheres minimum zone fitting and finding precise minimum zone values. It was concluded that the primal-dual interior point method algorithm exhibited decreased performance with increased data points. Rossi et al. [135] presented a hardware design utilizing distributed control logic and multi-gigabit transmission, enabling rapid data transfer and synchronization. The improved minimum zone circle (IMZC) method was developed by Li et al. [136] which utilized convex hull theory for roundness error assessment, demonstrating higher precision and reduced computation time compared to traditional methods. Nagahanumaiah et al. [137] investigated achievable form tolerance using direct rapid tooling methods, DMLS and SLA, highlighting SLA's better dimensional accuracy but relatively poor form accuracy compared to DMLS.

2.7 GAPS IN LITERATURE

While research on micro machining using EDM continues to pose challenges, the majority of studies conducted thus far have focused on effects of machining parameters and optimization, material removal mechanism, plasma characterization, influence of different dielectric, performance analysis and process improvement rather than the micro machining of polygonal shapes. After reviewing the existing literature, several gaps in knowledge have been identified:

- **Limited information on fabrication of different shapes:** The literature provides limited details regarding the fabrication of different shapes including polygonal shapes using EDM. Identifying and applying the methodology to produce polygonal microcavities is crucial for developing engineering solutions for generating macro and micro structures and analysing the physical behaviour of EDM machining.
- **Inadequate reporting of machining performance of EDM in production of different micro cavities:** Few researchers have reported a comprehensive study of performance of die-sinking EDM in the machining of different cavities. A deeper understanding of the shape discrepancies, tool wear rates, the formation of recast layers, the occurrence of micro cracks and elemental characterization is important to establish the guidelines and optimize the process.
- **Limited reporting of parametric analysis of EDM in machining of polygonal cavities:** There is a scarcity of comprehensive studies on the impact of EDM parameters over the quality of surface of machined cavities

with different shapes. It is essential to understand the interaction of parameters with performance measures to improve the overall machining efficiency by selection of optimized parameters.

Hence, this research is motivated by the urge to develop engineering solutions by generating cavities of various shapes and analyzing the behaviour of EDM machining in fabrication of these structures.

2.8 PROBLEM STATEMENT AND OBJECTIVE OF THE RESEARCH WORK

The research aims to address the current research gaps and challenges in the field of die-sinking EDM of different shapes including polygonal cavities on micro scale by conducting a comprehensive investigation into the application of this technique. The problem is formulated as follows:

“INVESTIGATIONS ON PART GEOMETRY AND SURFACE FINISH BY ELECTRICAL DISCHARGE MACHINING (EDM)”

The present research problem aims to accomplish the following objectives:

- To evaluate the dimensional accuracy of the shapes generated for different geometries
- To study the tool wear
- To investigate the overcut and recast layer
- To analyze the part geometry and surface finish

CHAPTER 3

METHODOLOGY AND EXPERIMENTATION

3.1 INTRODUCTION

Electrical Discharge Machining (EDM) of polygonal micro cavities in EN24 alloy steel presents significant challenges due to the material's high strength and elevated softening temperature. Conducting these experiments requires a carefully designed setup capable of handling the entire EDM process efficiently.

The experimental setup must include a robust EDM machine that can withstand the substantial forces involved in machining and provide precise control over discharge parameters. A secure fixture system is essential to firmly hold the EN24 alloy steel workpiece in place during machining.

EDM generates high temperatures, which can impact the machine's components and the dielectric fluid system. Proper cooling and insulation mechanisms are necessary to protect the machine and maintain process integrity. A reliable tool holder is crucial to securely hold the electrode and prevent slippage during discharge.

Selecting the appropriate electrode material is critical for machining EN24 alloy steel, as it directly affects machining performance and electrode wear. To ensure effective experimentation, it is important to choose an electrode material that offers optimal results and a sufficient lifespan. Additionally, a facility to swiftly produce electrodes with the required dimensions is necessary to support extensive trial runs.

3.2 METHODOLOGY

To achieve the objective of fabrication of microcavities of different shapes, the study started with the selection of tool and work material followed by the selection of machine tool, machining parameters and dimensions. The fabrication step started with the machining of the desired micro-scale patterns using a copper tool electrode with a diameter of 400 microns to perform the die-sinking EDM process on an alloy steel EN-24 workpiece. The resulting patterned samples were then subjected to dimensional measurement using a profile projector, and the standard deviation was estimated to assess their dimensional stability. Next, SEM and optical microscope examinations were conducted to study the formation of the recast layer and other surface features, including their shapes and the additional effects of the discharge pattern. Surface roughness testing machine was used to estimate profile uniformity. The achievable tolerances were calculated by collecting data from different locations of geometries using Olympus analysis five software and the profile projector. Figure 3.1 portrays the flowchart of the methodology involved.

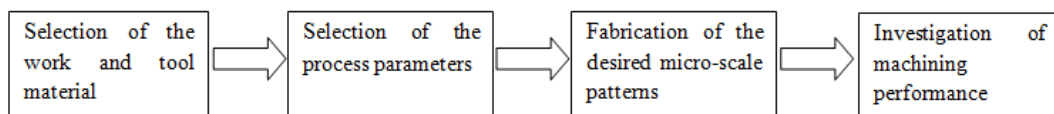


Figure 3.1: Flowchart of the Methodology

3.3 DIE-SINKING EDM TOOL AND ITS PERIPHERALS

Figure 3.2 shows the Die-sinking EDM Machine Tool, Model: Electronica XPERT-1 having accuracy of 0.01 mm accuracy and programmable frontal wear compensation cycle. This machine tool is equipped with CNC-controlled movement of axes and a

power supply unit consisting of electronic pulses (e-pulse 50 CNC), enabling the creation of intricate micro-scale structures with intricate tool path trajectories.

Features:

1. The erosion axes (X, Y, Z) are programmable
2. The monitor displays information and data
3. The machine tool features a 3-axis display of both actual and commanded positions, utilizing incremental encoders to achieve accuracy up to 0.001 mm
4. An External Machine Control Unit (MCU) is included in the machine tool
5. The machine tool provides assistance for G and M codes
6. Programmable Auto Flushing to enhance machining stability
7. The machine tool includes Programmable Auto Flushing, which helps to enhance machining stability
8. The machine tool supports serial data transfer of technology and programs via a serial mode
9. The machine tool offers an optional C-axis which serves as a rotating electrode device. This C-axis can be used for internal and external threading, indexing of electrodes, and cutting internal grooves
10. The machine tool also offers an optional automatic tool changer, which enables automatic electrode changing through a program
11. The machine tool is integrated with a software called Assist, which is a unique part programming software that guides the operator step by step in programming simple as well as complex cavities without requiring knowledge of G and M codes.

12. Unattended operation
13. Orbiting cycles can improve flushing conditions, preventing arcing and reducing the number of electrodes needed, while also maintaining dimensional uniformity of jobs
14. The machine tool has a programmable frontal wear compensation cycle, which helps to maintain the accuracy of machining by adjusting the tool electrode wear.

3.4 MATERIAL SELECTION

Workpiece material: The experiment utilizes a workpiece made of EN-24 alloy steel with dimensions of 100 mm × 100 mm x 15 mm, as depicted in Figure 3.3. EN-24 is a through-hardening alloy steel with excellent machinability in the "T" condition, which is commonly used in components such as gears, shafts, studs and bolts. The chemical composition of the workpiece material has been confirmed through spectroscopic analysis which has been represented in Table 3.1. EN24T can be further surface hardened using induction or nitriding processing to improve wear resistance. It has a tensile strength of 850-1000 N/mm² and a hardness of 248 HB.

Tool electrode material: A tool electrode of length 50 mm with a diameter of 400 μm is utilized, consisting of a cylindrical rod made of copper. Generally copper and its alloys are widely used as an electrode due to its high conductivity and low cost. Table 3.2 outlines the physical characteristics of the copper tool electrode.



Figure 3.2: EDM Xpert-1 Tool

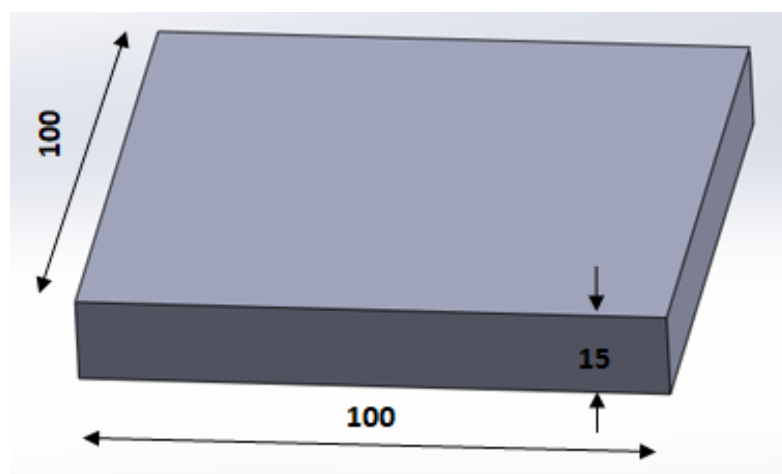


Figure 3.3: Dimensional Representation of Workpiece (in mm)

Table 3.1: Composition of EN-24 Alloy Steel

Elements	Percentage
Iron	96.0775
Nickel	1.35
Chromium	1.01
Manganese	0.601
Carbon	0.388
Silicon	0.302
Molybdenum	0.288
Phosphorus	0.0226
Sulphur	0.0209

Table 3.2: Properties of Tool Electrode

Properties	Values
Density	8.96 g/cm ³
Hardness	30-100 (Vickers)
Melting point	1085 °C
Thermal expansion coefficient	16.5 µm/m-K
Thermal conductivity	401 W/m-K

Dielectric fluid: During the machining process, the dielectric fluid employed is EDM oil, specifically IPOL SEO 450. This fluid is created using top-grade, low-aromatic hydrocarbon base stocks that have been carefully chosen. It is designed to possess the ideal viscosity to enable efficient EDM operation while minimizing electrode wear. Additionally, it is virtually colourless, and its low aromatic content promotes a reduction in odours and fumes. IPOL SEO 450 is highly recommended for use in electric discharge machining where a high degree of accuracy and precision is necessary.

Features:

1. This is a product that has been carefully selected for its narrow boiling range and is suitable for spark erosion
2. The low viscosity of this product provides excellent flushing and settling of metal fines and the higher flash point promotes better work safety
3. The negligible amount of aromatics in this product enhances safety and is beneficial for the environment
4. The acceptable odour of this product leads to greater acceptance
5. It has a long-lasting transparency that ensures clear operation and is non-corrosive and prolongs the life of the electrode
6. The excellent oxidation stability of this product guarantees a longer fluid life and the high dielectric strength of this product enhances precision and improves control over sparking.

3.5 MACHINING PARAMETERS

The gap voltage (V), pulse / spark on time (T_{ON}), pulse / spark off time (T_{OFF}), current (I), polarity, threshold and feed rate are the machining parameters that have been selected based on the limitations of the die-sinking EDM tool in micro machining. According to the machine operating instructions, the workpiece was kept negative and the tool electrode was kept positive in order to establish polarity [138], which leads to a higher rate of removal of material, lower rate of wear of tool and improved surface finish. A lower threshold value was chosen to ensure sensitivity in detecting short circuiting [139]. The appropriate machining parameters are listed in Table 3.3.

Table 3.3: Common Parameters used for Machining

Parameters	Values
I	1 A
T_{ON}	5 μ s
T_{OFF}	16 μ s
V	75 V
Polarity	Tool electrode +ve

3.6 MEASUREMENTS AND ANALYSIS

Measurements and analysis is the most important part of an experiment. For this, the machined workpiece is demounted from the machine after the machining is over and prepared for measurement and analysis.

3.6.1 Dimensional Measurement and Shape error

The shape geometry of the machined micro-cavities has been examined using a Japan-made Olympus optical microscope, as shown in Figure 3.4. The microscope has five objectives with magnifications of 5x, 10x, 20x, 50x, and 100x. A digital camera, the Olympus E-330 has been installed on top of the microscope to capture images of the micro-cavities. For dimensional measurement, a Nikon Profile projector is utilized having 0.001 mm / 1 minute of arc as a least count as represented in Figure 3.5.



Figure 3.4: Olympus Optical Microscope



Figure 3.5: NIKON Profile Projector

3.6.2 Tool wear rate (TWR)

The performance measure Tool wear rate (TWR) is evaluated to determine the volumetric material removed tool electrode, respectively. To calculate TWR, the length of the eroded tool, diameter of the tool electrode and machining time are determined using Equation (3.1). To measure the tool's eroding length, an electrical contact was made to a fixed spot both before and after machining.

$$\text{TWR} = \frac{\pi \times (\text{tool electrode diameter})^2 \times \text{length of eroded tool}}{4 \times \text{Time of machining}} \quad (3.1)$$

3.6.3 Surface roughness

The surface roughness measurement is performed using a Mitutoyo– SJ-400 contact-type Surface roughness tester, which is equipped with a diamond stylus tip and sapphire skid as shown in Figure 3.6. The instrument has a minimum resolution of $0.000125\mu\text{m}$. The cut-off length (L_c) used is 0.25 mm.

3.6.4 Surface characterization

ZEISS EVO Series Scanning Electron Microscope EVO 50 and EVO 18 is used to obtain surface characteristics of machined samples, as shown Figure 3.7. The SEM is having a maximum magnification of 50,000X with a resolution of 2 nm at 30 kV. To analyse elemental compositions, the SEM is integrated with an Energy Dispersive X-Ray Spectroscopy (EDS) attachment.



Figure 3.6: Mitutoyo Surface Roughness Tester – SJ-400



Figure 3.7: ZEISS EVO Series SEM EVO 50 and EVO 18

3.6.5 Geometric tolerance analysis

Minimum Zone circle (MZC) approach is a method for evaluating the roundness error of a machined part. It involves creating a circle that is the smallest possible size that can contain all of the measured points on the surface of the part. The difference between the radius of this circle and the nominal radius of the part is the roundness error. To calculate straightness tolerance of channels, the data obtained from Olympus Analysis Five software is used. Straightness tolerance is the measure of deviation from the perfect straight line. It can be calculated by comparing the measured data with the ideal straight line and calculating the deviation.

Finally, angularity error is measured using the profile projector. Angularity error is the difference between the actual angle of the machined part and the nominal angle. It can be calculated by measuring the angle of the machined part using the profile projector and comparing it with the nominal angle.

CHAPTER 4

RESULTS AND DISCUSSIONS

4.1 PERFORMANCE ANALYSIS IN DIE-SINKING EDM OF MICRO HOLES AND CHANNELS

The EDM process is used extensively in industries for fabricating micro-scale apparatus, devices, and micro-electro-mechanical systems (MEMS) characterized by their exceptional precision and narrower dimensional tolerances. The machining capability of EDM is increased by integrating it with short electrical pulses and CNC-controlled positioning steps, enabling the production of precise and dimensionally controlled microstructures even with minimal machining parameters.

The experiments were conducted using the Electronica Machine Tools XPERT-1 series model of EDM. The experiments started with the machining of micro holes as well as channels over alloy steel of EN-24 grade using cylindrical electrode with a diameter of 400 μ m. The EDM machining setup has been illustrated in Figure 4.1, with the workpiece positioned on the X-Y positioning table and the tool electrode fixed to the spindle. The electrode's diameter was used as a reference diameter, and the CNC-controlled tool trajectory machined microholes and channels at the selected parameters shown in Table 3.3. Table 4.1 displays the size and tool paths used in micromachining. To ensure repeatability, three micro holes and channels were created, and the average value of performance measures were recorded for further examination.

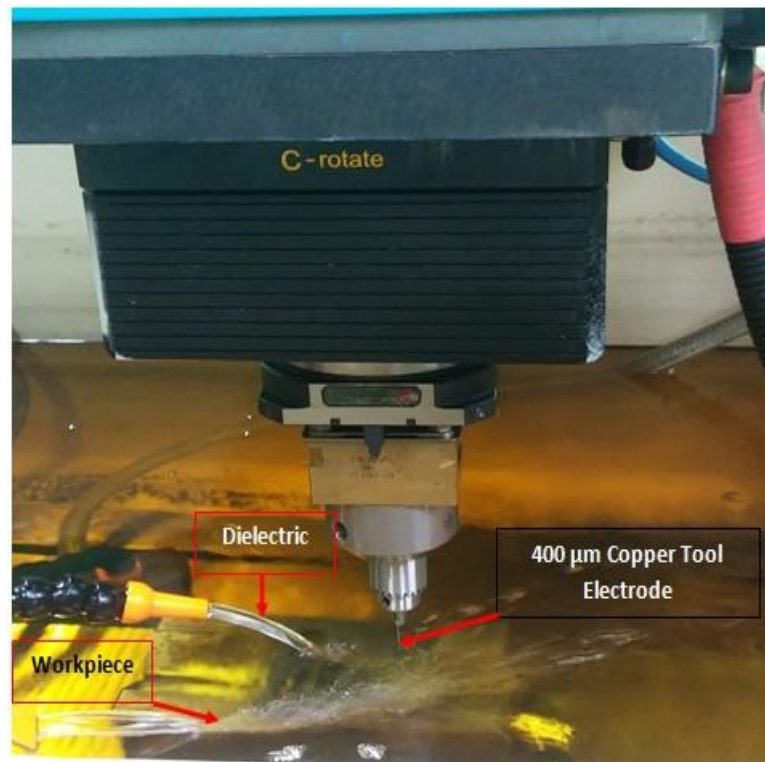
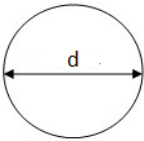

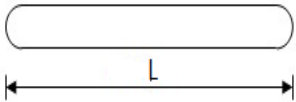
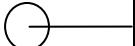


Figure 4.1: Die-sinking EDM Machining Setup

Table 4.1: Dimensions of Geometries

Geometry	Reference dimensions	Tool paths
 Circular	$d = 400\mu\text{m}$ $\text{depth} = 2000\mu\text{m}$	
 Channel	$W = 400\mu\text{m}$ $L = 2000\mu\text{m}$ $\text{depth} = 2000\mu\text{m}$	

4.1.1 Dimensional Accuracy and Shape Error

In order to examine the dimensions of the microscopic images of cavities, a profile projector with a count of no more than 0.001 mm/1 minute of arc has been used. Table 4.2 contains the values of the measured dimensions and their standard deviations from the reference dimensions. Based on estimated dimensions, it is observed that round micro holes have the lowest standard deviation of 9, the best dimensional control, whereas micro channels have rather inadequate dimensional control, with width and length standard deviations of 20.84 and 43.02, respectively. The difference between moving a tool along the Z axis just while creating holes and moving it simultaneously along the Z and X axes when creating channels might be assigned as the cause of this. As a result, the position of the spark discharge is constantly changing, which causes instability and discharge jumping.

In addition to the primary discharge happening at the tool electrode's front, there is also a secondary discharge that happens at the electrode's side due to inadequate flushing at the cavity depth is a major cause of spark leaping, short circuits, unstable spark gaps, overcuts, and recast layers. Table 4.2 shows that there is an overcut error because the machined cavities' diameters are larger than the recommended size. The microscopic images of micro holes and channels are shown in Figure 4.2. According to Figure 4.2, side discharges result in burrs at the cavity borders and absence of crisp corners (corner error) in micro channels, both of which call for the need for extra finishing operations.

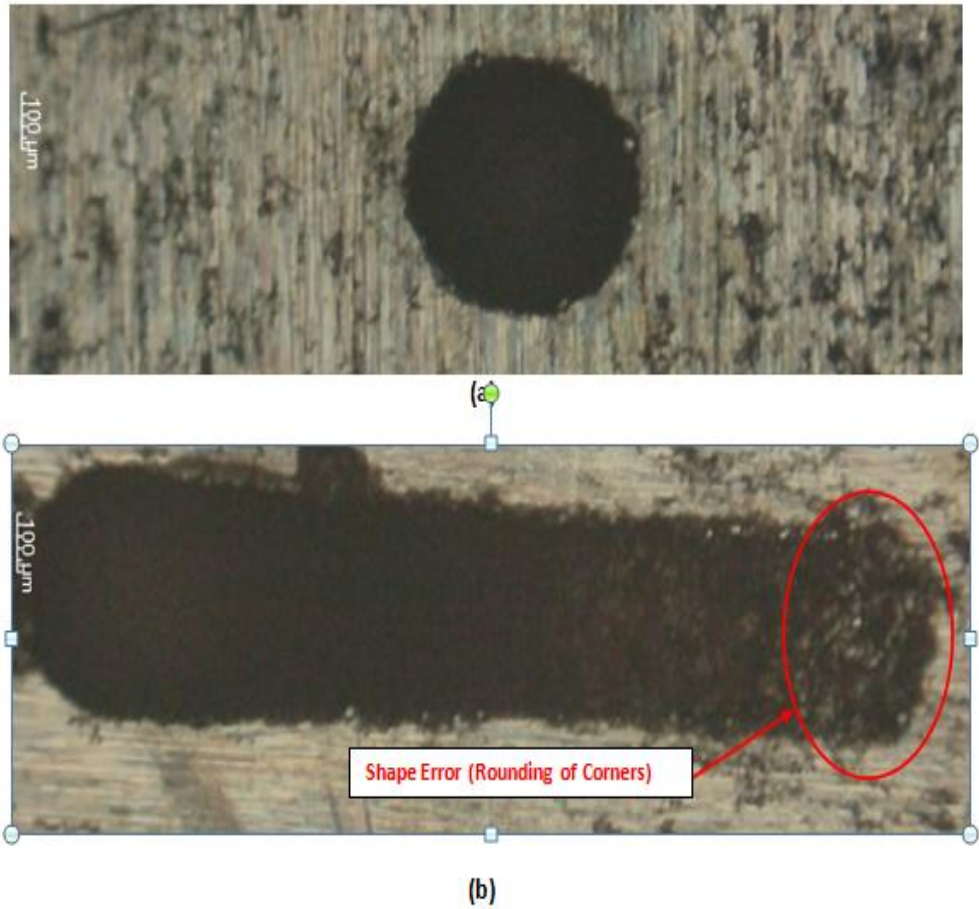


Figure 4.2: Microscopic Images (5X) of (a) Micro hole (b) Micro channel

Table 4.2: Dimensional error for micro holes and channels












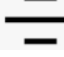


Geometries	Reference Dimension (μm)	Measured dimensions (μm)			Error		Standard deviations (S.D)
		1	2	3	Mean error (μm)	% error	
Circular	400	469	460	451	60	15 %	9
Channels	400 (width)	437	451	415	34.33	9 %	20.84
	2000 (length)	2097	2087	2018	67.33	3%	43.02

4.1.2 Geometric Tolerance Estimation

In essence, tolerances in geometry are employed to ensure that components are produced with the correct shape and form, which is critical for proper performance of the product. They are utilized in addition to the tolerances for dimensions, which control the size of a component. The most permitted deviation in shape or position from the true geometry is specified by geometric tolerances and are defined by a tolerance zone within which a surface or axis of a hole or cylinder can lie. Reference features such as planes, lines or surfaces can be developed in order to determine geometric tolerances on the drawing. The tolerance zone is then defined by specifying the relationship between the feature and the reference feature such as parallelism, perpendicularity and flatness. The tolerances are expressed using symbols.

Geometric tolerances are particularly important in the manufacturing of complex parts such as those used in aerospace or automotive industries, where tight tolerances are critical for proper fit and function. By using geometric tolerances, designers can ensure that parts will fit together properly and function as intended, reducing the need for rework or rejects and improving the overall quality of the product. Table 4.3 portrays the important geometric tolerances with their representation symbols.

Table 4.3: Geometric Characteristics Symbols [140]

TOLERANCE TYPE	CHARACTERISTIC	SYMBOL
FORM	Straightness	
	Flatness	
	Circularity (Roundness)	
	Cylindricity	
PROFILE	Profile of Line	
	Profile of Surface	
ORIENTATION	Parallelism	
	Perpendicularity	
	Angularity	
LOCATION	Position	
	Concentricity	
	Symmetry	
RUNOUT	Circular Runout	
	Total Runout	

4.1.2.1 Out of Roundness (for circular geometries)

The Minimum Circumscribed Circle (MCC), Minimum Zone Circle (MZC), Least Square Circle (LSC) and Maximum Inscribed Circle (MIC) can be used to measure roundness inaccuracy. In this study, minimum zone circle approach has been utilized to assess the roundness error. The Minimum Zone Circle method is a common approach used to assess the roundness error of a profile. To quantify the roundness error in this method, two circles are utilized as reference circles, as portrayed in Figure 4.3. The Minimum Circumscribed Circle (MCC) is one circle that is drawn outside the profile and completely encloses it. The Maximum Inscribed Circle (MIC) drawn inside the profile and only touching the profile at certain spots is the other circle. The MZC method is based on the concept that the roundness error is the difference between the radii of these two circles. The MCC represents the maximum possible deviation of the profile from a perfect circle, while the MIC represents the minimum possible deviation. The roundness error is then calculated as the difference between the radii of these two circles.

The MZC method is often preferred over other methods such as the Least Square Circle (LSC) and the Minimum Circumscribed Circle (MCC) because it is more robust to outliers and noise in the profile data. However, it should be noted that the MZC method only provides a measure of the roundness error and does not give any information about the shape of the profile or the specific features that are causing the error. For this, two tangent points on the maximum circle and two on the minimum circle are found. The process of identifying tangent points begins with locating two or three vertices spanning the maximum and minimum circles. This process is then

repeated until all points are contained within the two concentric circles. Lastly, the diameter difference between the largest (d_1) and smallest (d_2) circles is used to calculate the roundness error.

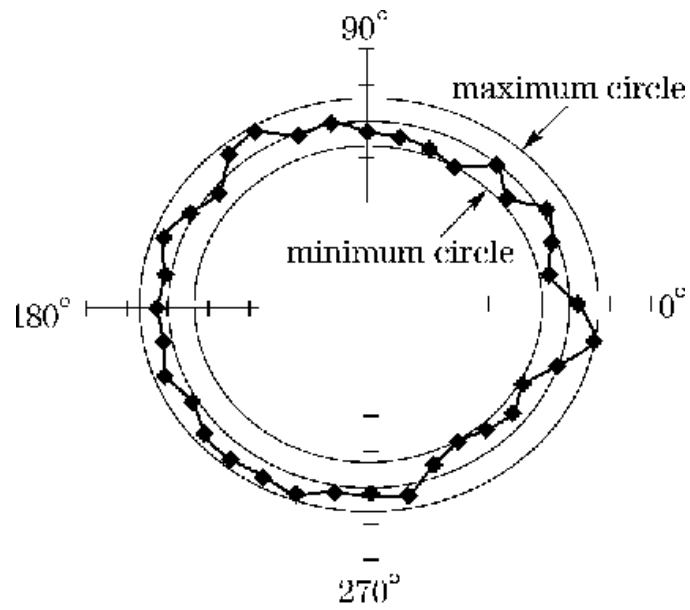


Figure 4.3: Minimum zone circle approach to find roundness error [136]

Table 4.4: Roundness Error of Micro holes

Geometry	Roundness Error (μm)	Average Roundness Error (μm)
Micro hole 1	45	46.33
Micro hole 2	41	
Micro hole 3	53	

Three circular micro holes' inaccuracy is computed independently, and the mean value is taken into consideration, as represented in Table 4.4. The roundness inaccuracy of circular micro holes is calculated to be 46.33 μm .

4.1.2.2 Straightness (for micro channels)

A straight element of a surface or an axis specifies a tolerance range that the axis or considered element must fall inside, and this requirement is known as straightness [137].

In terms of straightness, the evaluation line is:

$$y = y_0 + l_0 \quad (4.1)$$

The variation can be stated as follows::

$$e_i = y_i - (y_0 + l_0 x_i) \quad (4.2)$$

The following are the least square (LS) solutions:

$$l_0 = \frac{(N \sum x_i y_i) - \sum x_i \sum y_i}{(N \sum x_i^2) - (\sum x_i)^2} \quad (4.3)$$

$$y_0 = \frac{(\sum y_i - l_0 \sum x_i)}{N} \quad (4.4)$$

Straightness tolerance:

$$h_{\text{straightness}} = \frac{|e_{\text{MAX}(+)}| + |e_{\text{MAX}(-)}|}{\sqrt{1 + l_0^2}} \quad (4.5)$$

By utilising die-sinking EDM, three micro-channels with a total length of 2000 μm have been created in patterned form. After getting their microscopic views, dimensions are measured using Olympus Analysis Five software at ten distinct places spaced 200 μm apart (a preset spacing of X) to obtain measurement data (Y coordinates) represented in Table 4.5 for micro channel 1. The procedures for using the Olympus Analysis Five Software to analyse microscopic images are shown in

Figure 4.4. Equations (4.1), (4.2), (4.3), (4.4), and (4.5) have been used to calculate the straightness tolerance.

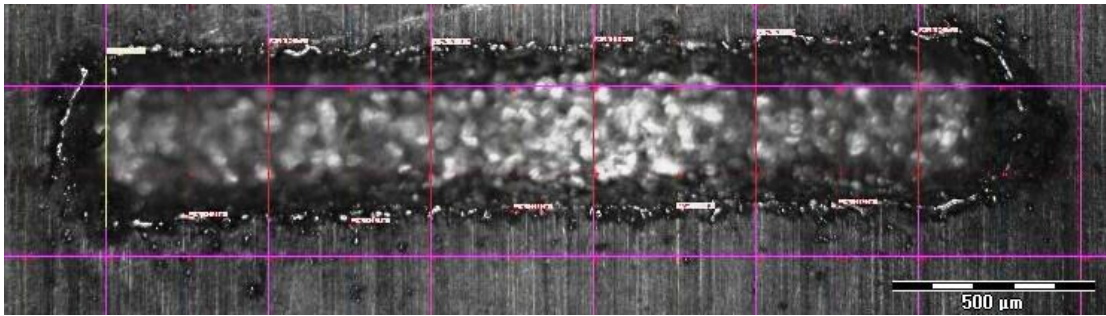


Figure 4.4: Analysis Process of Straightness of Micro channels using Olympus Analysis Five Software

For micro channel 1

Table 4.5: Dimensions of Micro-channel at different points

X (μm)	Y (measurement) (μm)	X (μm)	Y (μm)
0	431.34	1200	436.29
200	429.40	1400	426.37
400	430.52	1600	423.03
600	432.29	1800	425.49
800	434.69	2000	425.08
1000	436.96		

The LS solutions for this set are given by:

$$l_0 = [10 \times (200 \times 429.40 + 400 \times 430.52 + 600 \times 432.29 + 800 \times 434.69 + 1000 \times 436.96 + 1200 \times 436.29 + 1400 \times 426.37 + 1600 \times 423.03 + 1800 \times 425.49 + 2000 \times 425.08) - [(200 + 400 + 600 + 800 + 1000 + 1200 + 1400 + 1600 + 1800 + 2000)(429.40 + 430.52 + 432.29 + 434.69 + 436.96 + 436.29 + 426.37 + 423.03 + 425.49 + 425.08)] / [10 \times (200^2 + 400^2 + 600^2 + 800^2 + 1000^2 + 1200^2 + 1400^2 + 1600^2 + 1800^2 + 2000^2) - (200 + 400 + 600 + 800 + 1000 + 1200 + 1400 + 1600 + 1800 + 2000)^2]$$

$$l_0 = 0.004425 \text{ and}$$

$$y_0 = [(429.40 + 430.52 + 432.29 + 434.69 + 436.96 + 436.29 + 426.37 + 423.03 + 425.49 + 425.08) - 0.00266909(200 + 400 + 600 + 800 + 1000 + 1200 + 1400 + 1600 + 1800 + 2000)] / 10 = 425.144$$

Then the corresponding deviation (e_i) is calculated as:

$$e_1 = 429.40 - (425.144 + 0.004425 \times 200) = 3.371$$

$$e_2 = 430.52 - (425.144 + 0.004425 \times 400) = 3.606$$

$$e_3 = 432.29 - (425.144 + 0.004425 \times 600) = 4.491$$

$$e_4 = 434.69 - (425.144 + 0.004425 \times 800) = 6.006$$

$$e_5 = 436.96 - (425.144 + 0.004425 \times 1000) = 7.391 \text{ (Max. +ve error)}$$

$$e_6 = 436.29 - (425.144 + 0.004425 \times 1200) = 5.836$$

$$e_7 = 426.37 - (425.144 + 0.004425 \times 1400) = -4.969$$

$$e_8 = 423.03 - (425.144 + 0.004425 \times 1600) = -9.194 \text{ (Max. -ve error)}$$

$$e_9 = 425.49 - (425.144 + 0.004425 \times 1800) = -7.619$$

$$e_{10} = 425.08 - (425.144 + 0.004425 \times 2000) = -8.914$$

Therefore, $e_{\max(+)} = 7.391$,

and $e_{\max(-)} = -9.194$

Hence, straightness tolerance

$$h_{\text{straightness}} = \frac{|e_{\text{MAX}(+)}| + |e_{\text{MAX}(-)}|}{\sqrt{1 + I_0^2}} = \frac{7.391 + 9.194}{\sqrt{1 + 0.004425^2}} = 16.58 \mu\text{m}$$

Similarly for micro channel 2, $h_{\text{straightness}} = 9.57 \mu\text{m}$

and for micro channel 3, $h_{\text{straightness}} = 14.39 \mu\text{m}$

The average value is shown in Table 4.6.

Thus, $13.51 \mu\text{m}$ was determined as the micro channel's average straightness tolerance. It may be concluded that the generated geometries exhibit acceptable tolerance quality based on the computed value of the roundness of micro holes and straightness of micro channels.

Table 4.6: Straightness Tolerance of Micro channels

Geometry	Straightness Tolerance (μm)	Average Straightness Tolerance (μm)
Micro channel 1	16.58	13.51
Micro channel 2	9.57	
Micro channel 3	14.39	

4.1.3 Tool Wear Rate (TWR)

By calculating the volumetric material removal from the tool electrode, the performance metrics TWR is assessed. For each geometry, the TWR values are calculated using Equation (3.1) and the computed values of TWR are determined to be 0.91×10^4 and $0.71 \times 10^4 \mu\text{m}^3/\text{s}$, respectively which has been shown graphically in Figure 4.5. It is clear from Figure 4.5 that using micro channels as opposed to micro holes results in lower rates of tool wear. This might be explained by the fact that in the case of micro holes, the movement of tool occurs only along the Z-axis, which limits the discharge area. As a result, there is more tool wear since the side discharge occurs to a greater extent at depth. However, when creating micro channels, the discharge area is greater, which results in fewer side discharges and a lower rate of tool wear [123].

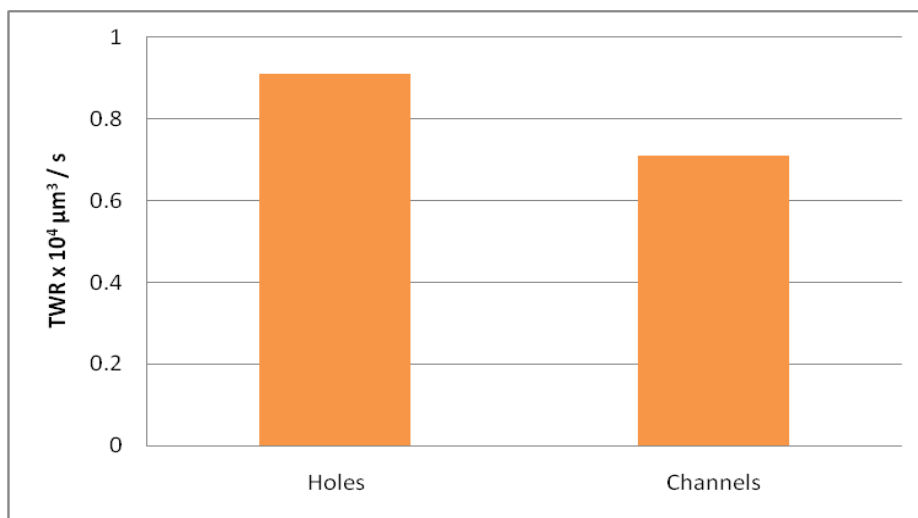


Figure 4.5: Average Tool Wear Rate of Micro holes and Channels

4.1.4 Surface Characteristics and Elemental Characterization

Recast layer is a whitish layer that forms on the surface as a result of the material being re-deposited as a result of secondary discharges caused by poor flushing of molten particles at deep. The trapped gases escape during the cooling process of these re-deposited components, causing the creation of pockmarks, gaps, and fragments of debris. Recast layer creation also causes the surface to experience residual stress, which leads to the emergence of microscopic fissures. However, because die-sinking EDM has been attempted at micromachining, machining was done at lower values of parameters which resulted in less recast layer formation. Hence, the development of micro cracks was similarly minimal. Yet, a comparison of machined geometries reveals that the formation of recast layers is more along the borders of the cavities than at the bottom due to occurrence of side discharges, as represented in Figure 4.6 which represents recast layer formation in micro holes and channels.

In order to examine the occurrence of elements present on the cavities' machined surface, energy dispersive X-ray (EDX) technology has been used. The EDX spectrogram of micro holes and channels together with their proportional weight % proportions is shown in Figure 4.7. It is clear from Figure 4.7 that there is deposition of copper tool material and a little quantity of the tool electrode material because of the heat flux on the surfaces of the cavities. This is due to localised metal evaporation at the surface. It has been also reported that numerous foreign elements, such as oxygen, silicon, sodium and others accumulated on the cavities' surface due to electrical discharge, manipulation of the dielectric and environmental factors.

It can also be because the materials used to make the work and the tools contain contaminants.

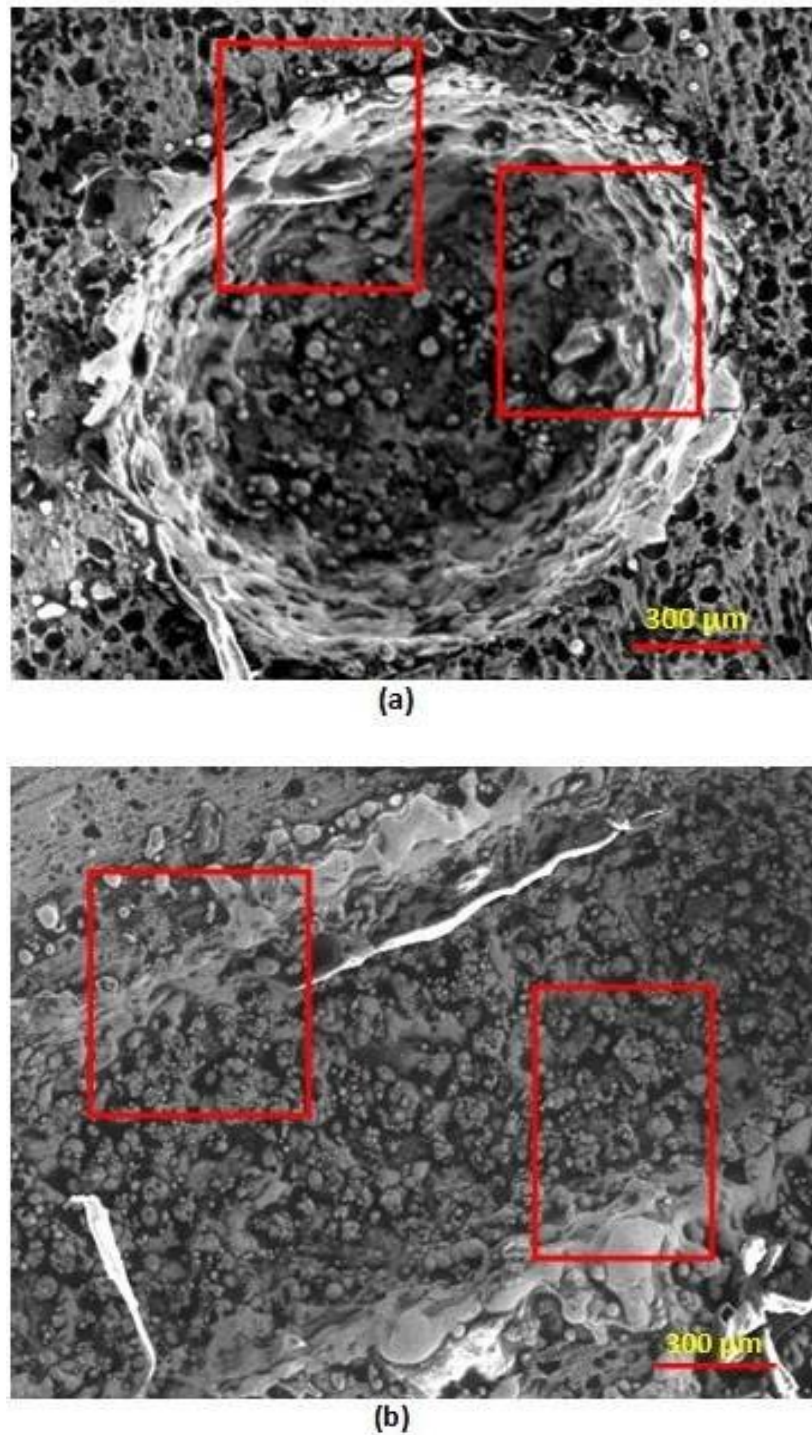
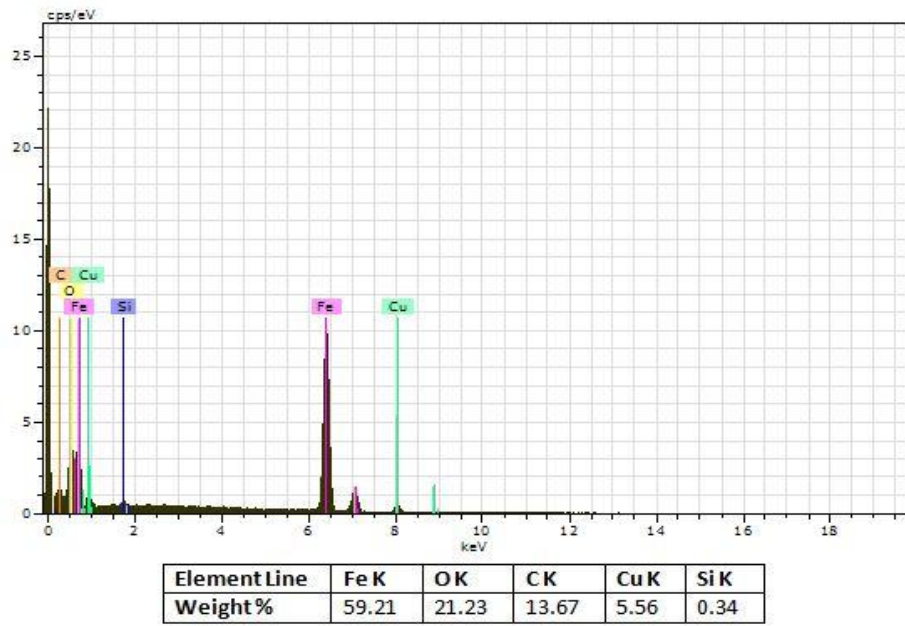
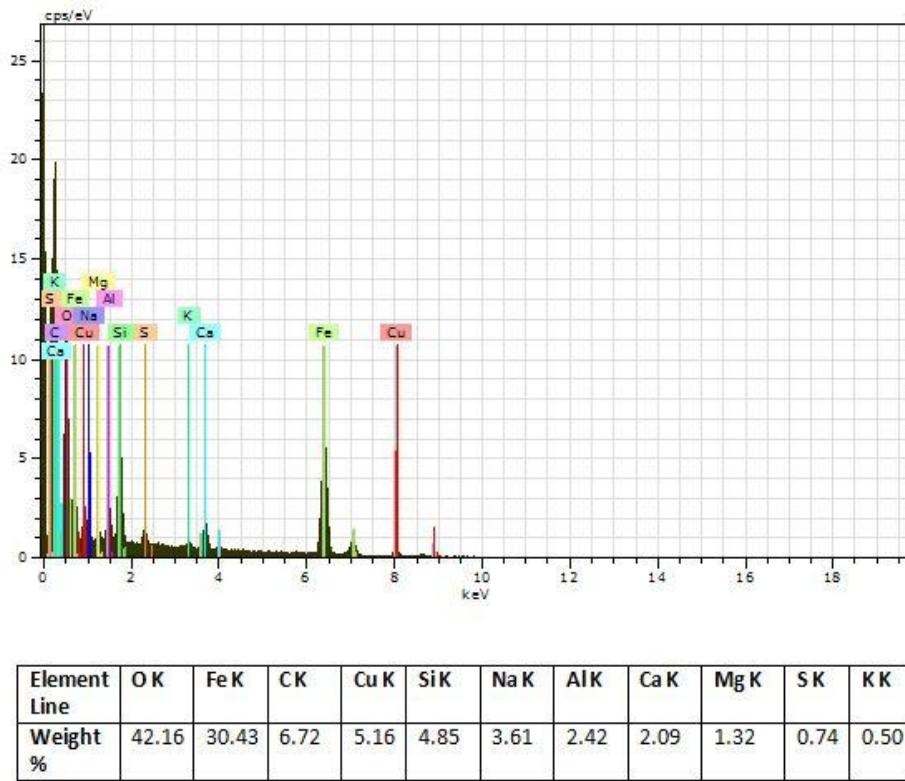


Figure 4.6: SEM Micrographs of Cavity Representing Recast Layer Formation:

(a) Micro hole (b) Micro channel



(a)



(b)

Figure 4.7: Machined surface EDX analysis of (a) Micro hole (b) Micro channel

4.2 PERFORMANCE ANALYSIS IN DIE-SINKING EDM OF POLYGONAL MICRO CAVITIES

The EDM Machining Centre used for the experiments is the XPERT-1 by Electronica Machine Tools including an electronic pulse 50 CNC power supply unit, which made it possible to design complex tool path trajectories. The electrolytic copper tools with different shapes like triangular, square, pentagon and hexagon have been used to erode EN-24 alloy steel work material. The shaped micro tools of required shapes have been prepared through CNC turning operation. The workpiece top and bottom faces were ground to a surface finish using a surface grinding machine before conducting the experiments. The bottom of the tool was also polished using a very fine grade emery sheet before every trial run. The EDM operation has been carried out with the tool and workpiece immersed in circulating liquid dielectric EDM oil, specifically IPOL SEO 450. The shape of the cavity follows the shape of tool electrode. The schematic representation of the design of the tool utilized for machining polygonal cavities i.e. (a) triangular, (b) square, (c) pentagonal and (d) hexagonal cavities are represented in Figure 4.8. Machining of an aspect ratio of 1:5 is easy, but higher aspect ratios can result in tool deflection. Lower values of current and ON time leads to very low material removal rate (MRR) and longer machining time, while higher values of current and ON time results in rough surfaces and increased tool wear. Based on the limitations of machining capabilities and conditions as well as preliminary research, the machining parameters listed in Table 3.3 have been chosen.

Polygonal geometries machined over EN-24 steel samples are examined using an optical microscope and the microscopic images of the cavities have been shown in Figure 4.9. The volumetric material removal from the tool electrode is used to determine TWR. The classification of the SEM-obtained micrographs is essential for identifying the surface integrity, creation of recast layers, micro cracks and material removal. The surface of machined polygonal cavities has been analysed through energy dispersive X-ray (EDS) analysis to ascertain the percentage composition of the elements present at the surface.

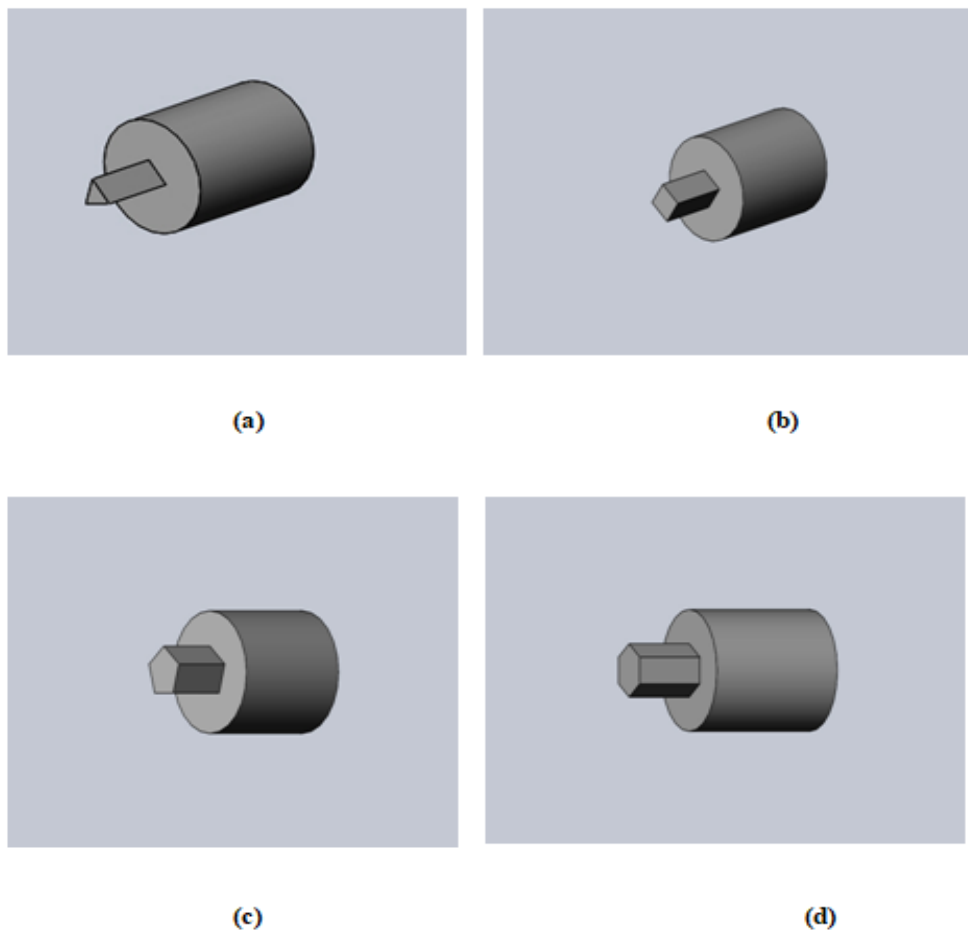
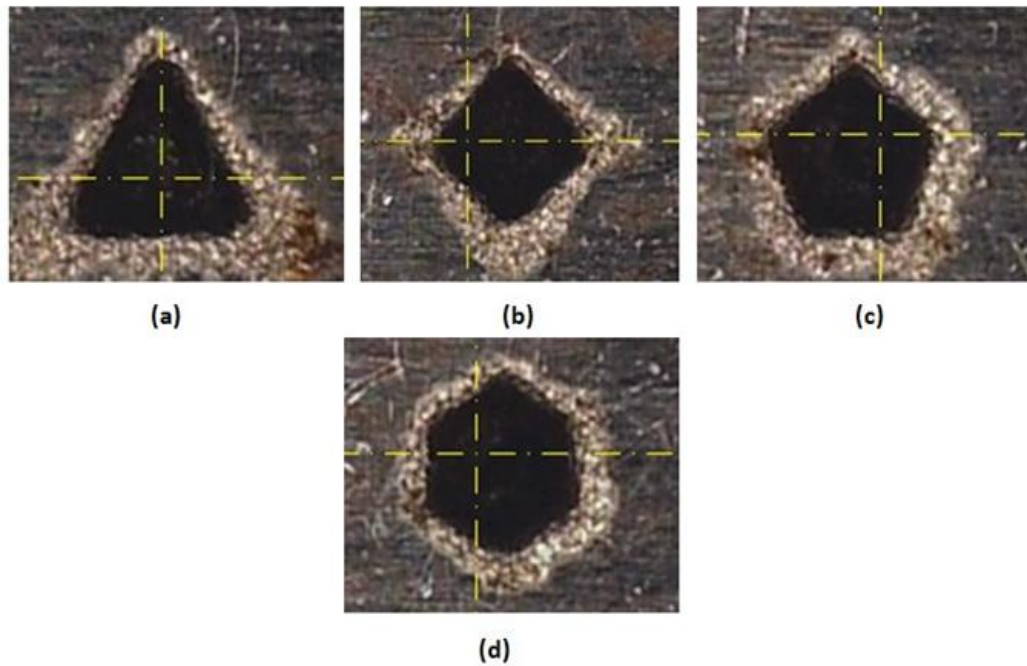


Figure 4.8: Schematic Representation of Polygonal Tools: (a) Triangular (b) Square (c) Pentagonal (d) Hexagonal



**Figure 4.9: Microscopic Images of Cavities: (a) Triangular (b) Square
(c) Pentagonal (d) Hexagonal**

4.2.1 Tool Wear Rate (TWR)

As mentioned in section 4.2, this EDM experiment utilizes a shaped electrode approach in which the machined cavity follows the shape of the tool electrode. The geometric profiles governing the discharge cause it to fluctuate in both direction and location. The side discharge contributes significantly to the material removal process in addition to the front discharge over the cavity and beneath electrode surfaces. This causes non-uniform electrode wear, spark gap instability, short circuiting, and discharge hopping. This causes shape errors, such as rounding of corners, perforated or distorted cavity edges, and recast layers. Due to the non-uniform discharge pattern in polygonal-shaped cavities, the tiny electrode may deflect due to the forces induced

by the combined effect of dielectric breakdown, ion bombardment, and thermo-mechanical waves, which require multiple experimental studies by various researchers for a better understanding.

Ion bombardment, uneven spark gaps, thermal effects, and microstructural flaws in the tool material all contribute to tool wear. Hence, EDM cannot avoid tool wear. The volumetric material removal from the tool electrode is used to determine TWR. According to Equation (3.1), the TWR is calculated using the length of the eroded tool, the diameter of the tool electrode, and the amount of machining time. To measure the length of the tool that has been eroded, an electrical contact is formed between the tool and a fixed point before and after machining.

Table 4.7 shows the calculated value of tool wear rate and Figure 4.10 is the graphical representation of the tool wear rate of different geometries. It is clear that as the complexity of polygonal shapes increases, tool wear rate also increases. Hence, $TWR_{\text{triangular}} < TWR_{\text{square}} < TWR_{\text{pentagonal}} < TWR_{\text{hexagonal}}$. As the tool electrode follows a more complex path to machine the workpiece, it may be subjected to more electrical discharges and sparks, which can accelerate wear. Longer tool paths also mean more exposure to the erosive effects of the electrical discharge.

Complex shapes may require longer machining times and the accumulation of heat generated during EDM can contribute to electrode wear. Prolonged exposure to high temperatures can cause electrode erosion. The extent of increase in tool wear rate with increase in the sides of polygon can be also attributed to the behaviour of flushability and dielectric flow. The flushing of debris and wear particles from intricate features in complex shapes can be challenging. If debris accumulates in

crevices and corners, it can act as an abrasive and accelerate tool wear. In EDM, dielectric fluid is used to remove debris and facilitate the machining process. Complex shapes may disrupt the flow of dielectric fluid, reducing its effectiveness in cooling and flushing, which can contribute to increased tool wear.

Table 4.7: Tool Wear Rate for Different Geometries

Cavity	TWR x 10 ⁴ (μm ³ / s)
Triangular	5.77
Square	6.17
Pentagonal	7.60
Hexagonal	7.69

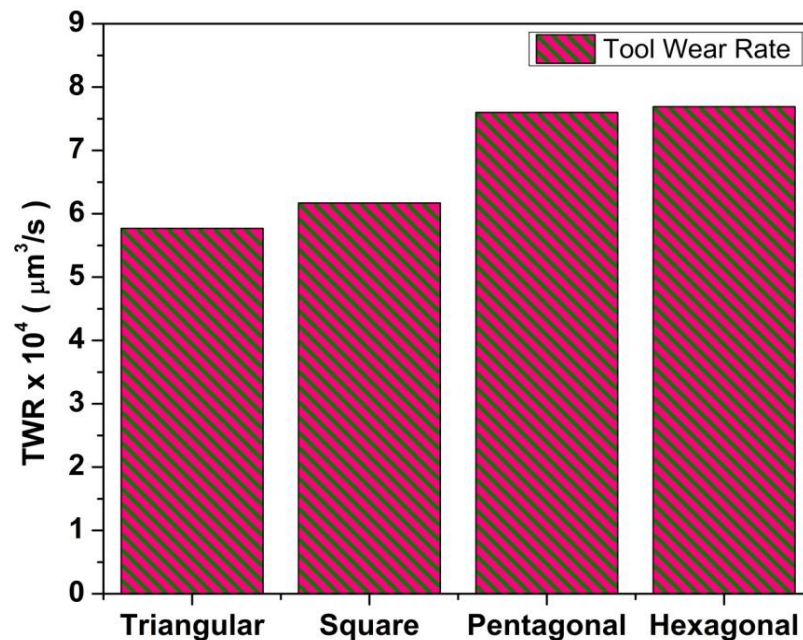


Figure 4.10: Graphical Representation of Tool Wear Rate for Different Geometries

4.2.2 Surface Characterization of Polygonal Cavities

Figure 4.9 reveals that the cavities, when examined under an optical microscope, exhibit burrs at their edges, leading to a decrease in their surface quality. Electrical discharge machining generates intense heat, causing localized melting or even evaporation of the workpiece material. Only a small percentage (15% or less) of the total molten material produced by the discharge is carried away by the dielectric [141], and the remaining molten material cools and solidifies to form a recast layer. During rapid cooling, entrapped gases are released from the material, resulting in the formation of debris globules, craters and pockmarks on the cavity surface. Additionally, residual stress generated by recast layer formation causes crack formation. The cracks originate at the machined surface and extend through the recast layer, as demonstrated by SEM micrographs in Figure 4.11. As the complexity of polygonal cavities increases, the uniformity of micro-cracks decreases gradually. Moreover, complex and higher-order polygons exhibit a higher formation of recast layer. The reason for this is that more complex and higher-order polygons have more intricate geometries which can lead to uneven thermal and mechanical stresses during the machining process. These stresses result in inconsistent micro-crack formation and a higher propensity for recast layer formation due to increased heat accumulation and material redeposition.

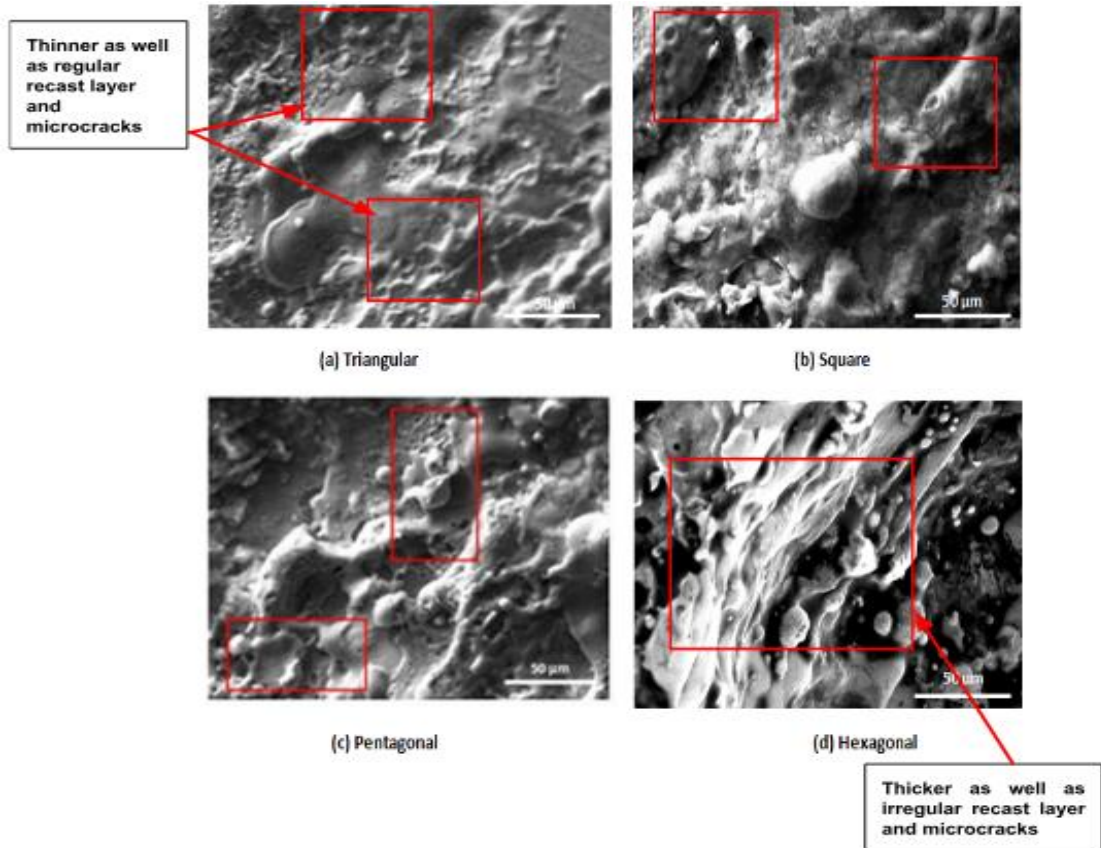
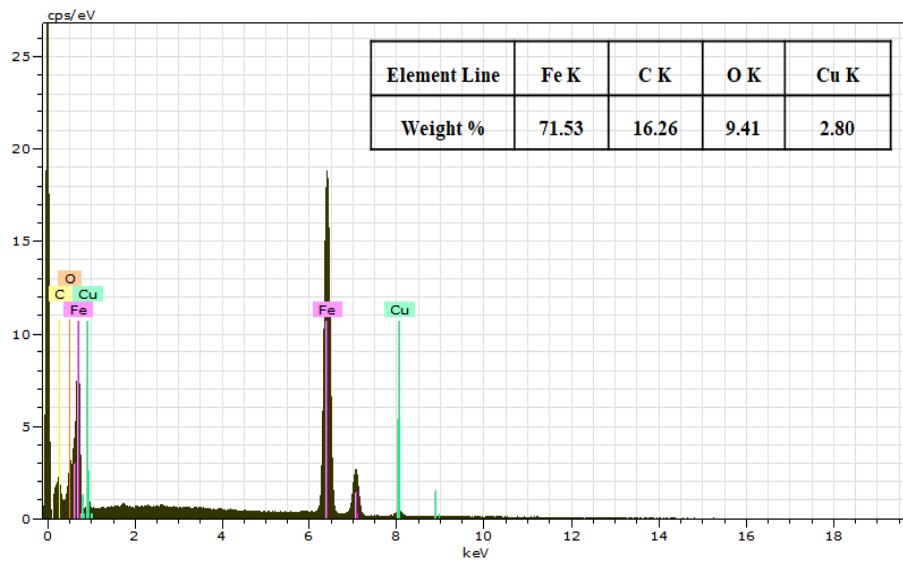


Figure 4.11: SEM Analysis of Cavities Representing Recast Layer with Micro Cracks: (a) Triangular (b) Square (c) Pentagonal and (d) Hexagonal

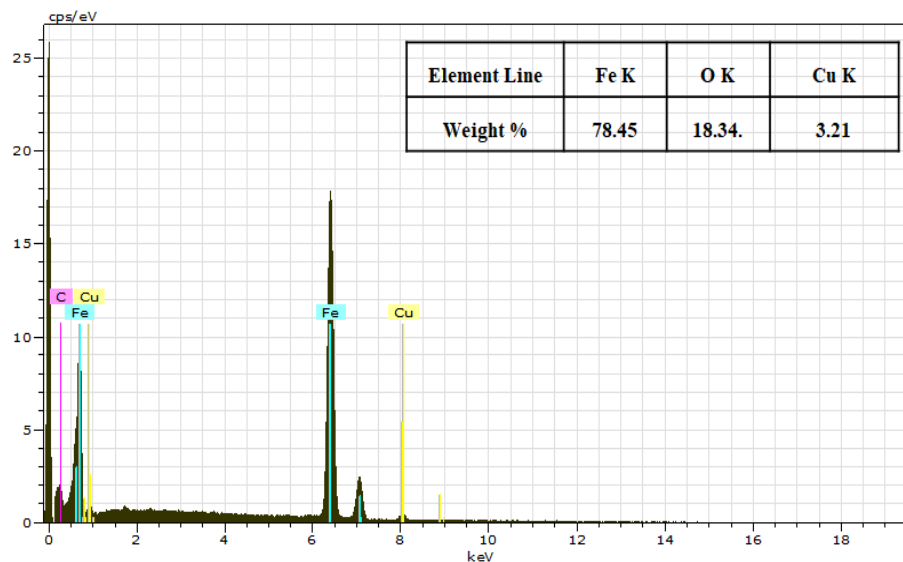
4.2.3 EDS Analysis of Polygonal Cavities

The elemental analysis of the polygonal cavities has been analyzed using the energy dispersive X-ray (EDS) technique based on the scanned area of the cavities. EDS spectrograms of various cavities and their respective weight percentage distributions are shown in Figure 4.12. According to the EDS investigation, local metal evaporation at the surface and a little quantity of electrode material occurring due to heat flux caused the tool electrode element copper to become deposited on the surfaces of the cavities. It is also found that a variety of foreign materials including

silicon, oxygen and other elements got collected on the cavities' surface during electrical discharge and handling of the dielectric as well as from surrounding environment.



(a)



(b)

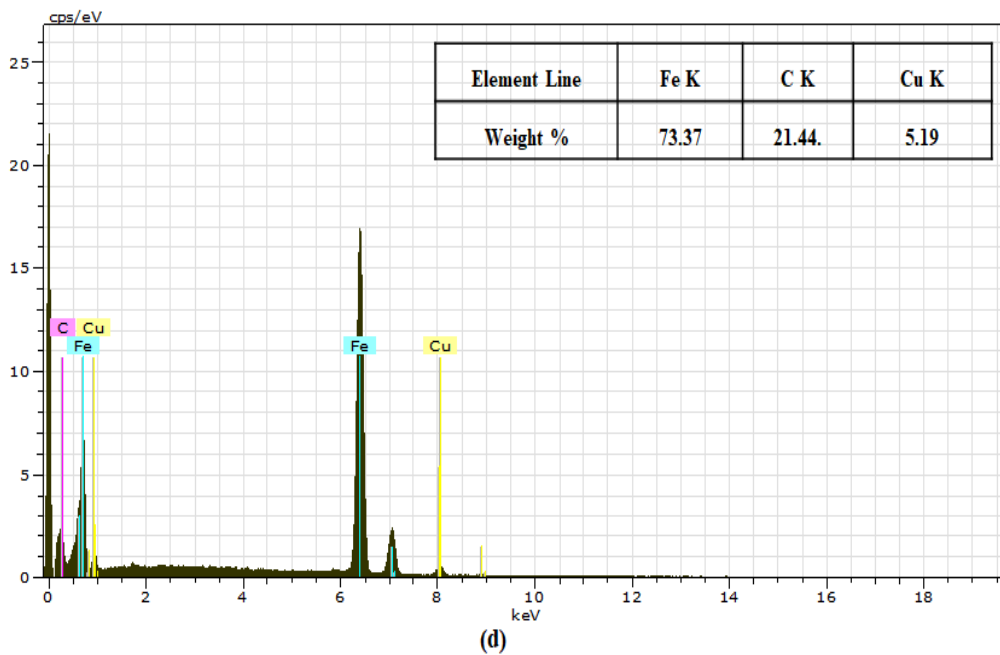
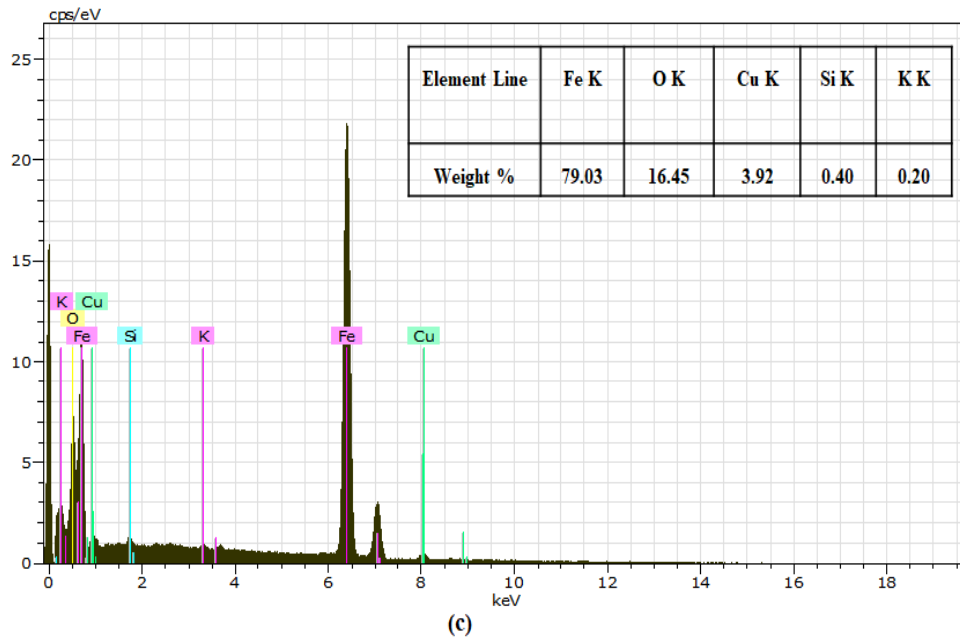


Figure 4.12: EDS Analysis of Machined Surface of Different Cavities:

(a) Triangular (b) Square (c) Pentagonal (d) Hexagonal

4.2.4 Software Based Analysis of Angularity Error

Three cavities with a depth of $2000\mu\text{m}$ each were created in order to micro-machine a selection of polygonal shapes using the machining parameters listed in Table 3.3. For every set of cavities, the angular disparities have been calculated, and their mean values are noted. Using an Olympus optical microscope, the machined micro-cavities' shape is studied, and the profile projector and Olympus Analysis Five software are used to evaluate the micro-cavities' tolerance. Figure 4.13 shows microscopic images of the machined micro-cavities and the analysis process used for the evaluation.

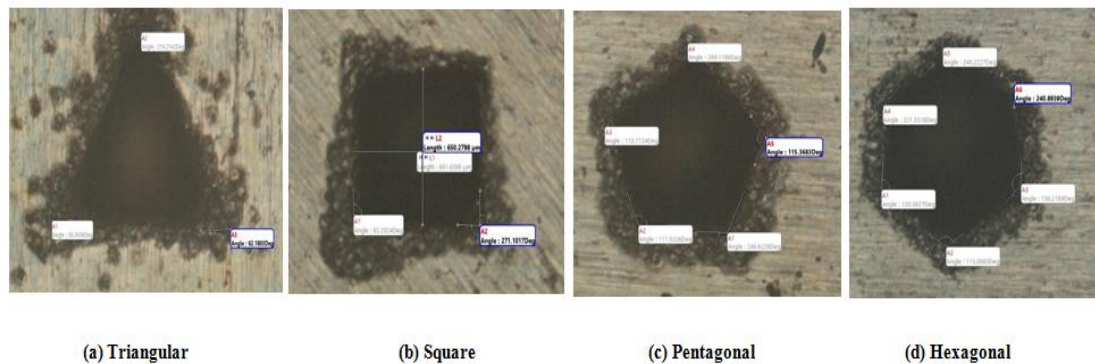


Figure 4.13: Microscopic Images along with Analysis Procedure of Cavities

The tolerance zone, bounded by two parallel planes at a given basic angle (which is not 90 degree) from a datum plane or axis, is known as the angularity tolerance. It is the area inside which the feature's surface or axis must lie.

Table 4.8 presents the angularity errors obtained through measurements performed by the measuring instruments.

Table 4.8: Angularity Error for Cavities

Cavity	Average Angularity Error (degree)						Mean Average Angularity Error (degree)
	<1	<2	<3	<4	<5	<6	
Triangular	5.39°	2.73°	4.91°	-	-	-	4.34°
Square	1.67°	0.10°	2.57°	0.98°	-	-	1.33°
Pentagonal	2.81°	11.67°	9.51°	11.60°	4.06°	-	7.93°
Hexagonal	2.90°	10.36°	13.97°	17.44°	5.62°	2.09°	8.74°

According to the statistics, square micro-cavities have the least amount of angularity error and the best degree of angular precision. On the other hand, triangular micro-cavities, which show higher angular precision than pentagonal and hexagonal micro-cavities, show the least amount of angularity error, followed by hexagonal micro-cavities. This might be because creating square cavities requires less complicated tool electrode movement than creating triangular, pentagonal, and hexagonal cavities, which need more complex route trajectories. Additionally, compared to the other three designs, the discharge area of square cavities is more constrained and less stochastic. Consequently, the increasing complexity of the electrode path and spark discharge area may be the cause of the variance in angular accuracy for hexagonal, pentagonal, and triangular micro-cavities.

CHAPTER 5

PARAMETRIC ANALYSIS IN DIE-SINKING EDM OF PENTAGONAL CAVITIES

5.1 INTRODUCTION

In the context of die-sinking EDM, parametric analysis refers to the systematic study and optimization of different machining factors that control the performance and outcome of the process. Parametric analysis in die-sinking EDM of pentagonal cavities is essential for optimizing the machining process and achieving high-quality results. By systematically studying and adjusting the process parameters, manufacturers can improve the efficiency, precision, and reliability of the EDM process. This leads to better performance, reduced costs, and enhanced capabilities in producing complex geometries and hard-to-machine materials. In general, parametric analysis is done in the following steps:

Step 1: Define Objectives and Parameters

Step 2: Design of Experiments (DoE)

Step 3: Conduct Experiments

Step 4: Data Analysis

Step 5: Validation and Verification

Step 6: Implementation and Documentation

5.2 EXPERIMENTAL EQUIPMENT AND DESIGN

Taguchi's orthogonal arrays (OAs) are a popular form of experimental design extensively applied in diverse domains, such as manufacturing, engineering, and product design. This design was developed by Dr. Genichi Taguchi, a Japanese engineer, who sought to create a more efficient and effective method for quality improvement and optimization of product and process design. Because of the method's robustness at the design or production stage, producers may make items of superior quality faster and for less money. Tong et al. [142] describe the Taguchi method as an implemented experimental technique that only optimizes one response, i.e. by utilizing an orthogonal array for experiments and the Signal-to-Noise (S/N) ratio as the metric for evaluating quality, the parametric parameters can be enhanced individually for each performance attribute. The optimal combination or collection of factor levels for quality improvement is determined to identify the most cost-effective solution for the product design specification taking into account of the requirements of the client.

The experiment was carried out using an Electronica XPERT-1-e-pulse 50 CNC die-sinking EDM machine, IPOL SEO 450 EDM oil, and a pentagonal-shaped copper tool electrode. Figure 5.1 depicts the experimental setup and tool preparation. The work piece is made of EN-24 alloy steel and has dimensions of 100 x 100 x 15 mm. Prior to conducting the trials, the top and bottom faces of the workpiece were ground to achieve a desired surface finish using a surface grinding machine.

The pentagonal shaped copper tool electrode of circumscribed diameter of 6.8 mm, side length 0.4 mm was prepared through CNC turning. For each run, new tool

electrode has been utilized to nullify the effects of electrode wear. Investigations have been conducted on the effects of three process factors in the die-sinking EDM process: current (I), pulse-off-time (T_{OFF}) and pulse-on-time (T_{ON}) on the rate of material removal, rate of tool wear and surface finish. The control parameters along with their levels have been represented in Table 5.1.

Taguchi makes use of a unique OA design to examine the whole parameter space with a minimal amount of experiments. The examination of S/N ratios often divides performance characteristics into three categories: Nominal-The-Better (NTB), Higher-The-Better (HTB), and Lower-The-Better (LTB).

For LTB response variable,

$$\eta_{ij} = -10 \times \log_{10}\left(\frac{1}{n} \sum_{k=1}^n y_{ijk}^2\right) \quad (5.1)$$

For HTB response variable,

$$\eta_{ij} = -10 \times \log_{10}\left(\frac{1}{n} \sum_{k=1}^n \frac{1}{y_{ijk}^2}\right) \quad (5.2)$$

For NTB response variable,

$$\eta_{ij} = 10 \times \log_{10}\left(\frac{\bar{y}_{ij}^2}{s_{ij}^2}\right) \quad (5.3)$$

Where, y_{ijk} is the experimental value of the j^{th} response variable in the i^{th} trial at the k^{th} replication, and n is the number of repeated experiments. The number of replies is p , and the number of experimental runs is m .

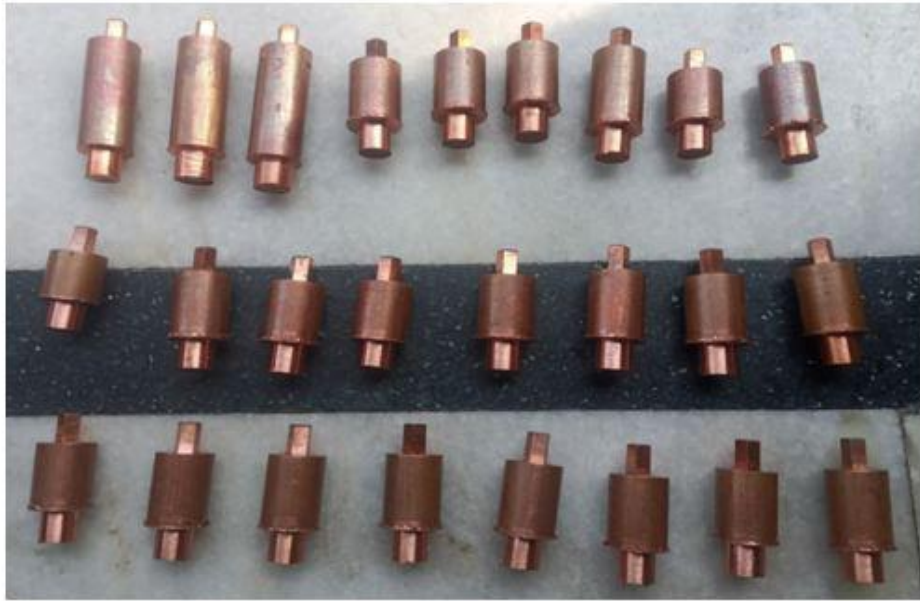
In this work, the effects of various machining parameters over machining performance in the EDM process have been studied through modelling utilizing the

Taguchi L_{25} OA and software (Minitab 18). The experimental layout based on L_{25} orthogonal array is given in Table 5.2.

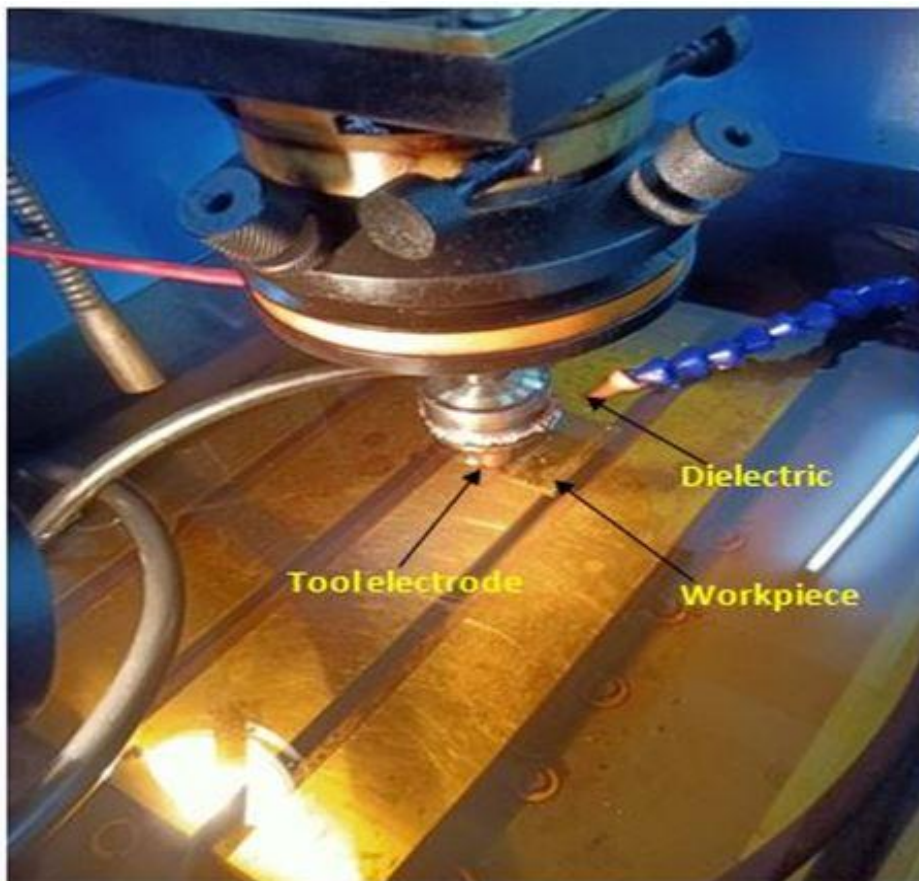
The assessment of rate of tool wear and rate of material removal is predicated on volumetric removal while the measurement of surface roughness has been carried out at three positions to give average value. The complete design matrix of input parameters with output parameters after experimental runs has been represented in Table 5.3. EDM machined sample and microscopic image have been represented in Figure 5.2.

Table 5.1: Control Parameters with their Levels

Sr. No.	Process Parameter	Unit	Level 1	Level 2	Level 3	Level 4	Level 5
1	Current (I)	A	5	6	7	8	9
2	Pulse-off-Time (T_{OFF})	μs	25	30	35	40	45
3	Pulse-on-Time (T_{ON})	μs	50	100	150	200	250



(a)

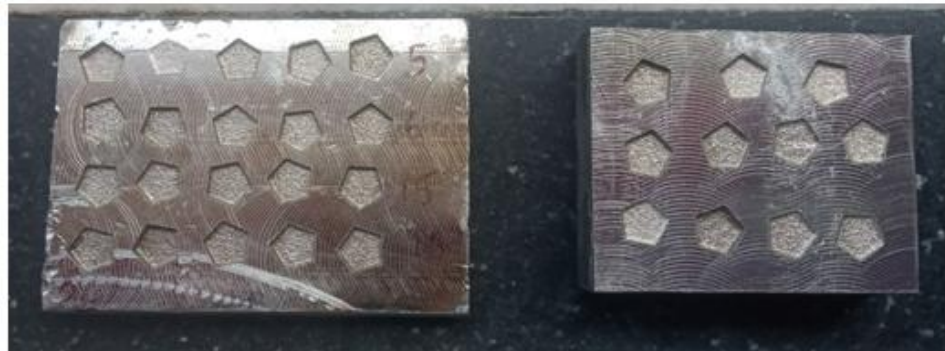


(b)

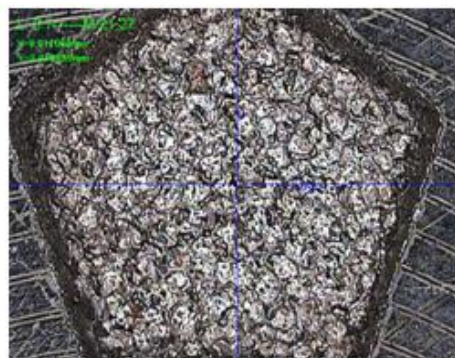
Figure 5.1: (a) Tool Preparation (b) EDM Machining Setup

Table 5.2: Experimental Layout

Expt. No.	I (A)	T_{OFF} (μs)	T_{ON} (μs)	Expt. No.	I	T_{OFF} (μs)	T_{ON} (μs)
1	5	25	50	14	7	40	50
2	5	30	100	15	7	45	100
3	5	35	150	16	8	25	200
4	5	40	200	17	8	30	250
5	5	45	250	18	8	35	50
6	6	25	100	19	8	40	100
7	6	30	150	20	8	45	150
8	6	35	200	21	9	25	250
9	6	40	250	22	9	30	50
10	6	45	50	23	9	35	100
11	7	25	150	24	9	40	150
12	7	30	200	25	9	45	200
13	7	35	250				



(a)



(b)

Figure 5.2: (a) Machined Sample (b) Microscopic Image of Cavity

5.3 PARAMETRIC ANALYSIS OF MRR

Due to the need for maximal material removal rate, the Higher-The-Better (HTB) characteristics are chosen for Taguchi analysis. The signal to noise ratio is then calculated using Equation 5.2. The signal-to-noise ratios for MRR are displayed in Table 5.4 while Tables 5.5 and 5.6 reflect the response table for signal-to-noise ratios and means, respectively. Figure 5.3 and Figure 5.4 depict the major effect plot for the means and S/N ratios of material removal rate (MRR) respectively. The most important element influencing the MRR after pulse-on-time and pulse-off-time is current, as shown by Tables 5.5 and 5.6 as well as Figures 5.3 and 5.4. On the basis

of higher the better characteristics, The highest MRR is obtained while using a combination of parameters consisting of a 9 A current, a pulse-off time of 35 μs , and a pulse-on time of 250 μs . Additionally, it is evident that the rate at which material is removed increases as both the current and pulse-on time increase.

Table 5.3: Design Matrix of Process Parameters with Performance Measures

Expt. No.	I (A)	T _{OFF} (μs)	T _{ON} (μs)	MRR (mm^3/min)	TWR (mm^3/min)	SR (Ra) (μm)	Expt. No.	I (A)	T _{OFF} (μs)	T _{ON} (μs)	MRR (mm^3/min)	TWR (mm^3/min)	SR (R _a) (μm)
1	5	25	50	0.112	0.021	2.6	14	7	40	50	0.609	0.881	6.57
2	5	30	100	0.127	0.081	3.01	15	7	45	100	0.612	0.922	6.83
3	5	35	150	0.222	0.12	3.69	16	8	25	200	1.152	1.549	7.68
4	5	40	200	0.231	0.259	4.45	17	8	30	250	1.247	1.502	7.81
5	5	45	250	0.314	0.212	4.96	18	8	35	50	1.015	1.211	7.27
6	6	25	100	0.329	0.611	5.71	19	8	40	100	1.028	1.252	7.53
7	6	30	150	0.425	0.651	5.83	20	8	45	150	1.112	0.991	7.62
8	6	35	200	0.434	0.789	5.97	21	9	25	250	1.767	1.732	8.53
9	6	40	250	0.517	0.742	6	22	9	30	50	1.535	1.441	7.83
10	6	45	50	0.304	0.451	6.18	23	9	35	100	1.548	1.482	8.03
11	7	25	150	0.729	1.081	6.91	24	9	40	150	1.632	1.221	8.17
12	7	30	200	0.739	1.219	7.31	25	9	45	200	1.612	1.651	7.93
13	7	35	250	0.823	1.172	7.61							

Table 5.4: Calculated S/N Ratios for MRR

Expt. No.	S/N Ratio	Expt. No.	S/N Ratio
1	-19.0156	14	-4.30765
2	-17.9239	15	-4.26497
3	-13.0729	16	1.22905
4	-12.7278	17	1.917329
5	-10.0614	18	0.129321
6	-9.65608	19	0.239862
7	-7.43222	20	0.922096
8	-7.25021	21	4.944731
9	-5.73019	22	3.722168
10	-10.3425	23	3.795419
11	-2.74545	24	4.254403
12	-2.62711	25	4.147301
13	-1.692		

According to the Analysis of Variance (ANOVA) table shown in Table 5.7, current and pulse-on time act as the most considerable characteristics at a 95% confidence level for material removal rate among all variables,. The degree of variance in MRR that may be attributed to the input components is expressed by the parameter R^2 . $R^2 = 99.9\%$ shows that the model has a high degree of accuracy in response prediction. The standard deviation of the error, $S = 0.0088072$. When the p-value is compared to the generally used confidence level of 0.05, it can be determined that if the $p \leq 0.05$,

the effect is significant. An essential addition to the model calculations are residual plots. To determine whether the data deviate from normality, the normal probability plot displays the standardized residuals of MRR, as shown in Figure 5.6. The residuals are nearly falling inside the confidence interval, as can be observed, suggesting that they are nearly regularly distributed.

Table 5.5: Response values for S/N Ratios - MRR

MRR (Larger is better)			
Level	Current (I)	Pulse-off-Time	Pulse-on-Time
1	-14.5603	-5.0487	-5.9629
2	-8.0822	-4.4688	-5.5619
3	-3.1274	-3.6181	-3.6148
4	0.8875	-3.6543	-3.4457
5	4.1728	-3.9199	-2.1243
Delta	18.7331	1.4306	3.8386
Rank	1	3	2

Table 5.6: Mean Response Values - MRR

Level	Current (I)	Pulse-off-Time	Pulse-on-Time
1	0.2012	0.8178	0.7150
2	0.4018	0.8146	0.7288
3	0.7024	0.8084	0.8240
4	1.1108	0.8034	0.8336
5	1.6188	0.7908	0.9336
Delta	1.4176	0.0270	0.2186
Rank	1	3	2

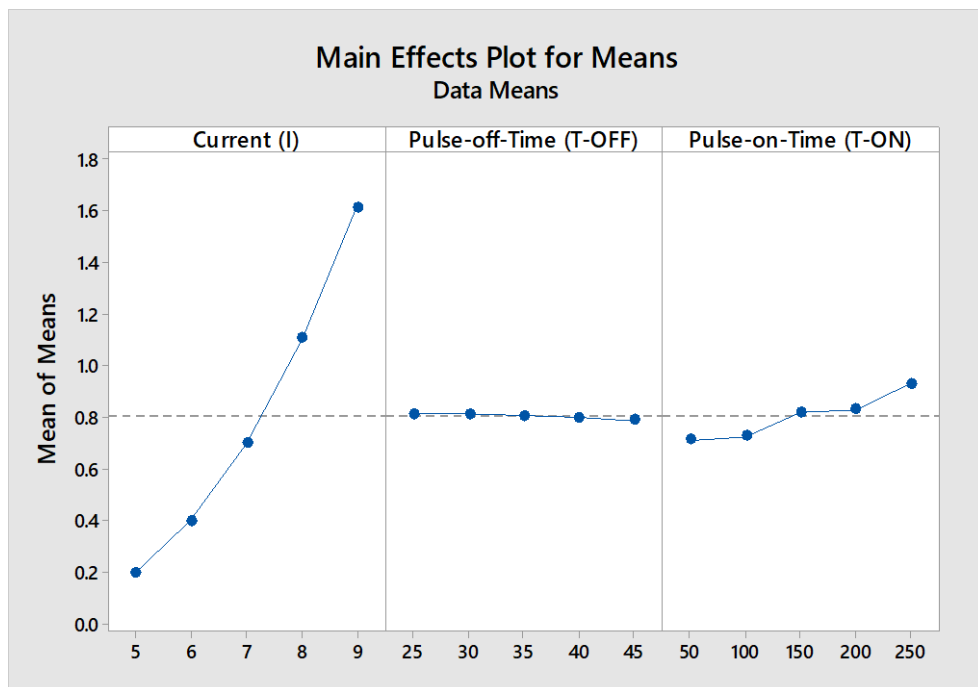


Figure 5.3: Primary Effects of Mean Values for MRR

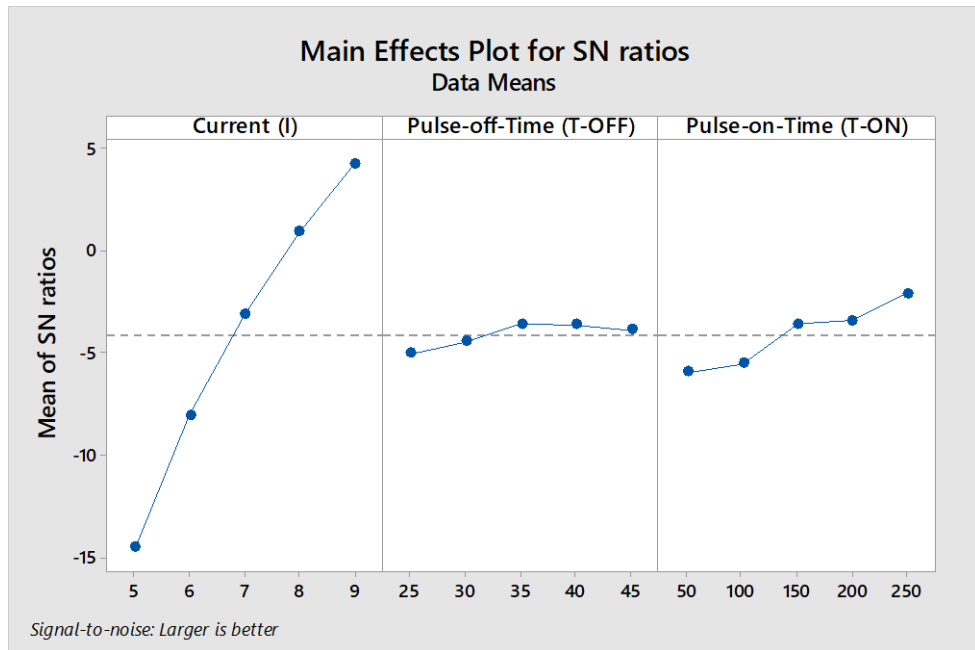


Figure 5.4: Primary Effects of Signal to Noise Ratios on material for MRR

Table 5.7: ANOVA Table for MRR

Source	DF	Adj SS	Adj MS	F-Value	P-Value
Current	4	6.46718	1.61679	20843.93	0.000
Pulse-off-Time	4	0.00226	0.00056	7.28	0.003
Pulse-on-Time	4	0.15802	0.03950	509.29	0.000
Error	12	0.00093	0.00008		
Total	24	6.62838			
S	R-sq	R-sq(adj)			
0.0088072	99.99%	99.97%			

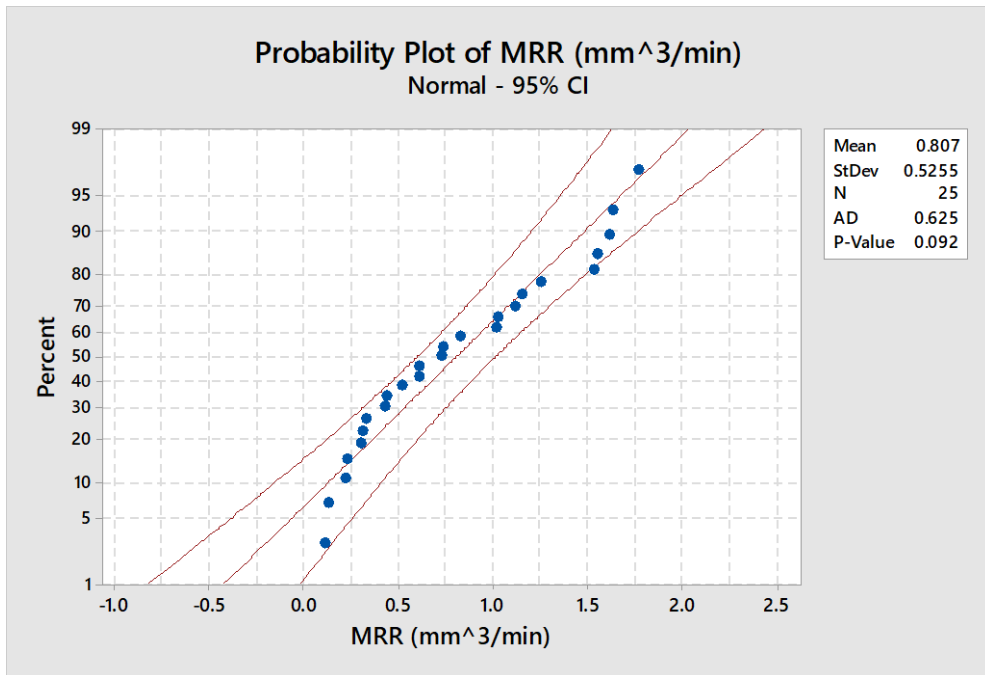
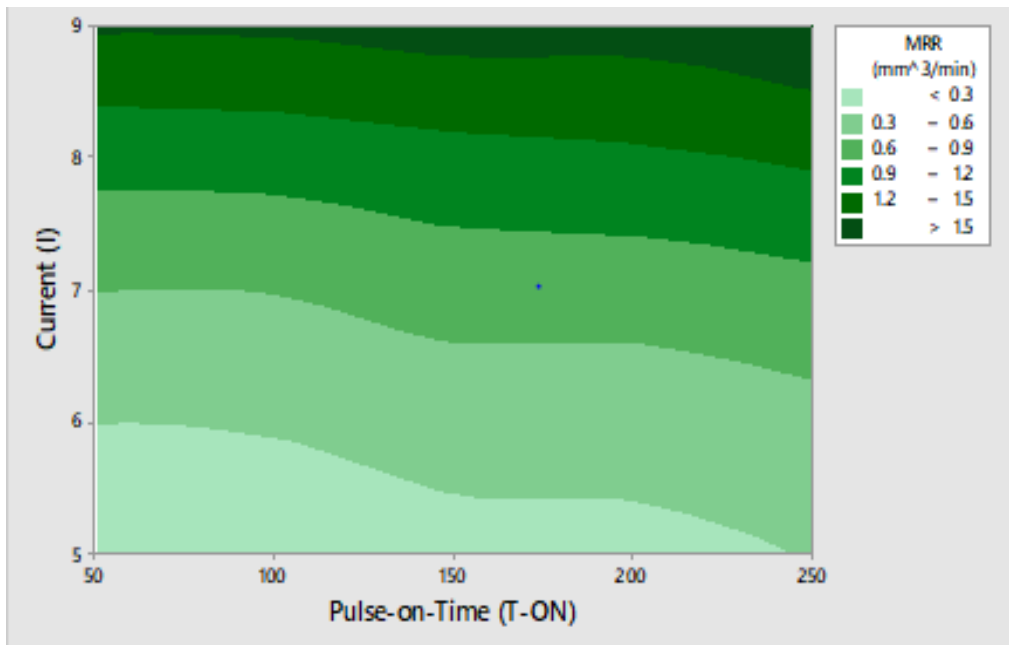
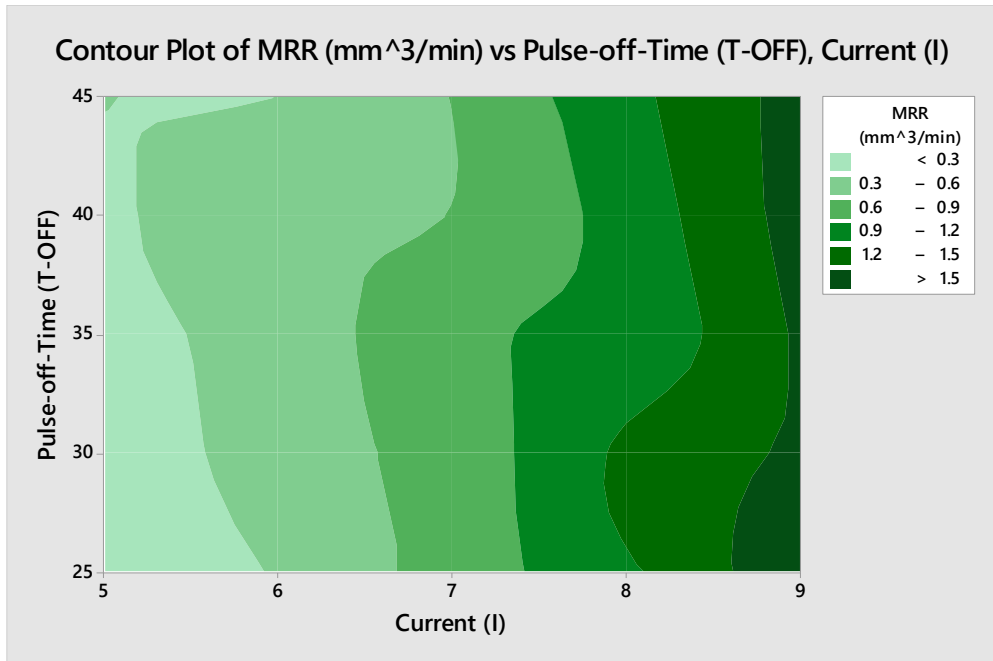


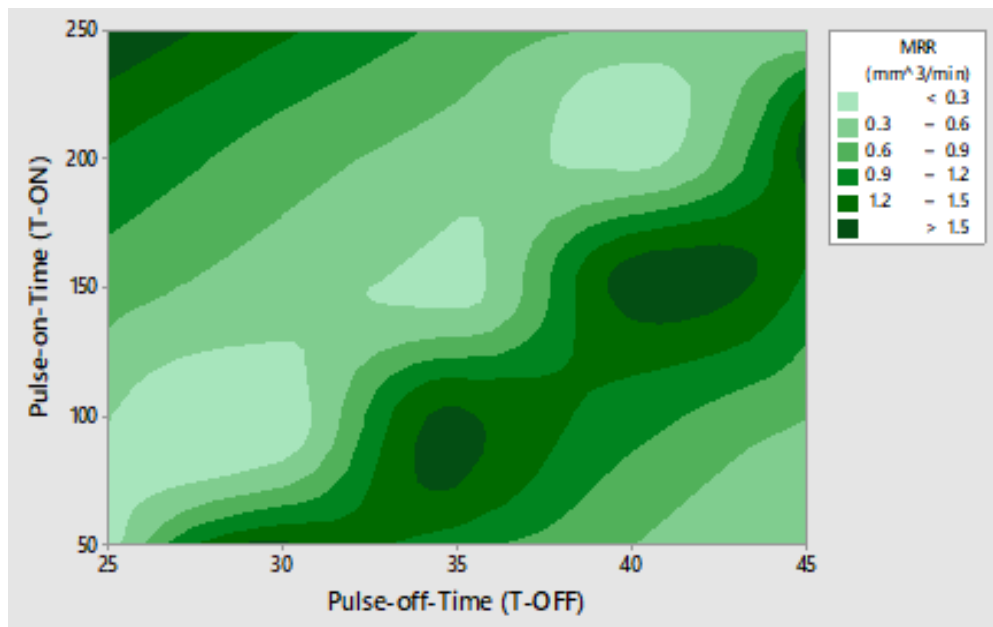
Figure 5.5: Residual plot of MRR



(a)



(b)



(c)

Figure 5.6: Contour Plots for MRR: (a) I vs T_{ON} (b) I vs T_{OFF} (c) T_{ON} vs T_{OFF}

Contour plots depicting the material removal rate (MRR) against current vs pulse-on time (a), current vs pulse-off time (b) and pulse-on time vs pulse-off time (c) are shown in Figure 5.6. When both current and pulse-on times are maximized, the maximum MRR is indicated by the darkest region in Figure 5.6(a). It is clear that the current must be at its maximum at all pulse-on times in order to get the maximum MRR. The relationship between pulse-off time and current in relation to MRR is shown in Figure 5.6(b). According to the findings, pulse-off time has less of an effect on MRR than current. Even with a high pulse-off time, a high current can still result in a high MRR. Figure 5.6(c) demonstrates the relationship between pulse-on time and pulse-off time, showing that in order to achieve the highest material removal rate (MRR), it is necessary to have a shorter pulse-off time and a longer pulse-on time.

Figure 5.7 illustrates the correlation between the current, pulse on time and pulse off time for the response of MRR. It has been noted that current is the most important aspect when taking pulse on time, pulse off time and current into account. In a similar vein, when comparing pulse on and off times, pulse on time shows a greater interaction effect on the MRR.

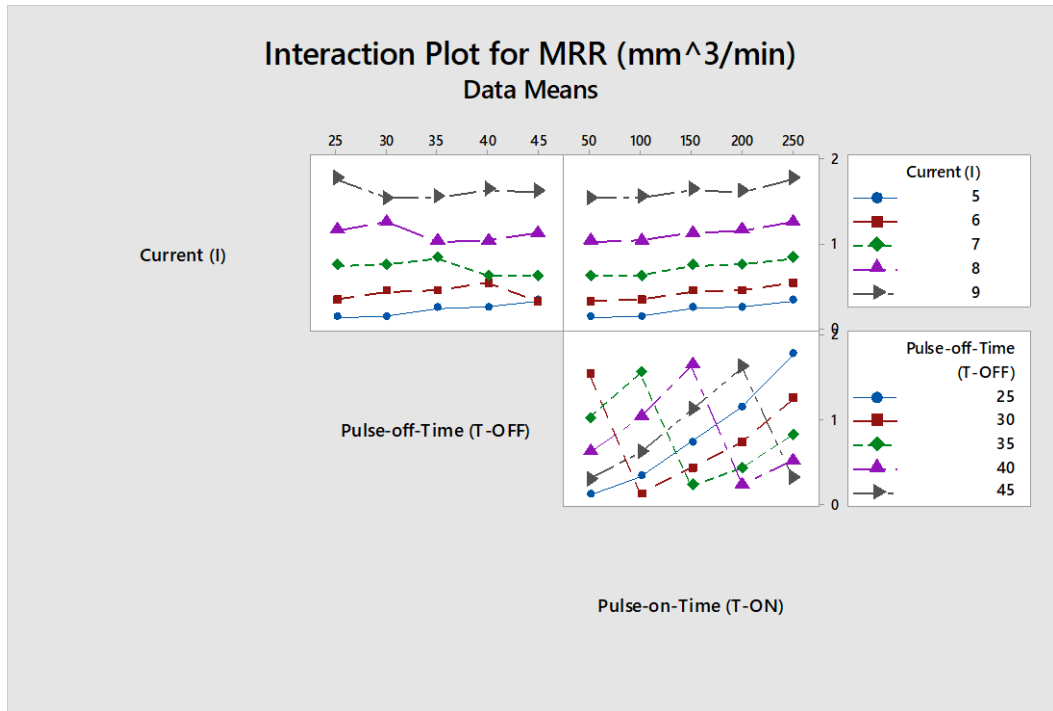


Figure 5.7: Interaction plot of MRR

5.4 PARAMETRIC ANALYSIS OF TWR

Since, tool wear rate must be the lowest, a Lower-The-Better (LTB) characteristic is selected for Taguchi analysis and the S/N ratio is determined using Equation 5.1. The S/N ratios for TWR are displayed in Table 5.8, while the response table for signal to noise ratios and means are listed in Table 5.9 and Table 5.10 respectively. Similarly, Figures 5.8 and 5.9 respectively, display the main effect plot for means and S/N ratios for TWR. It is evident from Tables 5.9 and 5.10 as well as Figures 5.8 and 5.9 that the most important component influencing the TWR is current, which is then followed by the pulse-on-time (T_{ON}) and pulse-off-time (T_{OFF}). On the basis of lower the better characteristics, the minimum TWR is achieved for the combination of

factors as Current of 5 A, 25 μ s as pulse-off-Time and 50 μ s as pulse-on-Time. It is evident that the rate at which the tool is removed increases when there is an increase in both the current and pulse-on time.

Table 5.8: Calculated SN ratios for TWR

Expt. No.	S/N Ratio	Expt. No.	S/N Ratio	Expt. No.	S/N Ratio
1	33.55561	10	6.916469	19	-1.95209
2	21.8303	11	-0.67651	20	0.078527
3	18.41638	12	-1.72007	21	-4.77096
4	11.734	13	-1.37855	22	-3.17328
5	13.47328	14	1.100482	23	-3.41696
6	4.279176	15	0.705382	24	-1.73431
7	3.72838	16	-3.80103	25	-4.35494
8	2.05846	17	-3.5334		
9	2.591922	18	-1.66288		

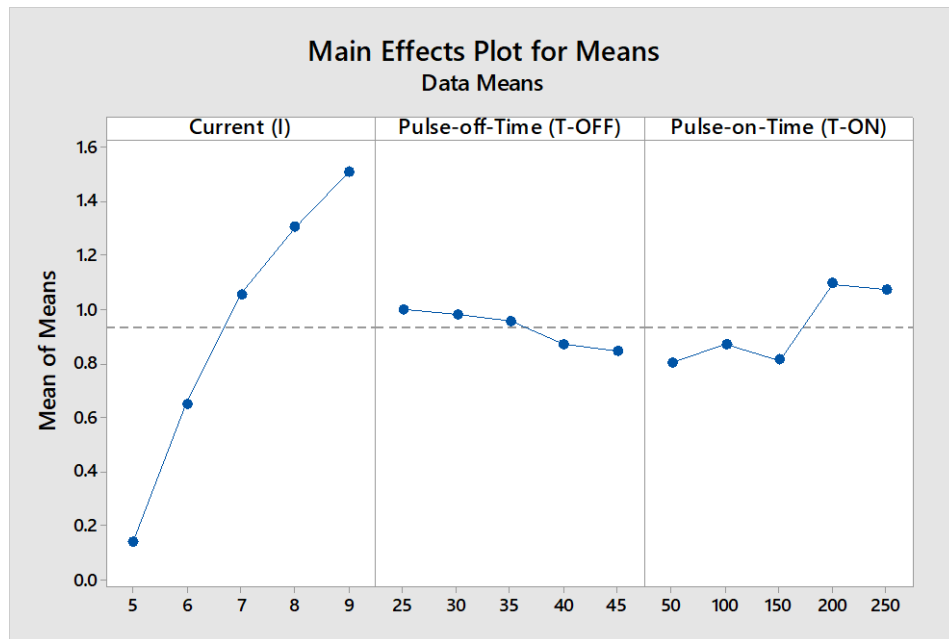


Figure 5.8: Primary Effects of Mean Values for TWR

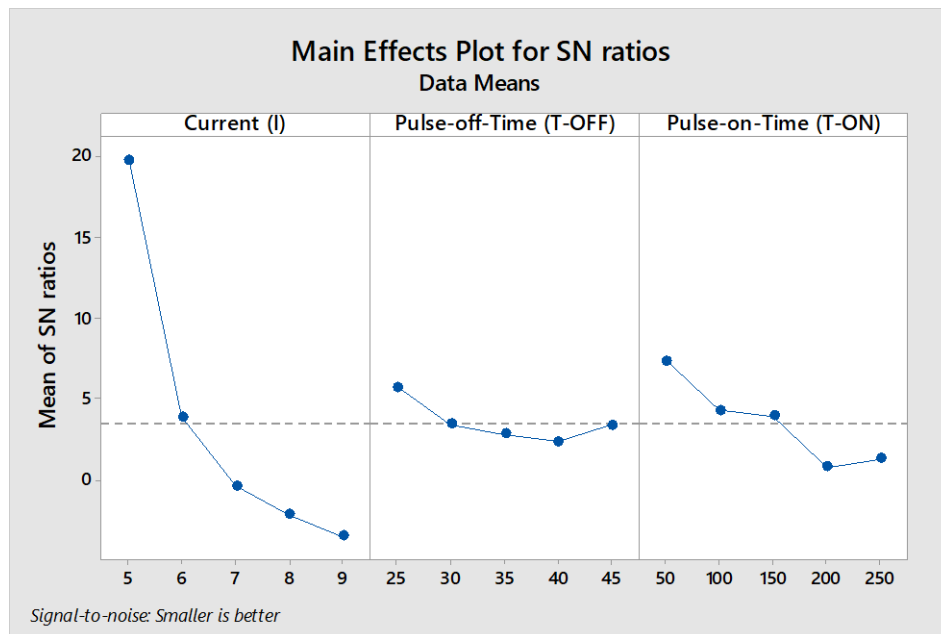


Figure 5.9: Primary Effects of Signal to Noise Ratios for TWR

Table 5.9: Response Values for TWR - S/N Ratios

TWR (Smaller is better)			
Level	Current (I)	Pulse-off-Time	Pulse-on-Time
1	19.8019	5.7173	7.3473
2	3.9149	3.4264	4.2892
3	-0.3939	2.8033	3.9625
4	-2.1742	2.3480	0.7833
5	-3.4901	3.3637	1.2765
Delta	23.2920	3.3693	6.5640
Rank	1	3	2

Table 5.10: Response Values for TWR - Means

Level	Current (I)	Pulse-off-Time	Pulse-on-Time
1	0.1386	0.9988	0.8010
2	0.6488	0.9788	0.8696
3	1.0550	0.9548	0.8128
4	1.3010	0.8710	1.0934
5	1.5054	0.8454	1.0720
Delta	1.3668	0.1534	0.2924
Rank	1	3	2

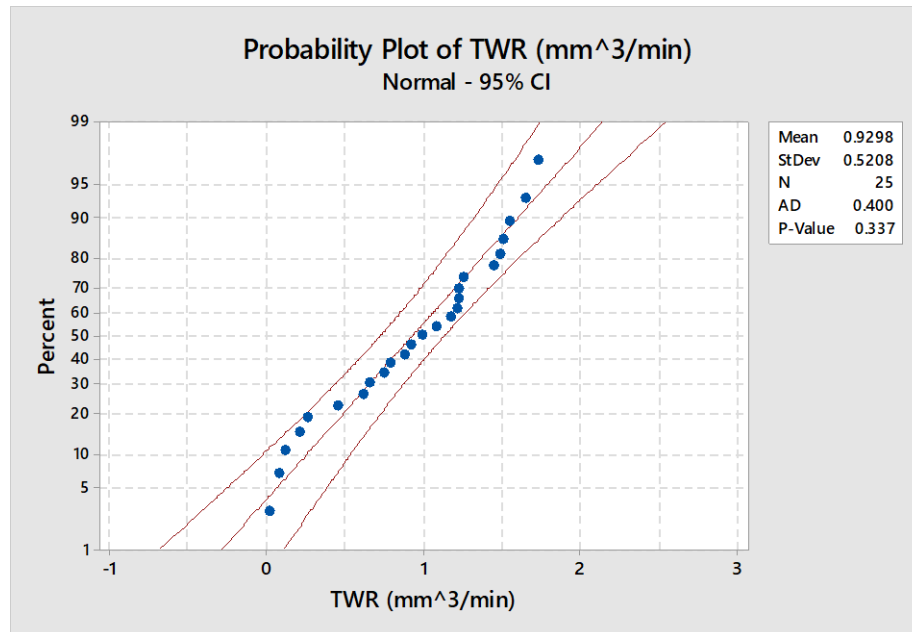


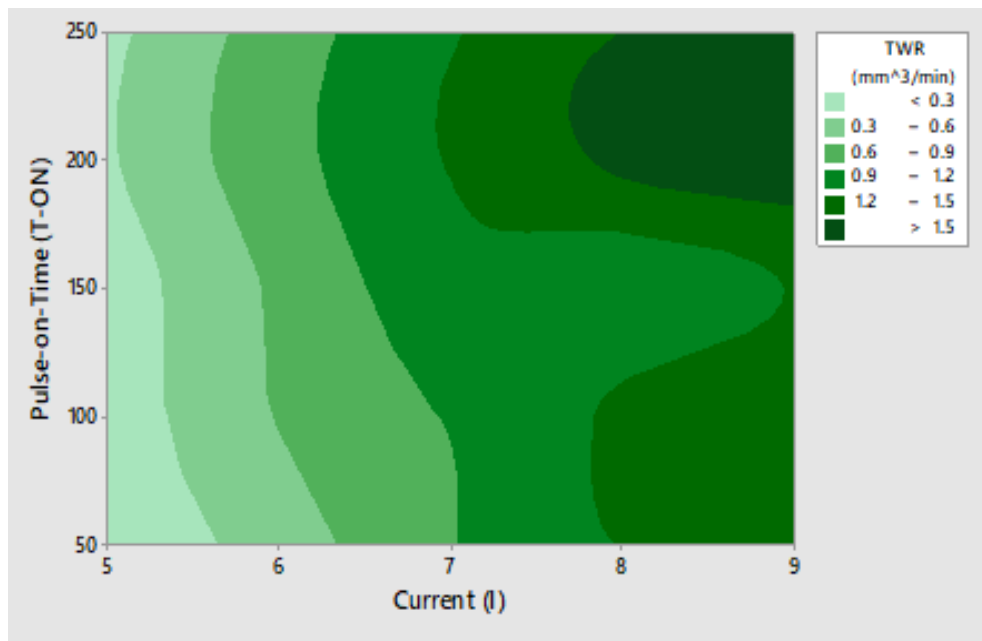
Figure 5.10: Normal Probability Plot of TWR

According to the Analysis of Variance (ANOVA) table provided in Table 5.11, the most important factors for tool wear rate, with a 95% confidence level, are the current and pulse-on time variables. The degree to which the input components account for the variation in TWR is shown by the metric R^2 . $R^2 = 98.9\%$ shows that the model has a high degree of accuracy for predicting the answer. The standard deviation of errors, $S = 0.0740804$. When the p-value is compared to the generally used confidence level of 0.05, it can be determined that if the $p \leq 0.05$, the effect is significant.

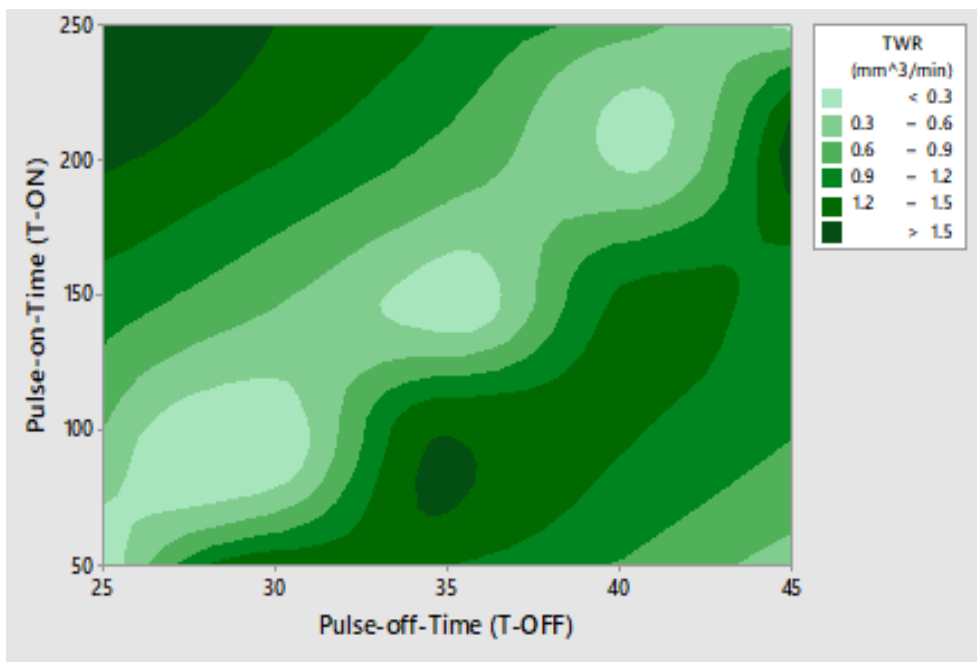
Table 5.11: ANOVA Table for the TWR

Source	DF	Adj SS	Adj MS	F-Value	P-Value
Current	4	5.94869	1.48717	270.99	0.000
Pulse-off-Time	4	0.09184	0.02296	4.18	0.123
Pulse-on-Time	4	0.40444	0.10111	18.42	0.000
Error	12	0.06585	0.00549		
Total	24	6.51083			
S	R-sq	R-sq(adj)			
0.0740804	98.99%	97.98%			

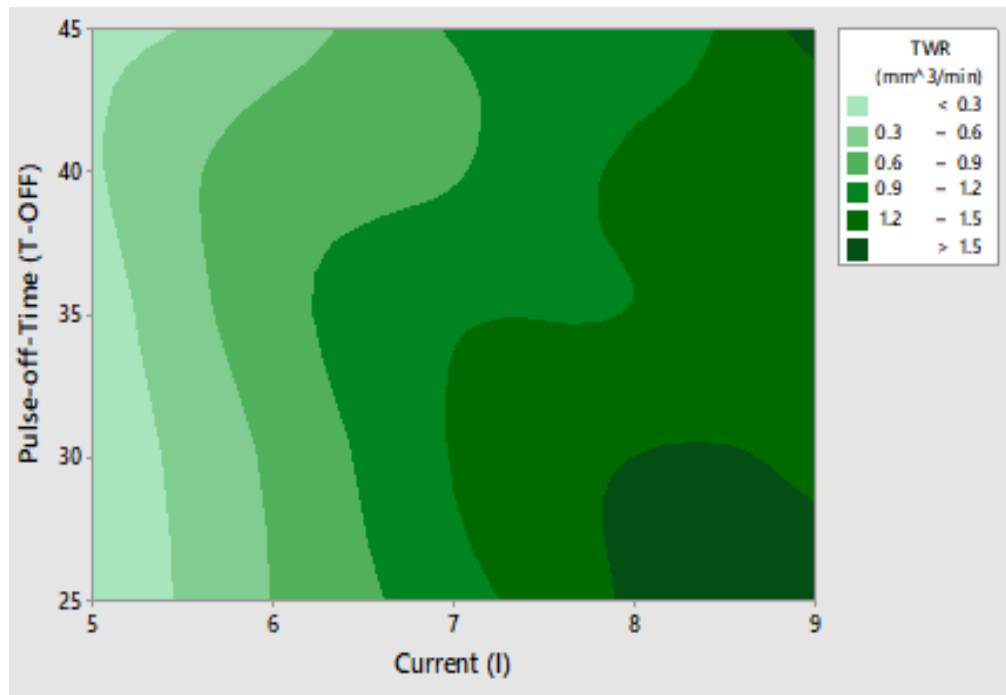
Figure 5.11 presents contour plots illustrating the tool wear rate in relation to: (a) current vs pulse-on time, (b) pulse-on time vs pulse-off time and (c) current vs pulse-off time. In Figure 5.11(a), the lightest region indicates the lowest TWR when both current and pulse-on time is minimized. It is evident that achieving the minimum TWR requires the current to be at its lowest across all pulse-on times. Figure 5.11(b) illustrates the relation between the duration of the pulse-on time and the pulse-off time with respect to TWR. According to the statistics, it is crucial to have a shorter pulse-on time (T_{ON}) and a longer pulse-off time (T_{OFF}) in order to obtain the lowest rate of tool wear. Figure 5.11(c) demonstrates the relationship between current and pulse-off time, showing that pulse-off time has a modest effect on TWR in comparison to current. Despite a reduced pulse-off time, a decrease in current can still lead to a lower rate of tool wear.



(a)



(b)



(c)

Figure 5.11: Contour Plots for TWR: (a) I vs T_{ON} (b) T_{ON} vs T_{OFF} (c) I vs T_{OFF}

The relationship between current, pulse on time and pulse off time for the response tool wear rate is displayed in Figure 5.12. It has been noted that current is the most important aspect when considering the pulse duration, pulse interval and current. Similarly while considering the pulse off time with pulse on time, pulse on time has the more interaction effect on the TWR.

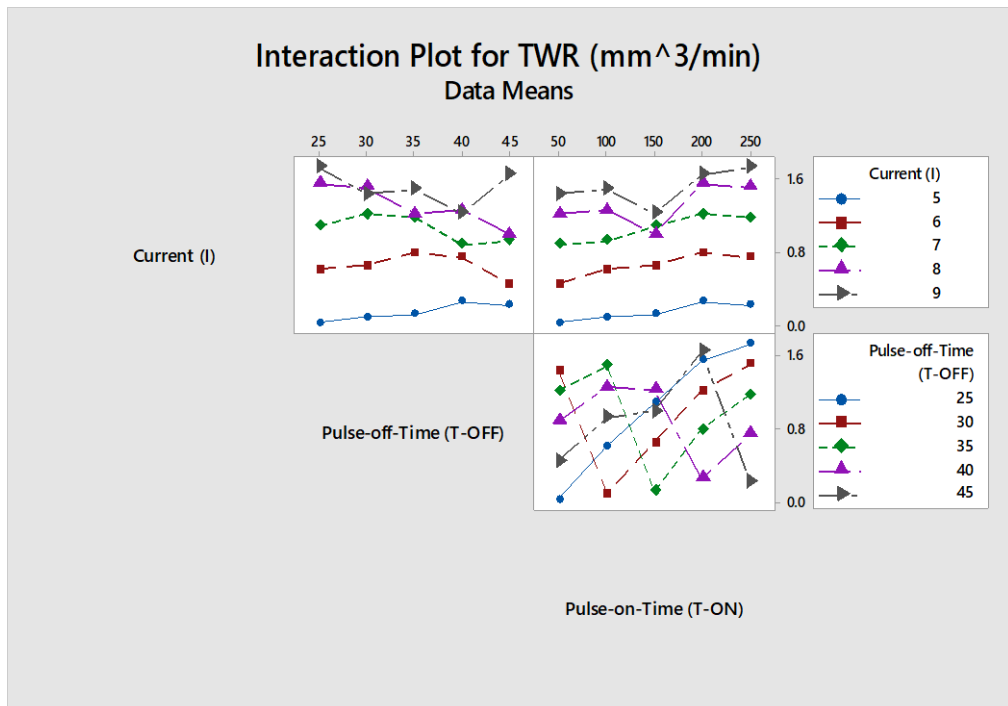


Figure 5.12: Interaction plot of TWR

5.5 PARAMETRIC ANALYSIS OF SURFACE ROUGHNESS (SR)

Since, surface roughness is considered to be minimum, Lower-The-Better (LTB) characteristics is selected for Taguchi analysis and the S/N ratio is determined using Equation 5.1. Table 5.12 displays the computed S/N ratio values for surface roughness, while Tables 5.13 and 5.14 display the response tables for S/N ratios and means, respectively. Similarly, the main effect plot for means and S/N ratios for SR have been shown in Figure 5.13 and Figure 5.14 respectively. From Tables 5.13 and 5.14 as well as Figures 5.12 and 5.13, it can be inferred that the most important component influencing the SR is current, which is then followed by the pulse-on time (T_{ON}) and pulse-off time (T_{OFF}). On the basis of lower the better characteristics; the minimum surface roughness is achieved for the combination of factors as current

5 A, pulse-off-time 25 μ s and pulse-on-time 50 μ s. It is also clear that the surface roughness increases with increase in current and pulse-on time generally.

According to the Analysis of Variance (ANOVA) table provided in Table 5.15, the most important factors for tool wear rate, with a 95% confidence level, are the current and pulse-on time variables. The degree of variance in surface roughness that is explained by the input parameters is expressed by the metric R^2 . $R^2 = 96.8\%$ shows that the model has a high degree of accuracy for predicting the answer. $S = 0.410024$ is the standard deviation of the errors. When the p-value is compared to the generally used confidence level of 0.05, it can be determined that if the $p \leq 0.05$, the effect is significant.

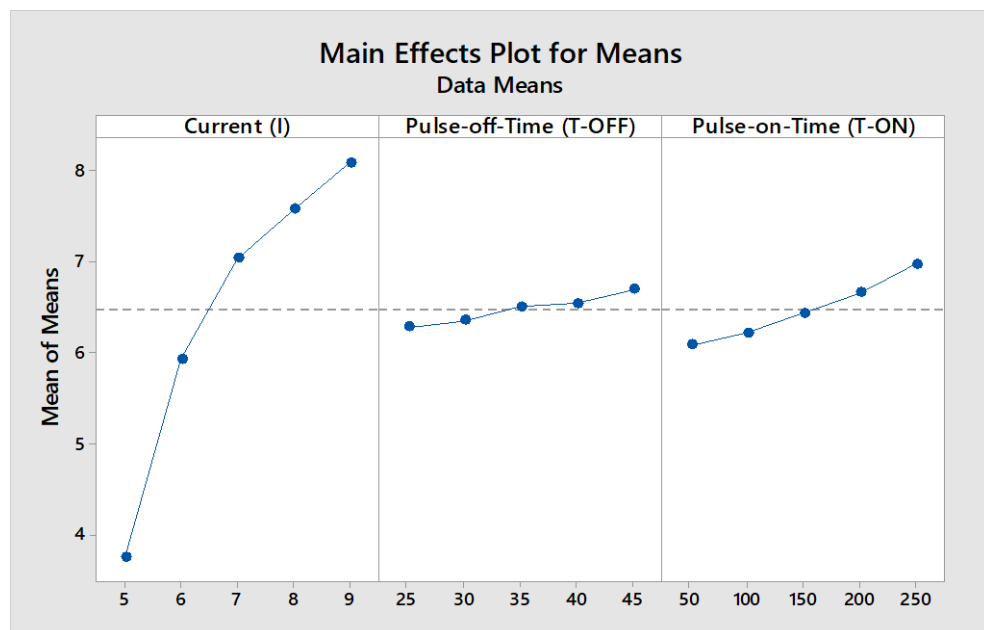


Figure 5.13: Primary Effects of Mean Values for SR

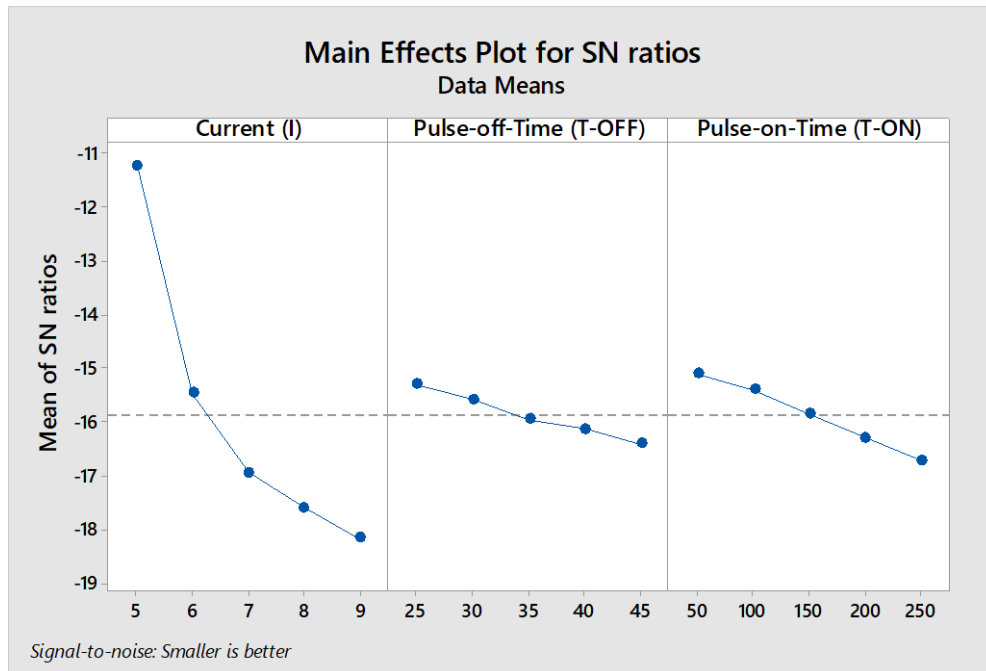


Figure 5.14: Primary Effects of Signal to Noise Ratios for SR

Figure 5.15 displays the SR residual charts. To determine whether the data deviate from normality, the standardised residuals are shown on a normal probability plot, as shown in Figure 5.15. The residuals are nearly falling inside the confidence interval, as can be observed, suggesting that they are nearly regularly distributed.

Contour plots showing the Surface Roughness (SR) in relation to T_{ON} vs T_{OFF} (c), current versus pulse-on time (a) and current versus pulse-off time (b) are shown in Figure 5.16. In Figure 5.16(a), the darkest region indicates the lowest surface roughness when both current and pulse-on time is minimum. Figure 5.16(b) illustrates the interaction between current and pulse-off time, indicating that pulse-off time has an insignificant impact on SR compared to current. Figure 5.16(c) illustrates the relation between the duration of spark-on time and spark-off time in respect to

SR. According to the statistics, reducing the pulse-on time is crucial in order to attain the minimum surface roughness.

Table 5.13: Calculated S/N Ratios for Surface Roughness

Expt. No.	S/N Ratio	Expt. No.	S/N Ratio
1	-8.29947	14	-16.3513
2	-9.57133	15	-16.6884
3	-11.3405	16	-17.7072
4	-12.9672	17	-17.853
5	-13.9096	18	-17.2307
6	-15.1327	19	-17.5359
7	-15.3134	20	-17.6391
8	-15.5195	21	-18.619
9	-15.563	22	-17.8752
10	-15.8198	23	-18.0943
11	-16.7896	24	-18.2444
12	-17.2783	25	-17.9855
13	-17.6277		

Table 5.14: Response Values for S/N Ratios - SR

SR (Smaller is better)			
Level	Current (I)	Pulse-off-Time (T-OFF)	Pulse-on-Time (T-ON)
1	-11.22	-15.31	-15.12
2	-15.47	-15.58	-15.40
3	-16.95	-15.96	-15.87
4	-17.59	-16.13	-16.29
5	-18.16	-16.41	-16.71
Delta	6.95	1.10	1.60
Rank	1	3	2

Table 5.15: Response Values for Means - SR

Level	Current (I)	Pulse-off-Time (T-OFF)	Pulse-on-Time (T-ON)
1	3.742	6.286	6.090
2	5.938	6.358	6.222
3	7.046	6.514	6.444
4	7.582	6.544	6.668
5	8.098	6.704	6.982
Delta	4.356	0.418	0.892
Rank	1	3	2

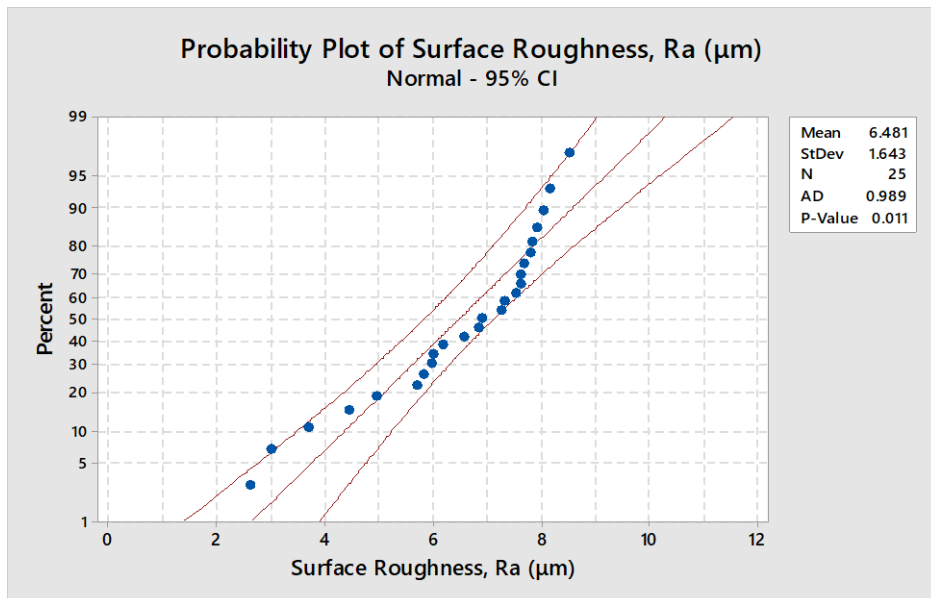
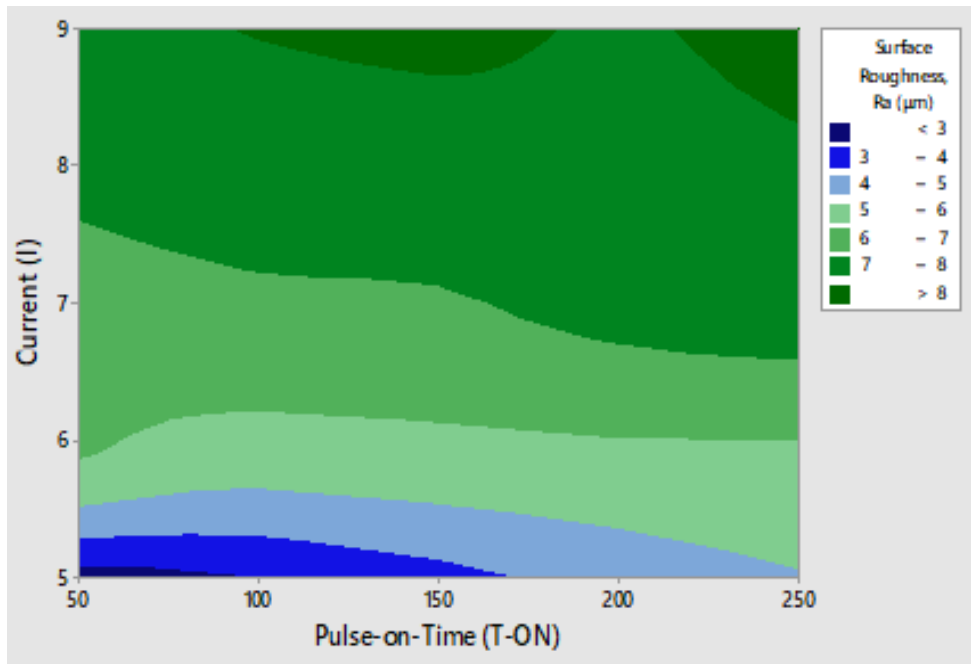


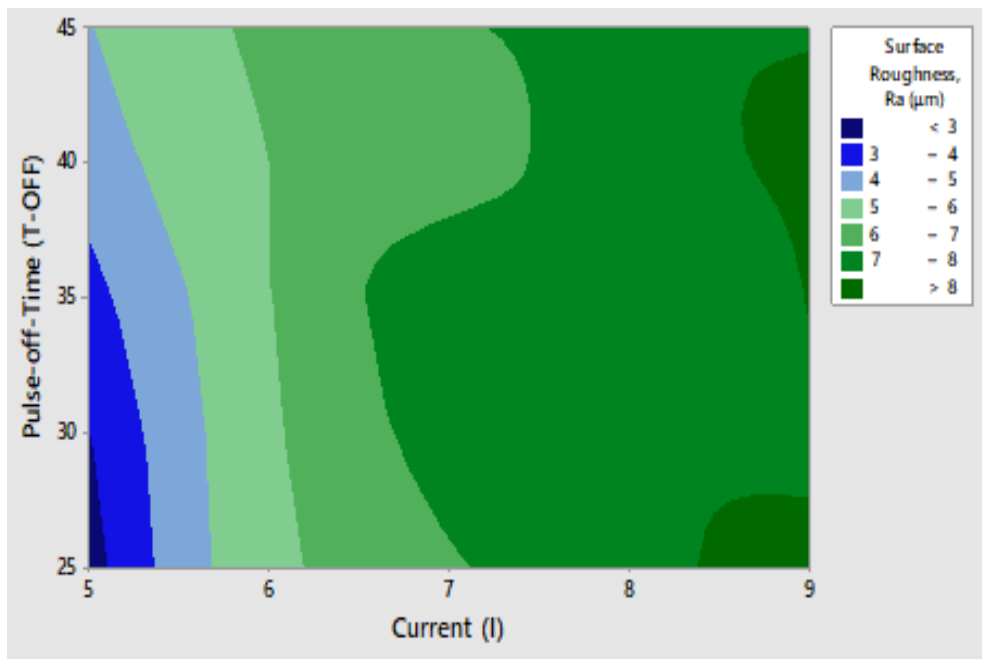
Figure 5.15: Residual Plot of SR

Table 5.14: ANOVA Table for the SR

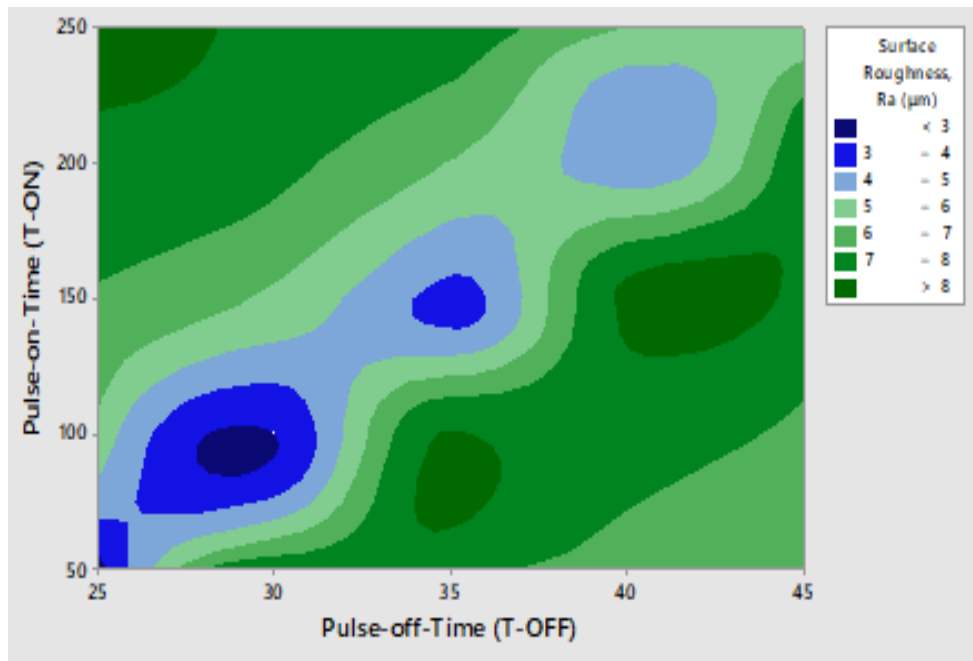
Source	DF	Adj SS	Adj MS	F-Value	P-Value
Current (I)	4	59.7154	14.9289	88.80	0.000
Pulse-off-Time (T-OFF)	4	0.5397	0.1349	0.80	0.547
Pulse-on-Time (T-ON)	4	2.5365	0.6341	3.77	0.033
Error	12	2.0174	0.1681		
Total	24	64.8091			
S	R-sq	R-sq(adj)			
0.410024	96.89%	93.77%			



(a)



(b)



(c)

Figure 5.16: Contour Plots for SR: (a) I vs T_{ON} (b) I vs T_{OFF} (c) T_{ON} vs T_{OFF}

Figure 5.17 demonstrates the relationship between I, T_{ON} , T_{OFF} and the response as SR. It has been noted that current is the most important aspect when taking current, pulse off time and pulse on time into account. In a similar vein, when comparing pulse on and off times, pulse on time significantly affects surface roughness.

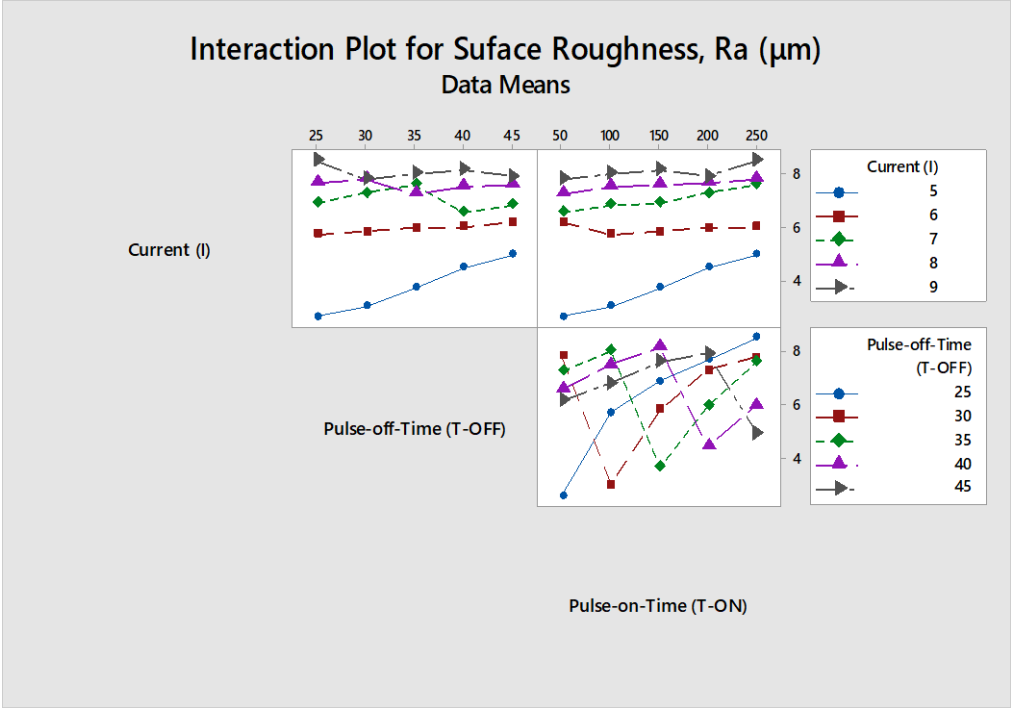


Figure 5.17: Interaction Plot of SR

CHAPTER 6

CONCLUSIONS AND FUTURE SCOPE

6.1 CONCLUSIONS

EDM's significant advantage of contactless machining and it has become the main tool in manufacturing due to its capacity to execute three-dimensional machining regardless of the hardness of the material. The incorporation of high-precision machining technologies like electronic pulses and CNC controlled movements of axes and electrodes has increased EDM's productivity in producing macro and micro-structures, as well as complex 3D structures.

The present study is decisive on the fabrication of micro geometries of different shapes using die-sinking EDM and exploring its micro-machining capabilities. Using a 400 micron-diameter copper tool electrode, the appropriate micro-scale designs are first generated over an alloy steel EN-24 work material using the die-sinking electrical discharge machining technique and then the machining performance is assessed by looking at geometric tolerances, surface integrity, micro cracks, TWR, recast layer, surface texture parameters, dimensional accuracy and shape variations brought on by the different geometries' shapes. The parametric analysis in die-sinking EDM of pentagonal cavities has also been conducted to examine how input parameters relate with performance metrics.

In light of the experimental findings, the following noteworthy conclusions can be drawn:

- The occurrence of random secondary discharges, alterations in discharge location and the joint impact of ion bombardment and thermo mechanical waves result in overcutting, corner rounding as well as tool wear. Among micro holes and micro channels, it is found that round micro holes have the lowest standard deviation of 9, the best dimensional control whereas micro channels have rather inadequate dimensional control with width and length standard deviations of 20.84 and 43.02 respectively
- The durability and functionality of mechanical components are significantly influenced by geometric tolerance. The roundness inaccuracy acquired by MZC and the straightness tolerance obtained by the least squares approach both meet ISO and ANSI requirements. According to the obtained geometric tolerance, the produced cavities are found to be of acceptable quality with fine tolerance, which means that the micro holes have very little roundness error of $46.33 \mu\text{m}$ and the micro channels are almost straight having average straightness tolerance of $13.51 \mu\text{m}$
- The tool wear rate is lower in channel machining because there is a greater discharge area, which also results in a smaller incidence of side discharge. According to the report, the computed TWR values are 0.91×10^4 and $0.71 \times 10^4 \mu\text{m}^3/\text{s}$, respectively
- In reference to investigation of tool wear in polygonal cavities, it has been found that the polygonal cavity's complexity directly affects the rate of wear of tool. Hence, in case of machining of hexagonal cavities, there is maximum

wear of tool of $7.69 \times 10^4 \mu\text{m}^3/\text{s}$ while minimum tool wear occurs during the machining of triangular cavities having value of $5.77 \times 10^4 \mu\text{m}^3/\text{s}$

- A detailed examination of the machined part's surface properties showed the presence of a recast layer, which was more noticeable around the cavity borders. Recast layer and micro cracks that start at the surface and travel vertically through the entire recast layer are revealed by analyzing the surface features of the geometry
- The formation of a recast layer becomes more prominent when working with complex and higher-order polygons. Sudden changes in the tool path's direction can cause uneven energy distribution, leading to inconsistent material removal and a thicker, irregular recast layer in higher-order polygons. This uneven energy distribution can also increase the likelihood of micro-cracks forming in the workpiece material. These micro-cracks may develop at the boundaries between different material removal passes due to stress concentration.
- Elemental examination of the machined surfaces indicates the presence of both tool electrode material and foreign contaminants
- Triangular micro cavities have an average angularity error of 4.34° , whereas square, pentagonal, and hexagonal micro cavities have average angularity errors of 1.33° , 7.93° and 8.74° respectively. The data acquired indicates that, in comparison to other cavities, the square cavities have the highest angular accuracy. It could be explained by the fact that limited tool motion and square cavities result in less secondary discharge.

- According to parametric analysis, the most important factor in the machining of pentagonal cavities is current, which has a P value of 0.000 and affects the MRR. The pulse-on-time and pulse-off-time have P values of 0.043 and 0.188 respectively. Regarding TWR, the most significant factor, with a P value of 0.000, is the current. The next most significant factors are the pulse-on-time and pulse-off-time which have values of 0.024 and 0.123 respectively
- Current is the most contributing factor for surface roughness having P value of 0.000 while the influence of pulse-on-time is insignificant.

6.2 SCOPE OF FUTURE WORK

This section highlights the scope of future work for the benefit of the research community and industry.

- There is a need to make use of die-sinking EDM's technological improvements for the construction of macro and micro scale functional systems in order to assess this method's capacity for micromachining and provide inspiring research
- Further research also exists to explore the long term effects of EDM machining of polygonal cavities on different materials utilizing wide range of electrode materials of different kinds and to develop more efficient parameter optimization techniques
- To improve the accuracy and dependability of results, research possibilities are also available in the improvement and implementation of computational

and mathematical tools for tolerance analysis as well as micro measurement techniques.

- Improving the flushing mechanism and tool rotation facility can enhance the process performance. To achieve synchronized rotation and translation of the tool, the feed speeds of axes need to be improved. This work represents significant progress towards utilizing the capabilities of multi-axis CNC electrical discharge machines, which have remained largely unexplored.
- After reporting hopeful results on the machining of polygonal cavities in EDM and investigating machining performance, the authors are continuing their investigation to establish process capability mapping for both regular and irregular geometries in order to facilitate the design of multi-scale serviceable devices which are becoming more popular because to their many excellent uses.

REFERENCES

- [1] El-Hofy, H. (2005). Advanced machining processes: nontraditional and hybrid machining processes. *McGraw-Hill*.
- [2] Singh, J., & Kumar, V. (2012). Investigation on the Material Removal Mechanism and the Thermal Aspects in the Electrical Discharge Machining Process. *International Journal of Engineering and Technology*, 2(9), 1503-1507.
- [3] Guu, Y. H. (2005). AFM surface imaging of AISI D2 tool steel machined by the EDM process. *Applied Surface Science*, 242, 245-250.
- [4] Kansal, H. K., Singh, S., & Kumar, P. (2007). Effect of silicon powder mixed EDM on machining rate of AISI D2 die steel. *Journal of Manufacturing Processes*, 9(1), 13-22.
- [5] Saha, S. K., & Chaudhary, S. K. (2009). Experimental investigation and empirical modelling of the dry electrical discharge machining process. *International Journal of Machine Tools and Manufacture*, 49, 297-308.
- [6] Abu Zied, O. A. (1996). The role of voltage pulse off time in the electro discharge machined AISI T1 high speed steel. *Journal of Materials Processing Technology*, 61, 287-291.
- [7] Crookall, J. R., & Heuvelman, C. J. (1971). Electro-discharge machining-the state of the art. *Annals of the CIRP*, 20, 113-120.
- [8] Amorim, F. L., & Weingaertner, W. L. (2002). Influence of duty factor on the die sinking electrical discharge machining of high-strength aluminum alloy under rough machining. *Journal of the Brazilian Society of Mechanical Sciences*, 24, 194-199.

- [9] Rao, G. K. M., Satyanarayana, S., & Praveen, M. (2008). Influence of machining parameters on electric discharge machining of maraging steels-An experimental investigation. *In Proceedings of the World Congress on Engineering*, Vol. II.
- [10] Lee, S. H., & Li, X. P. (2001). Study of the effect of machining parameters on the machining characteristics in electrical discharge machining of tungsten carbide. *Journal of Materials Processing Technology*, 115, 344-358.
- [11] Chow, H. M., Yan, B. H., & Huang, F. Y. (1999). Micro slit machining using electrodischarge machining with a modified rotary disk electrode (RDE). *Journal of Materials Processing Technology*, 91, 161-166.
- [12] Mohan, B., Rajadurai, A., & Satyanarayana, K. G. (2004). Electric discharge machining of Al-SiC metal matrix composites using rotary tube electrode. *Journal of Materials Processing Technology*, 153-154, 978-985.
- [13] Soni, J. S., & Chakraverti, G. (1997). Performance evaluation of rotary EDM by experimental design technique. *Defense Science Journal*, 47(1), 65-73.
- [14] Sommer, C. (2000). Non-traditional machining handbook (1st ed.). *Advance Publishing*.
- [15] Chen, S. L., Yan, B. H., & Huang, F. Y. (1999). Influence of kerosene and distilled water as dielectric on electric discharge machining characteristics of Ti 6Al 4V. *Journal of Materials Processing Technology*, 87(1-3), 107-111.
- [16] Murali, M., & Yeo, S. H. (2004). A novel sparks erosion technique for the fabrication of high aspect ratio micro-grooves. *Microsystems Technologies*, 10, 628-632.

- [17] Singh, S., Maheswari, S., & Pandey, P. C. (2007). Optimization of multi-performance characteristics in electrical discharge machining of Aluminium matrix composites (AMCs) using Taguchi DOE methodology. *International Journal of Manufacturing Research*, 2(2), 138-163.
- [18] Wang, Z. L., Cui, J. Z., Liu, X. F., & Zhao, W. S. (2004). Mechanism of electrode material removal in short pulse time electric discharge machining. *Materials Science Forum*, 471-472, 784-789.
- [19] Lauwers, B., Kruth, J. P., Liu, W., Eraerts, W., Schacht, B., & Bleys, P. (2004). Investigation of material removal mechanisms in EDM of composite ceramic materials. *Journal of Materials Processing Technology*, 149, 347-352.
- [20] Singh, A., & Ghosh, A. (1999). A thermo-electric model of material removal during electric discharge machining. *International Journal of Machine Tools and Manufacture*, 39, 669-682.
- [21] Yahya, A., & Manning, C. D. (2004). Determination of material removal rate of an electro-discharge machine using dimensional analysis. *Journal of Physics D: Applied Physics*, 37, 1467-1471.
- [22] Erden, A., & Kaftanoglu, B. (1981). Thermo-mathematical modelling and optimization of energy pulse forms in electric discharge machining (EDM). *International Journal of Machine Tool Design and Research*, 21, 11-22.
- [23] Bergs, T., Schneider, S., Harst, S., & Klink, A. (2019). Numerical simulation and validation of material loadings during electrical discharge machining. *Procedia CIRP*, 82, 14-19.

- [24] Yue, X., Li, Q., & Yang, X. (2020). Influence of thermal stress on material removal of Cf_SiC composite in EDM. *Ceramics International*, 46(6), 7998-8009.
- [25] Gostimirovic, M., Radovanovic, M., Madic, M., et al. (2018). Inverse electro-thermal analysis of the material removal mechanism in electrical discharge machining. *International Journal of Advanced Manufacturing Technology*, 97, 1861-1871.
- [26] Yue, X., Yang, X., & Kunieda, M. (2018). Influence of metal vapor jets from tool electrode on material removal of workpiece in EDM. *Precision Engineering*, 53, 278-288.
- [27] Govindan, P., Gupta, A., Joshi, S. S., Malshe, A., & Rajurkar, K. P. (2013). Single-spark analysis of removal phenomenon in magnetic field assisted dry EDM. *Journal of Materials Processing Technology*, 213(7), 1048-1058.
- [28] Yue, X., & Yang, X. (2020). Molecular dynamics simulation of material removal process and mechanism of EDM using a two-temperature model. *Applied Surface Science*, 528, 147009.
- [29] Bilal, A., Perveen, A., Talamona, D., & Jahan, M. P. (2021). Understanding material removal mechanism and effects of machining parameters during EDM of zirconia toughened alumina ceramic. *Micromachines*, 12, 67.
- [30] Lu, Y., Rao, X., Du, J., et al. (2022). Material removal mechanism of RB-SiC ceramics in dry impulse electrical discharge machining. *International Journal of Advanced Manufacturing Technology*, 122, 2407-2417.

- [31] Natsu, W., Ojima, S., Kobayashi, T., & Kunieda, M. (2004). Temperature distribution measurement in EDM arc plasma using spectroscopy. *JSME International Journal, Series C*, 47(1).
- [32] Panda, D. K. (2008). Study of thermal stresses induced surface damage under growing plasma channel in electro-discharge machining. *Journal of Materials Processing Technology*, 202(1-3), 86-95.
- [33] Natsu, W., Shimoyamada, M., & Kunieda, M. (2006). Study on expansion process of EDM arc plasma. *JSME International Journal, Series C*, 49(2).
- [34] Pandey, P. C., & Jilani, S. T. (1986). Plasma channel growth and the resolidified layer in EDM. *Precision Engineering*, 8(2), 104-110.
- [35] Shabgard, M., Ahmadi, R., Seyedzavvar, M., & Nadimi Babil Oliaei, S. (2013). Mathematical and numerical modeling of the effect of input parameters on the flushing efficiency of plasma channel in EDM process. *International Journal of Machine Tools and Manufacture*, 65, 79-87.
- [36] Li, Q., & Yang, X. (2020). Study on arc plasma movement and its effect on crater morphology during single-pulse discharge in EDM. *International Journal of Advanced Manufacturing Technology*, 106, 5033-5047.
- [37] Tanveer, A., Kapoor, S. G., Mujumdar, S., & Curreli, D. (2023). One-dimensional plasma model of electrical discharge machining in deionized water for prediction of plasma characteristics along the interelectrode gap. *ASME Journal of Manufacturing Science and Engineering*, 145(1), 011012.
- [38] Yue, X., & Yang, X. (2021). The role of discharge plasma on molten pool dynamics in EDM. *Journal of Materials Processing Technology*, 293, 117092.

- [39] Li, X., Wei, D., Li, Q., et al. (2020). Study on effects of electrode material and dielectric medium on arc plasma in electrical discharge machining. *International Journal of Advanced Manufacturing Technology*, 107, 4403-4413.
- [40] Lee, H. T., & Tai, T. Y. (2003). Relationship between EDM parameters and surface crack formation. *Journal of Materials Processing Technology*, 142, 676-683.
- [41] Sohani, M. S., Gaitonde, V. N., Siddeswarappa, B., & Deshpande, A. S. (2009). Investigations into the effect of tool shapes with size factor consideration in sink electrical discharge machining (EDM) process. *International Journal of Advanced Manufacturing Technology*, 45, 1131-1145.
- [42] Puertas, I., & LUIS, C. J. (2003). A study on the machining parameters optimization of electrical discharge machining. *Journal of Materials Processing Technology*, 521-526.
- [43] Guu, Y. H., & Hocheng, H. (2001). Effects of work piece rotation on machinability during electrical discharge machining. *Materials and Manufacturing Processes*, 16(1), 91-101.
- [44] Kumar, A., Kumar, V., & Kumar, J. (2012). Prediction of surface roughness in wire electric discharge machining (WEDM) process based on response surface methodology. *International Journal of Engineering & Technology*, 2(4), 708-719.
- [45] Nikalje, A. M., Kumar, A., & SaiSrinadh, K. V. (2013). Influence of parameters and optimization of EDM performance measures on MDN 300 steel using Taguchi method. *International Journal of Advanced Manufacturing Technology*, 69, 41-49.

- [46] Patel, K. M., Panday, P. M., & Rao, P. V. (2009). Determination of an optimum parametric combination using a surface roughness prediction model for EDM of Al₂O₃/SiCw/TiC ceramic composite. *Journal of Materials and Manufacturing Processes*, 24, 675-682.
- [47] Tzeng, Y., & Chen, F. (2007). Multi-objective optimisation of high-speed electrical discharge machining process using a Taguchi fuzzy-based approach. *Materials & Design*, 28(4), 1159-1168.
- [48] Kansal, H. K., Singh, S., & Kumar, P. (2005). Parametric optimization of powder mixed electrical discharge machining by response surface methodology. *Journal of Materials Processing Technology*, 169(3), 427-436.
- [49] Arooj, S., Shah, M., Sadiq, S., Iqbal, S. H., & Khushnood, S. (2014). Effect of current in the EDM machining of aluminum 6061 T6 and its effect on the surface morphology. *Arabian Journal for Science and Engineering*, 39, 4187- 4199.
- [50] Yu, Z., Tahasaki, J., Nakajima, N., Sano, S., Karatok, K., & Kunieda, M. (2005). Feasibility of 3-D surface machining by dry EDM. *International Journal of Electrical Machining*, 10, 15-20.
- [51] Zhang, Q. H., Zhang, J. H., Ren, S. F., Niu, Z. W., & Ai, X. (2005). A theoretical model of surface roughness in ultrasonic vibration assisted electrical discharge machining in gas. *International Journal of Manufacturing Technology and Management*, 7, 381-390.
- [52] Guu, Y. H., & Hou, M. T. (2007). Effect of machining parameters on surface textures in EDM of Fe-Mn-Al alloy. *Materials Science and Engineering A*, 466, 61-67.

- [53] Senthil, P., Vinodh, S., & Singh, A. K. (2014). Parametric optimisation of EDM on Al-Cu/TiB₂ in-situ metal matrix composites using TOPSIS method. *International Journal of Machining and Machinability of Materials*, 16(1), 80-94.
- [54] Tang, L., & Du, Y. T. (2014). Experimental study on green electrical discharge machining in tap water of Ti-6Al-4V and parameters optimization. *International Journal of Advanced Manufacturing Technology*, 70, 469-475.
- [55] Hascalik, A., & Caydas, U. (2007). Electrical discharge machining of titanium alloy (Ti-6Al-4V). *Applied Surface Science*, 253, 9007-9016.
- [56] Rebelo, J. C., Dias, A. M., Kremer, D., & Lebrun, J. L. (1998). Influence of EDM pulse energy on the surface integrity of martensitic steels. *Journal of Materials Processing Technology*, 84, 90-96.
- [57] Nakamura, M., Shigematsu, I., Kanayama, K., & Hirai, Y. (1991). Surface damage in ZrB₂-based composite ceramics induced by electro-discharge machining. *Journal of Materials Science*, 26, 6078-6082.
- [58] Dewangan, S., Gangopadhyay, S., & Biswas, C. K. (2015). Multi-response optimization of surface integrity characteristics of EDM process using grey-fuzzy logic-based hybrid approach. *Engineering Science and Technology, an International Journal*, 18(3), 361-368.
- [59] Marichamy, S., Saravanan, M., Ravichandran, M., et al. (2016). Parametric optimization of EDM process on α - β brass using Taguchi approach. *Russian Journal of Non-Ferrous Metals*, 57, 586-598.

- [60] Kumar, P., & Parkash, R. (2016). Experimental investigation and optimization of EDM process parameters for machining of aluminum boron carbide (Al-B₄C) composite. *Machining Science and Technology*, 20(2), 330-348.
- [61] Dang, X. P. (2018). Constrained multi-objective optimization of EDM process parameters using kriging model and particle swarm algorithm. *Materials and Manufacturing Processes*, 33(4), 397-404.
- [62] Baghel, R., Mali, H. S., & Biswas, S. K. (2019). Parametric optimization and surface analysis of diamond grinding-assisted EDM of TiN-Al₂O₃ ceramic composite. *International Journal of Advanced Manufacturing Technology*, 100, 1183-1192.
- [63] Mahdih, M. S., & Mahdavinejad, R. (2016). Recast layer and micro-cracks in electrical discharge machining of ultra-fine-grained aluminum. *Proceedings of the Institution of Mechanical Engineers, Part B: Journal of Engineering Manufacture*, 1-10.
- [64] Phan, N. H., & Muthuramalingam, T. (2021). Multi-criteria decision-making of vibration-aided machining for high silicon-carbon tool steel with Taguchi-TOPSIS approach. *Silicon*, 13, 2771-2783.
- [65] Phan, N. H., & Muthuramalingam, T. (2021). Multi criteria decision making of vibration assisted EDM process parameters on machining silicon steel using Taguchi-DEAR methodology. *Silicon*, 13, 1879-1885.
- [66] Phan, N. H., Banh, T. L., Mashood, K. A., Tran, D. Q., Pham, V. D., Muthuramalingam, T., Nguyen, V. D., & Nguyen, D. T. (2020). Application of TGRA-based optimisation for machinability of high-chromium tool steel in the EDM process. *Arabian Journal for Science and Engineering*, 45, 5555-5562.

- [67] Maradia, U., Benavoli, A., Boccadoro, M., Bonesana, C., Klyuev, M., Zaffalon, M., Gambardella, L., & Wegener, K. (2018). EDM drilling optimisation using stochastic techniques. *Procedia CIRP*, 67, 350-355.
- [68] Dikshit, M. K., Anand, J., Narayan, D., et al. (2019). Machining characteristics and optimization of process parameters in die-sinking EDM of Inconel 625. *Journal of the Brazilian Society of Mechanical Sciences and Engineering*, 41, 302.
- [69] Chakraborty, S., Mitra, S., & Bose, D. (2020). Performance analysis on eco-friendly machining of Ti6Al4V using powder mixed with different dielectrics in WEDM. *International Journal of Automotive and Mechanical Engineering*, 17(3), 8128-8139.
- [70] Ablyaz, T. R., Shlykov, E. S., Muratov, K. R., Mahajan, A., Singh, G., Devgan, S., & Sidhu, S. S. (2020). Surface characterization and tribological performance analysis of electric discharge machined duplex stainless steel. *Micromachines*, 11 (10), 926.
- [71] Viswanth, S., Srinivas, R., Radhakrishnan, R., Ramanujam, G., & Rajyalakshmi. (2020). Performance study of eco-friendly dielectric in EDM of AISI 2507 super duplex steel using Taguchi-fuzzy TOPSIS approach. *International Journal of Productivity and Quality Management*, 29 (4), 518-541.
- [72] Kliuev, M., Boccadoro, M., Perez, R., Dal Bó, W., Stirnimann, J., Kuster, F., & Wegener, K. (2016). EDM drilling and shaping of cooling holes in Inconel 718 turbine blades. *Procedia CIRP*, 42, 322-327.

- [73] Ahmed, A., Tanjilul, M., Rahman, M., et al. (2020). Ultrafast drilling of Inconel 718 using hybrid EDM with different electrode materials. *International Journal of Advanced Manufacturing Technology*, 106, 2281-2294.
- [74] Chuvaree, S., & Kanlayasiri, K. (2018). Improving the performance of EDM deep hole using multihole interior flushing electrode. *IOP Conference Series: Materials Science and Engineering*, 361 012013.
- [75] Khan, A. A., Ali, M. Y., & Haque, M. M. (2009). A study of electrode shape configuration on the performance of die sinking EDM. *International Journal of Mechanical and Materials Engineering*, 4, 19-23.
- [76] Lin, Z., Guo, Z., Jiang, S., Liu, G., & Liu, J. (2018). Electrical discharge drilling of metal matrix composites with a hollow hexagonal electrode. *Advanced Composites Letters*, 27(5), 193–203.
- [77] Nair, S., Dutta, A., Narayanan, R., & Giridharan, A. (2019). Investigation on EDM machining of Ti6Al4V with negative polarity brass electrode. *Materials and Manufacturing Processes*, 34, 1824-1831.
- [78] Bozdana, A. T., & Ulutas, T. (2015). The Effectiveness of Multichannel Electrodes on Drilling Blind Holes on Inconel 718 by EDM Process. *Materials and Manufacturing Processes*, 31(4), 504–513.
- [79] Chern, G. L., & Chuang, Y. (2006). Study on vibration-EDM and mass punching of micro-holes. *Journal of Materials Processing Technology*, 180, 151 - 160.
- [80] Khan, A. A. (2008). Electrode wear and material removal rate during EDM of aluminum and mild steel using copper and brass electrodes. *International Journal of Advanced Manufacturing Technology*, 39, 482-487.

- [81] Li, L., Gu, L., Xi, X., & Zhao, W. (2012). Influence of flushing on performance of EDM with bunched electrode. *International Journal of Advanced Manufacturing Technology*, 58, 187-194.
- [82] Syed, K. H., & Palaniyandi, K. (2012). Performance of electrical discharge machining using aluminium powder suspended distilled water. *Turkish Journal of Engineering and Environmental Sciences*, 36, 195-207.
- [83] Yilmaz, O., & Okka, M. A. (2010). Effect of single and multi-channel electrodes application on EDM fast hole drilling performance. *International Journal of Advanced Manufacturing Technology*, 51, 185-194.
- [84] Weng, F. T., & Her, M. G. (2002). Study of the batch production of micro parts using the EDM process. *International Journal of Advanced Manufacturing Technology*, 19, 266-270.
- [85] Flanoa, O., Ayesta, I., Izquierdo, B., Sanchez, J. A., Zhao, C., & Kunieda, M. (2018). Improvement of EDM performance in high-aspect ratio slot machining using multi-holed electrodes. *Precision Engineering*, 51, 223-231.
- [86] Puri, Y. M., & Gohil, V. (2017). Experimental study of material removal rate in electrical discharge turning of titanium alloy (Ti-6Al-4V). *IOP Conference Series: Materials Science and Engineering*, 187.
- [87] Li, L., Hao, J., Deng, Y., & Wang, H. (2013). Study of Dry EDM Milling Integrated with Electrode Wear Compensation and Finishing. *Materials and Manufacturing Processes*, 28(4), 403–407.
- [88] Moarrefzadeh, A. (2012). Study of workpiece thermal profile in Electrical Discharge Machining (EDM) process. *WSEAS Transactions on Applied and Theoretical Mechanics*, 7, 83-92.

- [89] Kim, B. H., Ok, J. G., Kim, Y. H., & Chu, C. N. (2007). Electrical discharge machining of carbon nanofiber for uniform field emission. *Annals of the CIRP*, 56, 233-236.
- [90] Liu, K., Reynaerts, D., & Lauwers, B. (2009). Influence of the pulse shape on the EDM performance of Si₃N₄-TiN ceramic composite. *CIRP Annals - Manufacturing Technology*, 58, 217-220.
- [91] Egashira, K., Matsugasako, A., Tsuchiya, H., & Miyazaki, M. (2006). Electrical discharge machining with ultralow discharge energy. *Precision Engineering*, 30, 414-420.
- [92] Shankar, P., Jain, V. K., & Sundararajan, T. (1997). Analysis of spark profiles during EDM process. *Machining Science and Technology*, 1, 195-217.
- [93] Khanra, A. K., Pathak, L. C., & Godkhindi, M. M. (2007). Microanalysis of debris formed during electrical discharge machining (EDM). *Journal of Materials Science*, 42, 872-877.
- [94] Singh, S., Maheshwari, S., & Pandey, P. C. (2004). Some investigations into the electric discharge machining of hardened tool steel using different electrode materials. *Journal of Materials Processing Technology*, 149, 272-277.
- [95] Lee, H. T., Rehbach, W. P., Tai, T. Y., & Hsu, F. C. (2004). Relationship between electrode size and surface cracking in the EDM machining process. *Journal of Materials Science*, 39, 6981-6986.
- [96] Ghanem F., Braham C., Sidhom. H., "Influence of steel type on electrical discharge machined surface integrity", *Journal of Materials Processing Technology*, 2003, 143, pp. 163-173.

- [97] Yadav, V., Jain, V. K., & Dixit, P. M. (2002). Thermal stresses due to electrical discharge machining. *International Journal of Machine Tools & Manufacture*, 42, 877-888.
- [98] Shen, Y., Liu, Y., Dong, H., & et al. (2017). Surface integrity of Inconel 718 in high-speed electrical discharge machining milling using air dielectric. *International Journal of Advanced Manufacturing Technology*, 90, 691-698.
- [99] Li, C., Xu, X., Li, Y., Tong, H., Ding, S., Kong, Q., Zhao, L., & Ding, J. (2019). Effects of dielectric fluids on surface integrity for the recast layer in high speed EDM drilling of nickel alloy. *Journal of Alloys and Compounds*, 783, 95-102.
- [100] Chakraborty, S., Mitra, S., & Bose, D. (2022). Performance characterization of powder mixed wire electrical discharge machining technique for processing of Ti6Al4V alloy. *Proceedings of the Institution of Mechanical Engineers, Part E: Journal of Process Mechanical Engineering*, 236(4), 1283-1295.
- [101] Kumar, V., Jangra, K. K., & Kumar, V. (2016). An experimental study on trim cutting operation using metal powder mixed dielectric in WEDM of nimonic-90. *International Journal of Industrial Engineering Computations*, 7, 135-146.
- [102] Patel, S., Thesiya, D., & Avadhoot, R. (2018). Aluminium powder mixed rotary electric discharge machining (PMEDM) on Inconel 718. *Australian Journal of Engineering*, 16, 21-30.
- [103] Prakash, C., Kansal, H. K., Pabla, B. S., et al. (2016). Experimental investigations in powder mixed electric discharge machining of Ti-35Nb-7Ta-5Zr β -titanium alloy. *Materials and Manufacturing Processes*, 32, 274-285.

- [104] Amorim, F. L., Dalcin, V. A., Soares, P., & Mendes, L. A. (2017). Surface modification of tool steel by electrical discharge machining with molybdenum powder mixed in dielectric fluid. *International Journal of Advanced Manufacturing Technology*, 91, 341-350.
- [105] Marashia, H., Sarhana, A. A. D., & Hamdia, M. (2015). Employing Ti nano-powder dielectric to enhance surface characteristics in electrical discharge machining of AISI D2 steel. *Applied Surface Science*, 357, 892-907.
- [106] Upadhyay, L., Aggrawal, M. L., & Pandey, P. M. (2018). Performance analysis of magneto rheological fluid assisted electrical discharge machining. *Materials and Manufacturing Processes*, 33(11), 1223-1232.
- [107] Lin, Y. C., Hung, J. C., Lee, H. M., Wang, A. C., & Fan, S. F. (2018). Machining performances of electrical discharge machining combined with abrasive jet machining. *Procedia CIRP*, 68, 162-167.
- [108] Zhang, Y., Liu, Y., Shen, Y., Ji, R., Li, Z., & Zheng, C. (2014). Investigation on the influence of the dielectrics on the material removal characteristics of EDM. *Journal of Materials Processing Technology*, 214(5), 1052-1061.
- [109] Kumar, S., Dhingra, A. K., & Kumar, S. (2017). Parametric optimization of powder mixed electrical discharge machining for nickel-based superalloy Inconel-800 using response surface methodology. *Mechanics of Advanced Materials and Modern Processes*, 3(7).
- [110] Sahu, D. R., & Mandal, A. (2020). Critical analysis of surface integrity parameters and dimensional accuracy in powder-mixed EDM. *Materials and Manufacturing Processes*, 35, 430-441.

- [111] Tamang, S. K., Natarajan, N., & Chandrasekaran, M. (2017). Optimization of EDM process in machining micro holes for improvement of hole quality. *Journal of the Brazilian Society of Mechanical Sciences and Engineering*, 39, 1277-1287.
- [112] Ziada, Y., & Koshy, P. (2007). Rotating curvilinear tools for EDM of polygonal shapes with sharp corners. *CIRP Annals*, 56(1), 221-224.
- [113] Gu, L., Li, L., Zhao, W., & Rajurkar, K. P. (2012). Electrical discharge machining of Ti6Al4V with a bundled electrode. *International Journal of Machine Tools and Manufacture*, 53, 100-106.
- [114] Singh, N. K., Pandey, P. M., & Singh, K. K. (2017). Experimental investigations into the performance of EDM using argon gas assisted perforated electrodes. *Materials and Manufacturing Processes*, 32, 940-951.
- [115] Tanjilul, M., Ahmed, A., Kumar, A. S., & Rahman, M. (2018). A study on EDM debris particle size and flushing mechanism for efficient debris removal in EDM-drilling of Inconel 718. *Journal of Materials Processing Technology*, 255, 263-274.
- [116] D'Urso, G., Maccarini, G., & Ravasio, C. (2016). Influence of electrode material in micro-EDM drilling of stainless steel and tungsten carbide. *International Journal of Advanced Manufacturing Technology*, 85, 2013-2025.
- [117] Raju, L., & Hiremath, S. S. (2020). Machining and characterization of micro-channels generated on phosphor bronze using μ -EDM. *Journal of Advanced Manufacturing Systems*, 19(01), 87-106.

- [118] Schubert, A., Zeidler, H., Hahn, M., Hackert-Oschätzchen, M., & Schneider, J. (2013). Micro-EDM milling of electrically nonconducting zirconia ceramics. *Procedia CIRP*, 6, 297-302.
- [119] Jahan, M.P., Wong, Y.S., & Rahman, M. (2009). A study on the fine-finish die-sinking micro-EDM of tungsten carbide using different electrode materials. *Journal of Materials Processing Technology*, 209(8), 3956-3967.
- [120] Li, G., & Natsu, W. (2020). Realization of micro EDM drilling with high machining speed and accuracy by using mist deionized water jet. *Precision Engineering*, 61, 136-146.
- [121] Singh, A.K., Patowari, P.K., & Chandrasekaran, M. (2020). Experimental study on drilling micro-hole through micro-EDM and optimization of multiple performance characteristics. *Journal of the Brazilian Society of Mechanical Sciences and Engineering*, 42, 506.
- [122] Karthikeyan, G., Garg, A. K., Ramkumar, J., & Dhamodaran, S. (2012). A microscopic investigation of machining behaviour in μ -ED-milling process. *Journal of Manufacturing Processes*, 14(3), 297–306.
- [123] Vidya, S., Vijay, Barman, S., Chebolu, A., Nagahanumaiah, & Das, A. K. (2015). Effects of different cavity geometries on machining performance in micro-electrical discharge milling. *Journal of Micro and Nano-Manufacturing*, 3(1), 011007.
- [124] Bellotti, M., Qian, J., & Reynaerts, D. (2018). Enhancement of the micro-EDM process for drilling through-holes. *Procedia CIRP*, 68, 610–615.

- [125] Feng, Y., Guo, Y., Ling, Z., & et al. (2019). Micro-holes EDM of superalloy Inconel 718 based on a magnetic suspension spindle system. *International Journal of Advanced Manufacturing Technology*, 101, 2015–2026.
- [126] Kar, S., & Patowari, P.K. (2019). Experimental Investigation of Machinability and Surface Characteristics in Microelectrical Discharge Milling of Titanium, Stainless Steel and Copper. *Arabian Journal of Science and Engineering*, 44, 7843–7858.
- [127] Khanafer, K., Eltaggaz, A., Deiab, I., & et al. (2020). Toward sustainable micro-drilling of Inconel 718 superalloy using MQL-Nanofluid. *International Journal of Advanced Manufacturing Technology*, 107, 3459–3469.
- [128] Meshram, D. B., & Puri, Y. M. (2020). Optimized curved electrical discharge machining-based curvature channel. *Journal of the Brazilian Society of Mechanical Sciences and Engineering*, 42, 82.
- [129] Phan, N. H., Muthuramalingam, T., Minh, N. D., et al. (2022). Enhancing surface morphology of machined SKD61 die steel in EDM process using DEAR approach based multi criteria decision making. *International Journal of Interactive Design and Manufacturing*, 16, 1155–1161.
- [130] Paswan, K., Pramanik, A., Chattopadhyaya, S., et al. (2023). An analysis of machining response parameters, crystalline structures, and surface topography during EDM of die-steel using EDM oil and liquid-based viscous dielectrics: A comparative analysis of machining performance. *Arabian Journal for Science and Engineering*, 48, 11941–11957.

- [131] Jiang, M., Li, L., Sun, X., et al. (2023). Research on the mechanism and process of polycrystalline diamond by EDM. *International Journal of Advanced Manufacturing Technology*, 125, 819–830.
- [132] Selvarajan, L., Sathiya Narayanan, C., Jeyapaul, R., Manohar, M. (2016). Optimization of EDM process parameters in machining Si₃N₄–TiN conductive ceramic composites to improve form and orientation tolerances. *Measurement*, 92, 114-129.
- [133] Liu, D., Zheng, P., Cao, M., Yin, H., Xu, Y., Zhang, L. (2021). A new method of roundness error evaluation based on twin support vector machines. *Measurement Science and Technology*, 32(7), 075008.
- [134] Arezki, Y., Zhang, X., Mehdi-Souzani, C., Anwer, N., Noura, H. (2018). Investigation of minimum zone assessment methods for aspheric shapes. *Precision Engineering*, 52, 300-307.
- [135] Rossi, A., Antonetti, M., Barloscio, M., Lanzetta, M. (2011). Fast genetic algorithm for roundness evaluation by the minimum zone tolerance (MZT) method. *Measurement*, 44(7), 1243-1252.
- [136] Li, J., Zhi-jing, Z., Wei-ren, W. U., Xin, J., & De-gang, J. (2013). Roundness Error Evaluation by Minimum Zone Circle via Microscope Inspection. *J. Beijing Inst. Technol.*, 22, 185–190.
- [137] Hanumaiah, N., & Ravi, B. (2007). Rapid tooling form accuracy estimation using region elimination adaptive search based sampling technique. *Rapid Prototyping Journal*, 13(3), 182-190.

- [138] Bhattacharyya, B., & Doloi, B. (2019). Modern machining technology: Advanced, hybrid, micro machining and super finishing technology. *Academic Press*.
- [139] Mikrottools Pte Ltd. (2006). *Programming Manual of Integrated Multi-process Machine Tool (model DT110)*, Ver. 1. Singapore.
- [140] Gust, P., Sersch, A., & Kuhlmeier, M. (2021). Influence of specifications according to the system of geometrical product specifications (GPS) on scrap in technical products. *Proceedings of the Design Society*, 1, 1847-1856.
- [141] Lim, L. C., Lee, L. C., Wong, Y. S., & Lu, H. H. (1991). Solidification microstructure of electrodischarge machined surfaces of tool steels. *Materials Science and Technology*, 7(3), 239-248.
- [142] Tong, L. I., Chen, C. C., & Wang, C. H. (2007). Optimization of multi-response processes using the VIKOR method. *The International Journal of Advanced Manufacturing Technology*, 31, 1049-1057.

LIST OF PUBLICATIONS AND RECOGNITIONS

PUBLICATIONS

1. Vidya, S., Wattal, R., & Rao, P. V. (2024). Performance evaluation in die-sinking EDM of polygonal micro cavities over EN-24 alloy steel using cylindrical electrode and polygon cycle approach. *Journal of Engineering Research*. <https://doi.org/10.1016/j.jer.2024.06.006>. (SCIE Indexed, Impact factor: 1.0) (Available Online on 13 June 2024).
2. Vidya, S., Wattal, R., & Rao, P. V. (2022). Experimental investigation on machinability and geometric tolerance in die-sinking EDM of microholes and channels. *MAPAN*, 37(399-407). <https://doi.org/10.1007/s12647-022-00532-x>. (SCIE Indexed, Impact Factor: 1.0).
3. Vidya, S., Wattal, R., & Rao, P. V. (2021). Investigation of machining performance in die-sinking electrical discharge machining of pentagonal micro-cavities using cylindrical electrode. *Journal of the Brazilian Society of Mechanical Sciences and Engineering*, 43(288). <https://doi.org/10.1007/s40430-021-03012-6>. (SCIE Indexed, Impact Factor: 2.0).
4. Vidya, S., Wattal, R., & Rao, P. V. (2023). Evaluation of material removal rate for different cavity geometries produced by die-sinking electrical discharge machining. *Materials Today: Proceedings*, 72(Part 3), 1132-1135. <https://doi.org/10.1016/j.matpr.2022.09.183>. (*International Conference and Exposition on Advances in Mechanical Engineering-2022, 23-25 June 2022, COEP, Pune*) (Scopus Indexed, Cite Score: 2.3).

5. Vidya, S., Wattal, R., & Rao, P. V. (2022). Software based analysis of angularity error for polygonal micro-cavities produced by die-sinking EDM. *Materials Today: Proceedings*, 56(Part 1), 559-562. <https://doi.org/10.1016/j.matpr.2022.02.355>. (International Conference on Materials, Machines & Information Technology-2022, 24-25 January 2022, Amity University, Ranchi) (Scopus Indexed, Cite Score: 2.3).

RECOGNITIONS

1. Research Excellence Award 2023 at DTU, New Delhi.
2. Research Excellence Award 2022 at DTU, New Delhi.

CURRICULUM VITAE

SHRIKANT VIDYA

PROFILE SUMMARY

- Ten years of work experience, having taught a diverse range of subjects at both the undergraduate and postgraduate levels which has provided a comprehensive understanding of engineering principles and pedagogical techniques.
- The research interests primarily focus on Electrical Discharge Machining (EDM) of steel, aiming to fabricate different shapes on micro scale, assess machining performance, optimize process parameters and exploit micromachining capabilities of EDM.

ACADEMIC QUALIFICATIONS

- Pursuing Ph.D. in the area of Electrical Discharge Machining of steel; this thesis is submitted to obtain Ph.D. degree from Delhi Technological University, Delhi, India.
- M.Tech (Manufacturing Engineering) from Indian Institute of Technology – Indian School of Mines (IIT-ISM), Dhanbad, India with 9.12 CGPA (2012-2014).
- B.Tech (Mechanical Engineering) from Ranchi University, Ranchi, India with 76% (2008-2012).

PROFESSIONAL EXPERIENCE

- Assistant Professor in the Department of Mechanical Engineering at Galgotias University, Greater Noida, India from August 2016 to till date.
- Assistant Professor in the Department of Mechanical Engineering at C. V. Raman College of Engineering, Bhubaneswar, India from August 2014 to July 2016.

GOOGLE SCHOLAR PROFILE AND ORCID ID



<https://shorturl.at/WpHrw>



<http://orcid.org/0000-0002-6806-3791>